# Design of a Soft Pneumatic Oscillator

by
Johannes Roelf Vegter

*Thesis presented in partial fulfilment of the requirements for the degree of Master of Engineering (Mechatronic) in the Faculty of Engineering at Stellenbosch University*

Supervisor: Dr Martin Venter

March 2020

# Plagiarism Declaration

By submitting this thesis electronically, I declare that the entirety of the work contained therein is my own, original work, that I am the sole author thereof (save to the extent explicitly otherwise stated), that reproduction and publication thereof by Stellenbosch University will not infringe any third party rights and that I have not previously in its entirety or in part submitted it for obtaining any qualification.

Date: March 2020

# Abstract

The field of soft robotics and more specifically flexible fluidic actuators makes use of conventional control systems that are usually tethered and cumbersome. This project followed a systems engineering approach to produce a soft robotic focused controller that aims to address the shortcomings of conventional controllers used for soft robots. The conceptual design stage identified flexible fluidic actuators as technology in need of a controller to increase robustness, reduce inputs, and increase simplicity. The type of controller identified was an oscillator, which takes inspiration from central pattern generators that are seen as a biological oscillator used to control rhythmic motions. Finally, the conceptual design identified the directional control valve and soft valve as two controller technologies that can produce a soft robot focused oscillator. The oscillator should be able to produce two oscillating outputs from a single constant input, with the frequency of the oscillations proportional to the magnitude of the input.

In the preliminary design stage, the oscillator technologies were evaluated in terms of their functionality and manufacturability. A design of each concept was made and evaluated with regards to three mechanisms namely switching, latching and flow control. These mechanisms were identified to be necessary to produce two oscillating outputs. Both designs produced functional mechanisms, but the directional control valve does not satisfy the manufacturability criteria.

In the detail design stage, a soft valve oscillator was design and evaluated. The oscillator was found to be functional, producing two asynchronously oscillating outputs from a single constant supply pressure, with the frequency of the oscillations dependant on the magnitude of the supply pressure.

# Uittreksel

Die veld van sagte robotika en meer spesifiek buigsame vloeistofaktuators maak gebruik van konvensionele beheerstelsels wat gewoonlik vasgemaak en omslagtig is. Hierdie projek het 'n stelselingenieurswese benadering gevolg om 'n sagte robot-gefokusde beheerder te vervaardig wat daarop gemik is om die tekortkominge van konvensionele beheerders wat vir sagte robots gebruik word, aan te spreek. Die konseptuele ontwerpstadium identifiseer buigsame vloeistofaktuators as 'n tegnologie wat 'n beheerder nodig het om robuustheid te verhoog, insette te verminder en eenvoud te verhoog. Die tipe beheerder wat geïdentifiseer is, is 'n ossillator wat inspirasie verkry uit sentrale patroongenerators wat gesien word as 'n biologiese ossillator wat gebruik word om ritmiese bewegings te beheer. Laastens identifiseer die konseptuele ontwerp die rigtingreëlingskontroleklep en sagte klep ten opsigte van beheertegnologieë wat 'n sagte robot gefokusde ossillator kan produseer. Die ossillator moet in staat wees om twee ossilerende uitsette vanaf 'n enkele konstante inset te lewer, met die frekwensie van die ossillasies afhanklik van die grootte van die inset.

In die voorlopige ontwerpstadium word die ossillatortegnologieë beoordeel aan die hand van hul funksionaliteit en vervaardigbaarheid. 'n Ontwerp van elke konsep word gemaak en geëvalueer met betrekking tot drie meganismes, naamlik skakel, vashou en vloeibestuur. Daar word geïdentifiseer dat hierdie meganismes nodig is om twee ossillerende uitsette te lewer. Albei ontwerpe lewer funksionele meganismes, maar die rigtingreëlingsklep voldoen nie aan die vervaardigbaarheidskriteria nie.

In die detailontwerpstadium word 'n sagte klep-ossillator ontwerp en beoordeel. Dit blyk dat die ossillator funksioneel is, en lewer twee asinchronies ossilerende uitsette vanaf 'n enkele konstante toevoerdruk, met die frekwensie van die ossillasies afhanklik van die grootte van die toevoerdruk.

# Contents

# List of Figures

# List of Tables

# Chapter 1

# Introduction

## 1.1 Motivation

The field of soft robotics is explored in this project for its potential impact on other fields in the future, since soft robots open up the possibility of integration of robots into applications that allow for contact, or close proximity working, with humans. This is an important factor behind the development of soft robots and is referred to as human-robot interaction (HRI). HRI is an important consideration in applications where humans and robots share a working environment, such as on a production line, or in a medical application where the safety of the human being treated is a priority. Soft robots have an advantage in this regard compared to their rigid link counterparts due to their inherent compliance that absorbs much of the energy resulting from a collision [1].

The HRI present in the medical application of soft robots is focused around human motor assistance where a robot that comes into direct contact with humans where robots function without endangering the patient. Cases of lost mobility or rehabilitation are able to integrate new methods and supporting equipment based on soft robotics.[2].

The field of soft robotics is in a unique position where considerable inspiration can be drawn from nature. Inspiration can be drawn from the way creatures function, the way they move, and the way they interact with their environment. As soft robots are in their infancy with regards to movement and functioning as a system, mimicking early lifeforms that have basic locomotory systems should give insight that leads to more complex soft robot locomotion.

This biomimicry can go beyond the biological systems that cause motion and delve into the underlying systems that control motion. In nature, much of the rhythmic motions that cause locomotion is controlled by central pattern generators (CPGs) [3]. CPGs are neural circuits found in invertebrate and vertebrate animals that have the ability to create rhythmic patterns in neural activity whilst receiving non-rhythmic inputs. CPGs are sometimes used as control systems that produce oscillating outputs that are modulated by simple input signals [3].

Incorporating a CPG mimicking soft robotic counterpart may result in a more robust soft robot. Specifically, in fluid-based soft robots, reducing the number of inputs necessary is an important step in producing untethered soft robots that are capable of relatively complex locomotion compared to conventional untethered robots. The complex type of motion considered in this project is the undulatory locomotion of the salamander.

The salamander is seen by many morphologists as the link to primitive tetrapods that are amongst the first land-going vertebrates. It is also known that the undulations of the body of the salamander during locomotion is controlled by a CPG network that responds to simple stimuli [4]. Being able to replicate some of the locomotion methods used by the salamander should provide a stepping stone to even more complex locomotion methods.

## 1.2 Problem Definition and Aim

The field of soft robotics is innovative in its application of materials and techniques to develop new and interesting functional robots. These innovations are bringing the way robots function and interact with the environment ever closer to that of biological creatures. However, soft robots fall behind in the implementation of their control systems. Most soft robots use re-purposed conventional control systems that cause the robot and its control to be bulky even when resulting in simple movement types.

The motion of soft robots is achieved through the use of soft actuators. Most soft actuators have a single movement type, such as extending or bending and require a corresponding input to achieve that single movement. These inputs are usually pressure sources, such as pumps, which are large in relation to electronic input sources used by conventional robots. Many soft robots consist of a system of soft actuators that work together to achieve a movement more complex than extending or bending, therefore they require many inputs that scale with the number of actuators. Accordingly, the input system for a complex soft robot can quickly become large. The reduction of required inputs will increase the simplicity and practicality of soft robotic systems.

This study aims to provide a solution to soft robotic systems that require many inputs to produce a dual-acting output by developing a soft robotic focused soft oscillator. The control mechanism is aimed at applications where size and operational constraints require a controller that is smaller and more robust in comparison to conventional control systems used for soft robotic applications.

The test case used to explore the development and application of soft oscillators in this study is the spinal undulations of the salamander. A three-section elongated body with antiphase oscillations of the sections should provide ample opportunity to implement a soft control system of sorts. The control of the soft robot salamander will draw inspiration from the functioning of the motor system of a real salamander, namely the functioning of central pattern generators (CPGs).

## 1.3 Objectives and Activities

### 1.3.1 Objectives

This project aims to deliver an oscillating mechanism for use in soft robotic applications under soft robotic operating conditions.

- The oscillator should be able to produce two asynchronous outputs from a single power source. This reduces the amount of inputs required.
- The oscillation frequency should be linked to the magnitude of the input. Therefore a higher magnitude input should produce a output frequency that is higher than that of a case with a lower magnitude input.
- The input pressure should act as both the working fluid and the control fluid, allowing the controller and actuator function at the same pressure.

### 1.3.2 Activities

The conceptualisation of the problem at hand starts with the conceptual design which will consist of a literature study that covers the following:

- Review and evaluation of the current state of the soft robotics field.
- Identify a bio-inspired solution to the problem statement of the project.
- Determine the scope of the project in relation to available soft robot technologies.
- Identify soft technologies applicable to this project.
- Select the most applicable soft technology for this project after the evaluation of applicable technologies.
- Select a design methodology to be followed by the project.

After the conceptual design, a preliminary design is done which will consist of the following activities:

- Identify oscillating mechanisms applicable to selected soft technology.
- Evaluate oscillation mechanisms and select the most applicable.

The final step of the project is to design the oscillator and evaluate its functionality, which will consist of the following activities:

- Develop an oscillator using the chosen mechanism.
- Evaluate the developed mechanism with regards to functionality and applicability.

## 1.4 Project Scope

This project covers the design of a soft pneumatic oscillator that can be used to control two soft actuators that are capable of mimicking the bending of a section of the spine of salamander during its terrestrial locomotion. The oscillator must be able to produce two asynchronously oscillating outputs from a single constant supply pressure, where the frequency of the oscillations is dependant on the magnitude of the supply pressure. In order to provide a robust design process, rapid and cost-effective prototyping is considered.

The project relies on a build, test, and evaluate prototyping method. The development of a computer model for the system is not done due to the dynamic and nonlinear behaviour of the silicone rubbers used. Therefore development of the controller does not take into account the parameters of the system it is used in, limiting the the specification definition of the oscillator to values that are independent of the influence of a connected system.

The project does not cover the design of a soft robot, but just the design process of a controller that is focused on soft robotics and is limited by a financial restriction. The financial restrictions limit the choice in material, and manufacturing methods to readily available options. The available facilities will be determining factor in the decisions made in this project.

# Chapter 2

# Literature Study

In this chapter, available soft actuator technologies applied to soft robotic systems that aim to mimic biological systems are studied. This information is used to gain insight into the type of movement most soft actuators are designed for as well as the type of control that is beneficial in producing simpler and more robust robot designs. Following the identification of soft actuator technology and desired functioning for a controller, a suitable biological example is sought to provide guidance. The biological example provides an example of control implementation used to produce a complex movement from simple input control signals. Thereafter existing control technologies applicable to the chosen biological system are explored. A applicable designing methodology is then researched to ensure designing method is applicable to development of the chosen technology. This chapter serves as the conceptualisation of the problem statement. A clear understanding of soft technology used, the biological system to be mimicked, and a selection of suitable controllers are delivered by the end of the chapter.

## 2.1 Soft Robotics

There are a few technologies that are implemented when considering soft actuators, namely shape memory alloys, smart polymers, and flexible fluidic actuators. These technologies vary in functionality, each with their own limitations and advantages. It is important to gain knowledge of the different technologies with regards to their power source, as this influences the design of the controller. This knowledge will be used to distinguish between the need for an electronic controller or a fluidic controller. Each actuator technology will be explored and insight into their capability and applicability will be assessed. Special attention will be given to their need for a controller and their feasibility. At the end of this section, a soft actuator technology will be identified as the chosen technology for this project, along with a clear statement of the functional requirements of the soft control mechanism this project aims to deliver.

### 2.1.1 Shape Memory Alloy Soft Actuators

Shape Memory Alloy (SMA) actuators work on the principle that wire contacts, made from alloys such as nickle titanium, contract when experiencing Joule heating; therefore, a nickle titanium coil functions as an actuator when an electrical current is passed through it. The inclusion of an SMA coil can reduce the fabrication complexity of a soft robotic system and simplify control by only needing a current supply for actuation and control [5], this is counter to the aim of this project though due to this type of implementation not requiring a novel controller. Advantages of SMA actuators are their large force to weight ratio and volumes small enough to be considered negligible [6]. These attributes provide for robust designs, and their negligible volume makes them ideal for biomedical applications where having the smallest intrusiveness possible is very important.

SMA coils are used as agonist or antagonist actuators, similar to the way the bicep is used to bend the arm [7]. SMA coils have also been embedded in flexible housings to cause a twisting motion [8]. Notable soft robotics implementations of SMAs are the octopus and caterpillar of [9] and [10] respectively.

The limitations that need to be considered when looking towards the implementation of SMAs are the high electrical currents needed for actuation, the relatively low efficiency of the process that transfers the electrical energy into the actuation force, and the hysteresis in the material activation that makes the precise control difficult [6].

### 2.1.2 Smart Polymer Soft Actuators

Smart polymer soft actuators cover a variety of technologies, the two most common forms are electroactive polymer (EAP) actuators and shape memory polymer (SMP) actuators.

SMP actuators are functionally almost identical to SMAs, the main difference being the stimuli that cause actuation. Thermal, chemical, light, or magnetic field stimuli can be used for activation at the cost of an increase in response time [6]. Theoretically, SMPs can replace SMAs in any application, whilst addressing some of the shortcomings of SMAs making SMPs a more favourable technology in some applications. With higher efficiency in transforming the input energy to actuation force, biocompatibility, and flexibility, SMPs are favourable to SMAs in many biomedical and micro-electromechanical applications [6].

[11] designed and manufactured micro-vascular SMP actuators, in claw and coil configuration, that use warm water for activation, the devices are shown in rest and activated form in Figure 2.1.1. Many implementations of SMPs in

soft actuators result in a hinge mechanism as in [5], as seen in Figure 2.1.2, and the studies reviewed by [12].

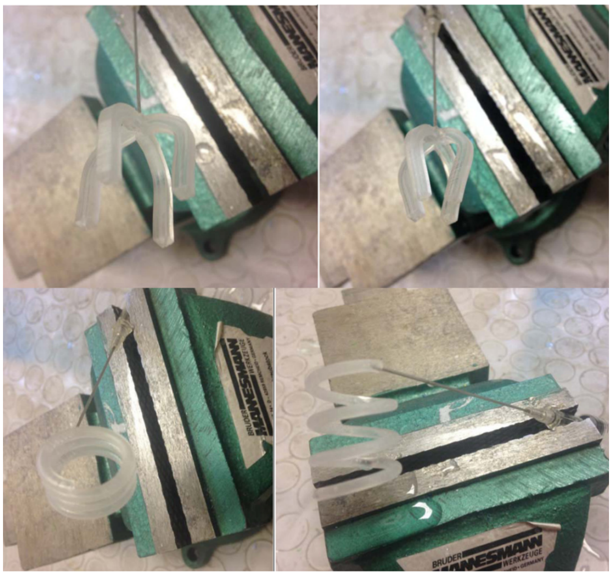

**Figure 2.1.1:** Rest and Activated Forms of Micro-Vascular SMP Actuators Left: At rest, Right: Actuated [11]

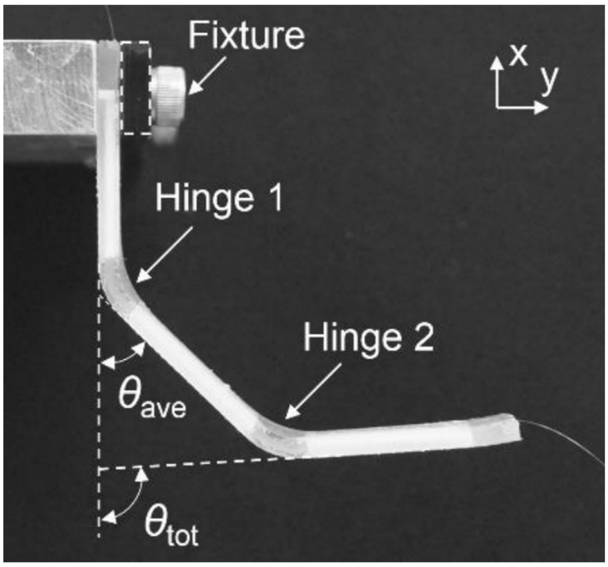


**Figure 2.1.2:** SMP Hinge Example [5]

EAP actuators have an electro-mechanical response with a high strain that closely resembles that of natural muscles [13]. EAPs have similar advantages to SMPs, such as biocompatibility, flexibility, and relatively high efficiency.

Where EAPs separate themselves from SMPs is in their greater property change when subjected to electrical stimulation [6], with much larger actuation distances than SMPs. Electrolytically active polymers, polyelectrolyte gels, and gel-metal composites have been used as bending type actuators as shown by [14], [15], and [16].

The most attractive EAP technology for this project are dielectric elastomer actuators (DEAs) due to their high specific power, ease of manufacturing, and low cost [17]. DEAs have found widespread applications, many of which make use of so-called constrained DEAs. [18] designed a bicep inspired muscle using this technique, [19] designed a earthworm locomotion imitating robot, [20] designed a pneumatic valve, [21] designed a quadruped robot, and [22] designed a tunable lens. These applications work on the principle that a DEA changes in surface area when activated. The change in surface area causes an increase or decrease in thickness, which functions as the actuation, as shown in Figure 2.1.3.

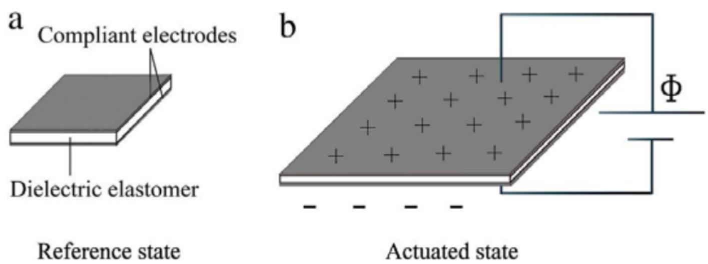


**Figure 2.1.3:** Forms of Constrained DEA
Left: At Rest, Right: Activated [22]

[23] is responsible for work that may be more applicable to this study than the technologies previously mentioned, namely, a soft artificial muscle with high strain at relatively low voltages. The artificial muscle is composed of ethanol distributed throughout a silicon elastomer matrix that experiences large volume change when exposed to an electrical stimulant. The increase in volume when activated is illustrated in Figure 2.1.4.

As with SMAs, the EAP biomimetic applications tend to be as agonist or antagonist actuators. Most EAPs are still limited by their slow response or high voltage requirements which may prove to be parameters that are important for this study [6].

### 2.1.3 Flexible Fluidic Actuators

Flexible fluidic actuators (FFAs) function by inflating a chamber that deforms in a prescribed manner. Two common types of flexible fluidic actuators to con-

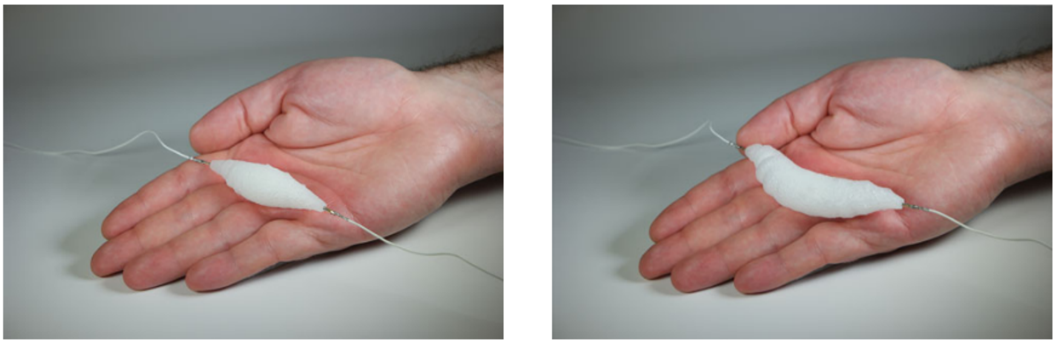

**Figure 2.1.4:** DEA Soft Artificial Muscle Activation
Left: Not Activated, Right: Activated [23] [22]

sider are pneumatic artificial muscles (PAMs) and elastic inflatable actuators (EIAs).

### Pneumatic Artificial Muscles

A typical PAM is an inflatable tube wrapped in a deformation restricting braided mesh. The structure contracts or expands in length and increases or decreases in radius as the tube is pressurised and halts when the radial deformation is stopped by the mesh [24]. The behaviour of the actuator when inflated is reliant on the weave pattern of the mesh and is operated with a driving pressure much higher than that required by EIAs [7].

PAMs are almost exclusively used as agonistic or antagonistic actuators as reported by [24]. [25] proposed series pneumatic artificial muscles (sPAMs) to create a soft continuum robot arm, illustrated in Figure 2.1.5. sPAMs are PAMs connected in series, as to achieve contraction whilst still having the flexibility to bend. The robot arm in [25] achieved bending by using a larger centre tube as a rigidity providing element and two sPAMs on opposite sides of the centre tube that controlled bending. This application delivers a robot that functions much the same as the EIAs.

### Elastic Inflatable Actuators

EIAs are comprised of an expansion chamber that is in some way restricted by its physical properties. The structure of the actuator can control the motion path of the actuation, this is seen as a sort of embedded intelligence that is programmed into the hardware design of EIAs [26]. Being able to control actuation paths by configuring the hardware of the EIAs is a powerful tool in actuator design. These actuators are able to achieve a variety of motions as a result of their structure. Many of these motions and practical examples of each are shown in Figure 2.1.6.

From Figure 2.1.6 it can be seen that expanding and bending motions are

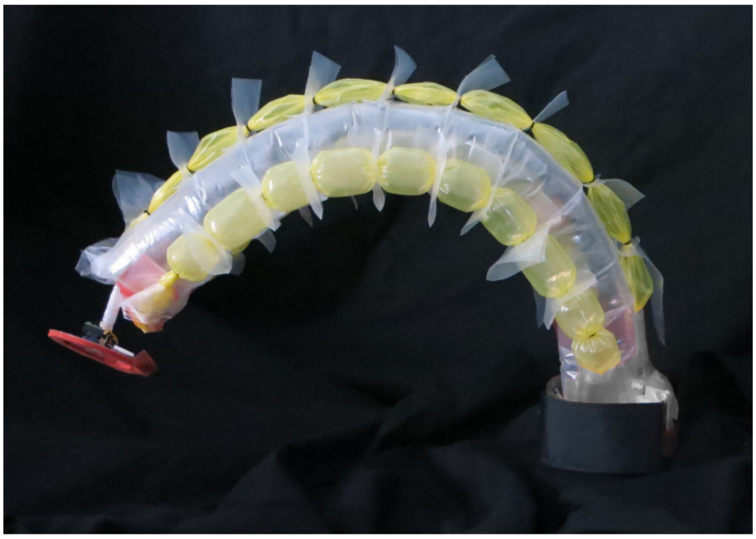

**Figure 2.1.5:** sPAM Continuum Arm [25]

produced by material expansion due to being exposed to an internal pressure, whilst other types of motions similar to contracting and twisting are achieved by used a reinforcement that restricts inflation.

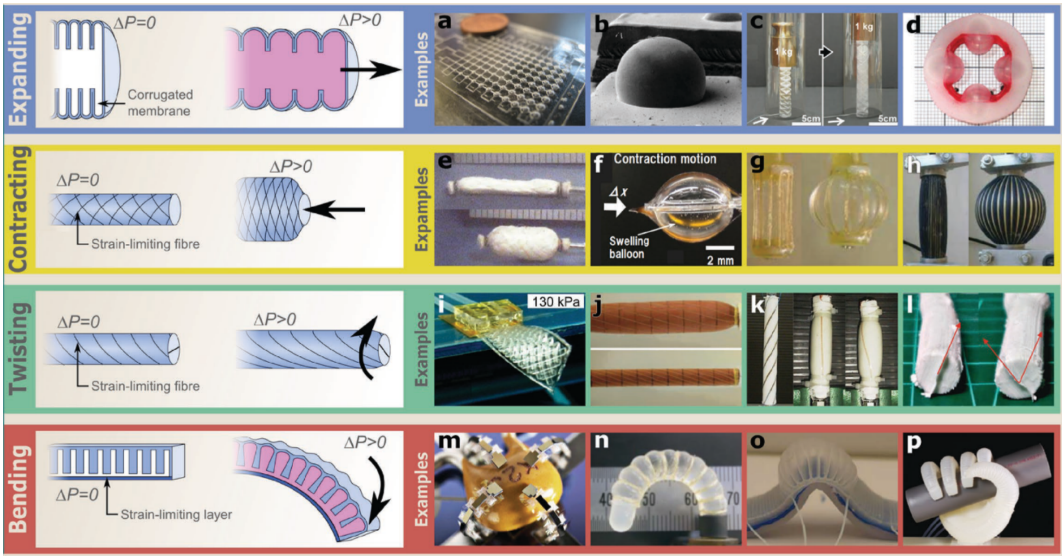


**Figure 2.1.6:** Examples of EIAs [26]: The types of actuation paths with included examples are divided into rows

This flexibility in functionality is paired with independence from high pressure, electrical power, or temperature to power actuation. The operating pressure of EIAs is less than ten percent of that required by PAMs [7]. EIAs have found widespread adoption in research with advancements made in modern manufacturing techniques [26]. EIAs have been used to make crawling robots capable of multiple gaits, as shown in Figure 2.1.7 adapted from [27] and in soft robots that make use of travelling wave undulations, in a soft robot developed by [28], such as the one shown in Figure 2.1.8.

The drawback of EIAs is the dependence on an external pressure source, and the slow response time due to the mass flow required to inflate large volumes that function at low pressures relative to conventional robots. There have been noticeable advancements made with respect to response time by [29].

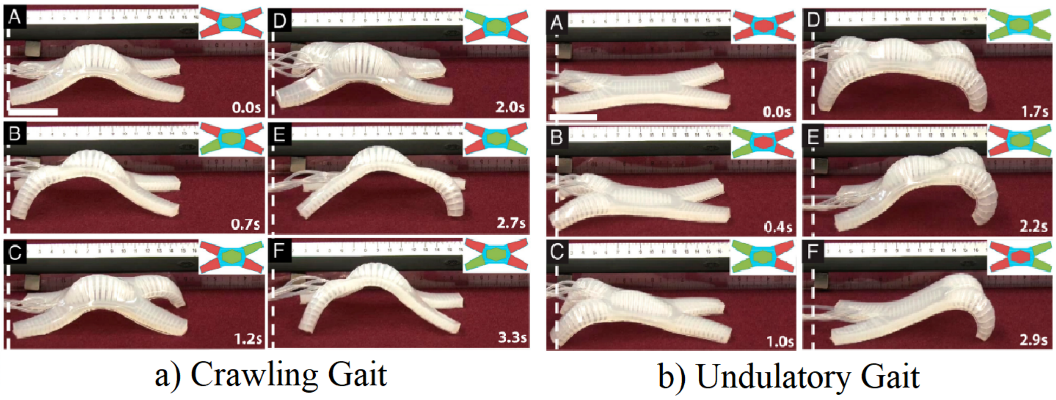


**Figure 2.1.7:** Multigait EIA Soft Robot [27]: a) shows a limb-by-limb actuation method of locomotion and b) a body undulation method of locomotion

## 2.1.4 Evaluation and Discussion

To evaluate the soft technologies in relation to one another, they are ranked according to actuation speed, actuation accuracy, power requirements, manufacturability, cost, robustness, and the need for control. These are seen as criteria that will produce an effective choice for a soft technology due to important functional requirements and viability requirements being evaluated. The four technologies considered are SMAs, PMAs, EIAs, and PAMs. The distinction between EIAs and PAMs is made due to the actuation paths of PAMs being much more limited than that of EIAs even though both are considered FFAs. The following paragraphs provide the reasoning behind the rankings shown in Figure 2.1.9. Figure 2.1.9 is a radar plot in which the technologies are ranked in comparison to one another, with a larger radius equating to a higher preferability.

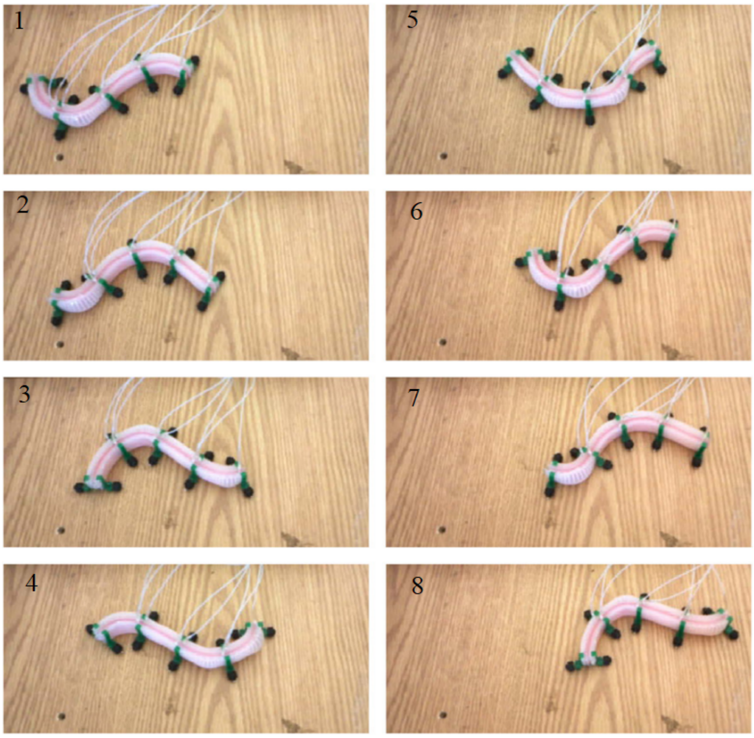


**Figure 2.1.8:** Undulatory Locomotion EIA Soft Robot [28]

### Actuation Speed

SMAs have slow actuation speeds due to the actuation being reliant on thermal reactions, with SMPs having a similar disadvantage. SMPs have other actuation mechanisms but are also limited in speed.

EIAs and PAMs are actuated a working fluid, therefore the speed is dependant on the use of pneumatic or hydraulic working fluids, with hydraulic actuation being a faster actuating technology. Both these technologies actuate faster than SMAs and SMPs, with PAMs actuating the fastest. The actuation speeds of EIAs can be improved as seen in [29].

### Actuation Accuracy

SMAs and SMPs have difficult to control actuation methods, due to being reliant on thermal or chemical reactions. SMAs have hysteresis in material activation that causes difficulty in precision, which is a disadvantage that SMPs can improve.

The actuation accuracy of PAMs and EIAs are dependant on their power supply but are more accurate than SMAs and SMPs. PAMs are more accurate than EIAs due to their actuated stated being geometrically constrained and defined by a restrictive enclosure although EIAs can also be structurally reinforced or constrained to limit actuation. Over-inflation does therefore not cause inaccuracy as in the case of PAMs or the specific case of constrained EIAs.

### Power Requirement

Regarding power requirements, fluidic and electrical power supplies are considered. The fluidic power requirements are reliant on the volume and scale of the actuator, with a larger actuator requiring lower pressure. Therefore it is difficult to provide a concrete difference between PAMs and EIAs. They are ranked similarly in this criteria, with both requiring a simple pressure source. EIAs are slightly more favourable due to their flexibility in design that can influence the required power supply, demonstrated in [29]. The availability of pneumatic power supplies is considered as an advantage for these technologies.

SMAs and SMPs actuate with electrical stimulation, with SMAs requiring large electrical currents. Large electrical currents are seen as a disadvantage in this project due to safety concerns. SMPs have other power supply options as previously discussed and lower electrical requirements in some cases, making them more favourable than SMAs.

### Manufacturability

SMA and SMP based actuators require specialised manufacturing techniques. In some cases, the use of polymers used by SMP actuators also includes specialised materials that require their own manufacturing process. This project is not focused on the development of an actuator technology thus this is seen as a disadvantage for SMPs.

EIAs are cast silicone parts that require the designing and manufacturing of a mould. This can be done using computer-aided design and 3D printed parts, which are available facilities. A variety of silicone are also readily available for constructing of EIA based designs, making EIAs an easily manufacturable option. PAMs have the most simple manufacturing process, requiring only an inflatable bladder and a constraining layer. These parts can be manufactured from available plastic sheeting. Therefore both EIA and PAM technologies are more favourable than SMA and SMP options, with PAMs being the most favourable in regards to manufacturability.

### Cost

Although all actuator technologies considered are low cost relative to store bought conventional actuators, EIAs and PAMs are more favourable due to the availability of plastic sheeting, silicone, 3D printing facilities, and power sources. SMAs and SMPs will both require the purchase of the metal or polymer around which the actuator is based.

### Robustness

SMA and most SMPs have rigid components which are sensitive to external forces, that may bend or break these rigid components. The SMPs that do not make use of rigid components, such as the one shown in Figure 2.1.4, can not function in uncontrolled situations with restrictions to external contaminants.

EIAs and PAMs are very robust due to their inherent flexibility as a result of their soft nature, making them impervious to external forces. Silicone and plastics also have low chemical reactivities, making the use of these technologies in various conditions possible. EIAs and PAMs are able to deform and absorb the energy of collisions and function in various environments due to their flexibility and low chemical reactivity, making them more robust than SMAs and SMPs.

PAMs require a rigid structural component or constant power supply to be self-supporting; however, EIAs can be design to be self supporting by using a harder silicone or by designing a silicone structure with a sufficient stiffness to stop prominent out-of-plane bending whilst remaining what is considered to be a soft structure.

### Need For Control

SMA and some SMP actuators are electrically controlled, and therefore make use of a mature technology. The SMPs that are not electronically controlled require the development of a control system that provides the required stimulant, making a specialised control system more attractive for this technology.

EIAs and PAMs make use of conventional fluidic control systems that are not conventionally designed with robustness and portability as a consideration. Therefore a specialised controller that can reduce the need for external controllers is an attractive prospect. Due to the fully soft nature of EIAs, the design of a fully soft controller that will complement the robustness of the technology makes the introduction of a specialised controller for EIAs a more attractive option than for PAMs.

### Evaluation

Although technologies such as SMAs and SMPs show promise in advancement in soft control systems, their electrical-power requirement is unsuitable for this project since the electronic control system is a mature science, with many control options. SMPs have other power sources, but the available facilities do not include these methods.

From Figure 2.1.9 it can be concluded that EIAs and PAMs are both suitable for this project due to their simplicity, ease of use, and cost-effectiveness. They require only a pressure source for functioning, which is a very important consideration with regard to ease of use. Both technologies are also a cost-effective solution by only needing readily available and less costly plastic sheeting or silicone for manufacturing, in comparison to the polymers and exotic materials of the other technologies. In regards to their simplicity, the wide variety of actuation types of EIAs makes them ideal for this project by providing adaptability for unforeseen challenge. EIAs are also more robust due to being self-supporting without the need for a rigid component or constant power supply. Therefore EIAs are the most applicable technology for this project.

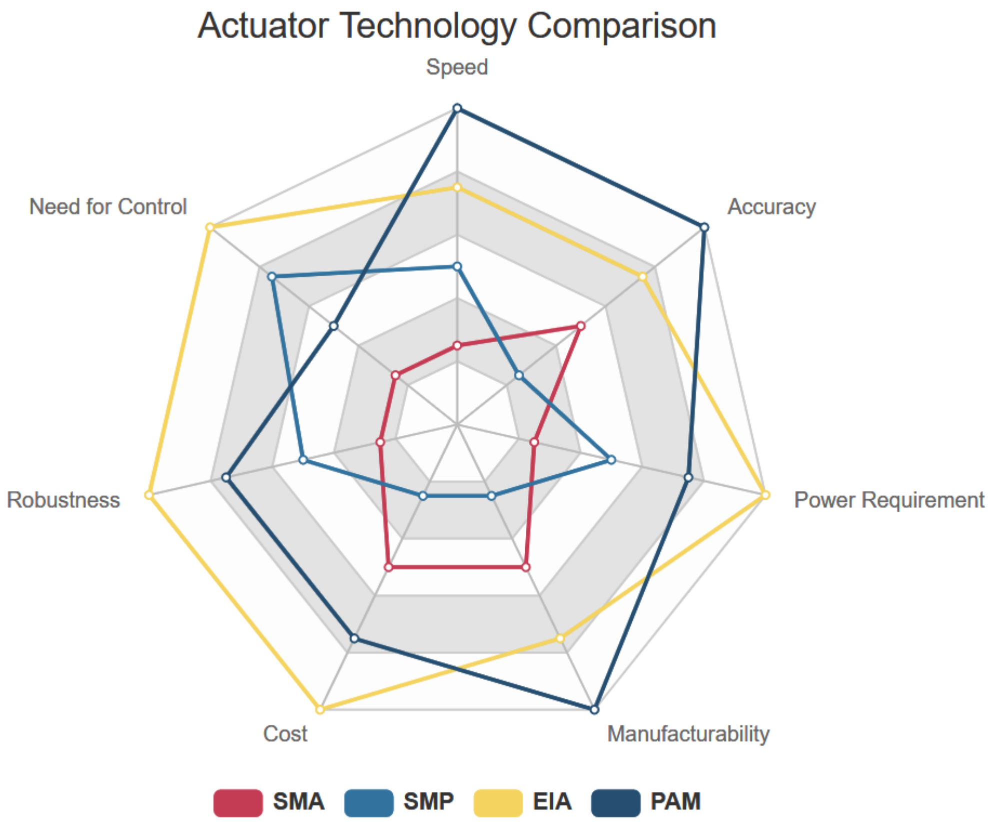


**Figure 2.1.9:** Actuator Technology Comparison Radar Plot: For each criterion the technologies are ranked decreasingly in radius from first to fifth with a smaller radius equating to a lower ranking.

## 2.2 Existing Elastic Inflatable Actuator Based Soft Robots

### 2.2.1 Introduction

This section looks at existing soft robots that make use of EIAs, that have the same undulating motions that this project aims for, as well as controllers that may be implemented in this project. Insight into the limitations of soft robot oscillators and what type of motion is possible with the use of EIAs is gathered to give guidance in determining a realistic scope with regards the complexity of motion achievable whilst making use of a soft robotic focused controller.

### 2.2.2 Existing Undulating Soft Robots

Body undulation is a motion often used in nature, often for locomotion. Replicating this motion is an avenue for many soft robotic scientists. The soft robot briefly mentioned in Section 2.1.3 and shown in Figure 2.1.8 was developed by [28] in an effort to implement onboard control in soft robots. This was done to increase usability and independence by reducing the amount of control and power transmissions the robot is connected to whilst still performing a complex type of serpentine locomotion. Figure 2.1.8 shows the soft robot making use of external control, used as a proof of concept on inducing undulating motion, whilst Figure 2.2.1 shows the soft robot with onboard control. The robot makes use of four bidirectional EIAs in series with the control and power systems located in the tail and the control valves located in between each segment. The pressure is distributed to the required segments at the required intervals by the control system via the control valves. This robot is, in essence, a soft robot with conventional electronic control systems.

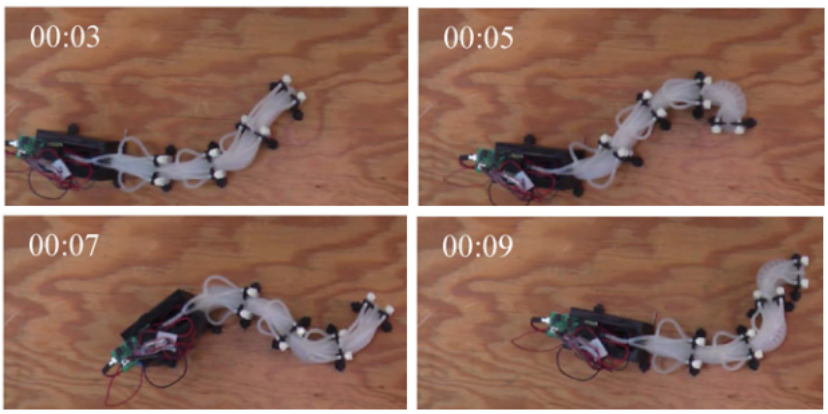


**Figure 2.2.1:** Undulatory Locomotion EIA Soft Robot with Onboard Control and Power Source[28]

Another interesting use of EIAs to perform undulatory locomotion is that of [27]. The soft robot with multigait functionality is briefly discussed in Section 2.1.3 and the two gaits are shown in Figure 2.1.7. The soft robot designed is a quadruped with four actuators as legs and one as a spine. The actuators in the legs are inflated either one at a time with the spine always inflated to induce a crawling gait, or the rear legs, spine, and front legs are inflated cyclically to induce a body undulation. The gaits along with their inflated sections for each method of locomotion is also shown in Figure 2.1.7.

The soft robot in [27], although capable of undulatory locomotion, makes use of external control and a pressure source for each actuator. An important insight gained from [27] is that undulation is reproducible by cyclically inflating the sections of a soft robot without requiring a mechanism that allows the working fluid to cascade through the robot. The sections of the soft robot can therefore be independently inflated to mimic a smooth undulation, whilst making use of minimal sections. In this case, three sections are used, but producing an s-shaped undulation is achievable by using two anti-phase bidirectional bending sections in series.

[30] makes use of buckling elastomer beams to enable movement in soft robots. Making use of strategically chosen geometries and buckling under negative pressure loads, torque output is achieved. Figure 2.2.2a illustrates the geometry, Figure 2.2.2b illustrates the functioning and the schematic, and Figure 2.2.2c illustrates the actual functioning of the mechanism. This design functions both as an actuator and soft robot, integrating the two parts into a self-contained soft machine.

A challenge in implementing the mechanisms of [30] into this project is the reliance on negative pressure. The design of [30] may be reversible by having the original shape be the buckled shape achieved after the vacuum load is applied, inflation could then cause the already buckled shape to expand causing rotation in the different direction. Torque output is unique for soft mechanisms and may lead to interesting developments if implemented.

## 2.3 Control in Nature

### 2.3.1 Introduction

Just as in engineering, biologists that seek to model and describe a complex problem simplify the underlying elements in order to gain insight and understanding. This approach can be followed to determine the underlying biological systems in control of locomotion. Since the 1980's biologists interested in the neural mechanisms in control of locomotion have been studying animals that possess simple locomotor systems, such as the lamprey and the salamander [31], [32], [33], [34]. These vertebrates have the locomotory control systems that are considered to very closely resemble that of the prehistoric vertebrates

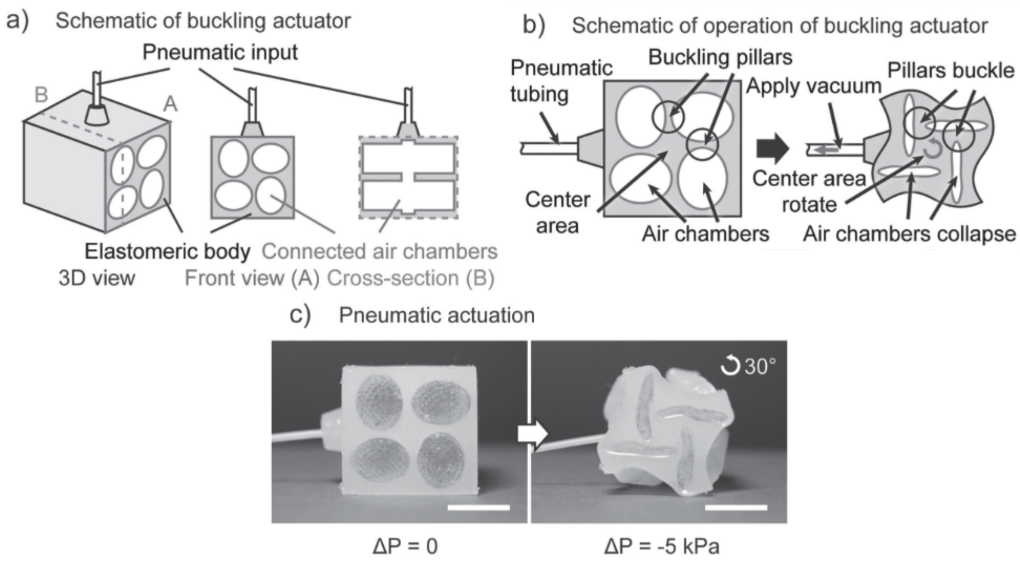


**Figure 2.2.2:** Buckling Elastomer Beam Soft Robot: a) schematic of buckling actuator, b) schematic of operation of buckling actuator, c) pneumatic actuation of physical robot [30]

that evolved from aquatic to terrestrial modes of locomotion.

As an amphibian, the locomotor system of the salamander must be very dynamic in switching between locomotion methods to adapt to ever-changing environmental conditions. The ability to switch between various terrestrial and aquatic gaits. The salamander provides an invaluable case study for engineers looking to design a multigait robot, due to salamanders using variations of the same motions to produce different locomotion methods.

Adding to the attractiveness of the salamander and lamprey locomotion case is the simple nervous system that controls the locomotion of the salamander, within which a simple solution to complex control systems may be held.

At this point, it is important to note that although both the lamprey and salamander are very close locomotory speaking, the flexibility provided to the aims of this project by the terrestrial and aquatic gaits of the salamander cements it as the case study for this project.

## 2.3.2 Salamander Morphology

Vertebrate morphologists have used the salamander to gain insight into the locomotory systems of primitive tetrapods. Along with the sprawling posture and the undulatory movements of the spine during locomotion the salamander has in common with its prehistoric ancestor, its skeleton structure is also accepted as the closest representation of the earliest tetrapods [35].

Studying the skeletal structure of the salamander gives valuable insight into the design of the theoretical soft-robot of this project. The skeletal structure is responsible for guiding the kinematics of locomotion, therefore an accurate representation of the structure is needed to enable an accurate replication of locomotion.

The typical salamander skeleton is divided into four components, namely the skull, the spine, the forelimbs, and the hindlimbs. The spine is further divided into components, namely the cervical, trunk, sacrum, and tail. An illustration of the skeletal structure of the salamander is provided in Figure 2.3.1.

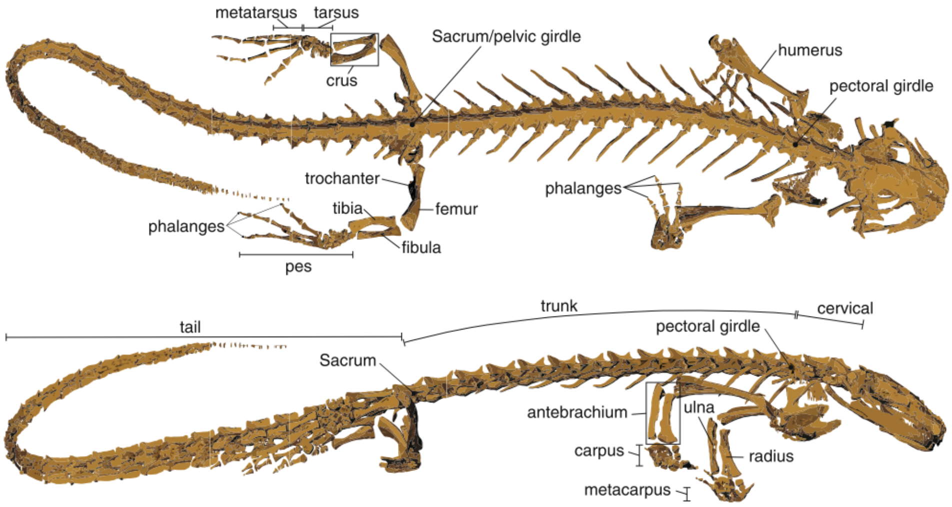


**Figure 2.3.1:** The Skeleton of the Salamander [36]

### 2.3.3 Locomotion Kinematics

There are two gaits to consider in the locomotion of the salamander, namely the terrestrial and aquatic gait. These gaits vary greatly with respect to not only the speed of the axial undulations but also to the propagation of the undulation through the body of the salamander as well as the magnitude of these undulations [4], [32], [34], [35], [37].

[34] and [37] distinguish between a travelling wave axial undulation during the swimming gait, and a combination of standing and travelling wave axial undulation for the trotting gait depending on the walking speed. The difference between the two gaits are illustrated in Figure 2.3.2, adapted from [37], with the swimming gait shown in a and the trotting gait in b. The shape of the gaits are gathered experimentally by monitoring the location of certain points on a salamander during terrestrial and aquatic locomotion.

The main differences between the two gaits is the type of undulation the spine undergoes and the limb use. During the swimming gait the limbs are

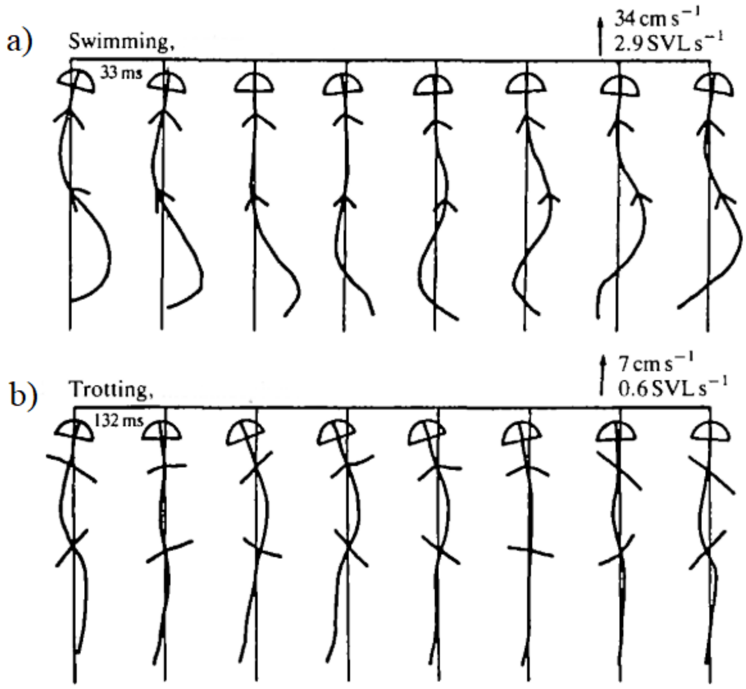


**Figure 2.3.2:** Swimming and Trotting Gaits of the Salamander [37]: a) illustrates the travelling wave undulation during aquatic locomotion and b) illustrates the standing wave undulations during terrestrial trotting

retracted and not needed for locomotion, whereas the limbs are extended and in use in the terrestrial. The other difference is the type of undulation the spine performs.

The swimming gait is achieved by making use of a travelling wave undulation. The travelling wave can be seen in a of Figure 2.3.2, where the pectoral and pelvic girdles do not stay in-line and the amplitude of the oscillation increasing as it travels down the length of the spine.

During terrestrial locomotion, the pectoral and pelvic girdles remain in-line and serve as pivot points for the cervical, trunk, and tail as illustrated in b of Figure 2.3.2. Alternating bending of the sections of spine then produce an s-shape undulation.

The terrestrial gait of the salamander is accomplished with a combination of three movements, namely: i) limb retraction, ii) limb rotation, and iii) girdle rotation [36]. Limb retraction refers to the bending of the limbs in the plane of the body, limb rotation refers to the rotation of the limbs around the girdles without bending, and girdle rotation refers to the rotation of the limbs purely as a result of the girdle's rotation caused by spinal undulations. Salamanders can be made to walk using each of these motions individually, but in nature, the salamander always combines all three of the motions. The standing wave undulations of the body during the terrestrial gait causes the girdles to rotate, the pelvic girdle much more so than the pectoral girdle [35], this rotation gives the limbs a larger range of motion and therefore enables larger steps. Combining the extra range of motion due to girdle rotation with limb retraction and limb rotation gives the salamander faster and more stable locomotion than using a single locomotion method.

### 2.3.4 Locomotion Control

Just as in other vertebrates, the salamander's gait is generated by a central pattern generator (CPG). The CPG network for the axial undulations runs along the entire length of the spinal cord and is responsible for the activation of the muscles along the spine. The limb movements are controlled by separate CPGs that work in conjunction with the spinal CPG for the correct activation of the muscles along the spine and limbs to enable locomotion [4]. This is seen as a form of distributed control where a central control system is not required to produce various forms of output signals, but rather distribute the control to other sections that produce various types of output signals in response to an input signal from the central control system.

Interestingly, the locomotion mode of the salamander can be induced and changed with a simple electric stimulation of the mesencephalic locomotor region of the brain [38], [39]. Low levels of stimulation induce a trotting gait that increases in speed as the stimulation strength increases; at a certain stimulation level the swimming gait is induced. In both locomotion modes, the frequency of movement is proportional to stimulation strength [4]. What is important to note is that the standing wave undulations change into travelling wave undulations by merely increasing the strength of the stimulation, this shows two different types of undulation produced by the same CPG network, dependent only on the input signal strength sent to the CPG network.

Effectively CPGs allow for the decoupling of control from a central control system. Requiring only a simple constant input to produce an oscillating output lessens the burden on a central control system by simplifying the control signal the control system needs to produce.

### 2.3.5 Evaluation and Discussion

The locomotion of the salamander induced by CPGs is a biological application of an oscillator for control that has the potential for application in the field of soft robotics. Having an oscillator that needs only a constant input to deliver an oscillating output provides the opportunity to decouple the control of the actuator from a large central control system. Along with the CPG implementation, the undulation of the spine of the salamander is also a valuable case study for this project. The simplicity in structure and motion makes it a suitable candidate to be modelled by an EIA. Two back-to-back bending actuators will be be able to mimic the bending of a section of the salamander, therefore a combination of three of the back-to-back bending actuators will be able to mimic the spinal undulations of the salamander. This application will need an oscillator that is able to produce two asynchronous outputs, in order to actuate the bending actuators one at a time. This type of oscillator will supports the previous specification that requires the controller to reduce the number of inputs.

## 2.4 Existing Mechanisms for Oscillation

### 2.4.1 Introduction

This section looks at three suitable oscillating technologies to implement and adapt in this study in order to select an option most suitable based on the criteria set up in the introduction. Taking into consideration the difficulty of achieving oscillation using a passive soft mechanism, soft, hybrid, and conventional technologies are considered. More attention is given to technologies that focus on soft materials, but conventional technologies are explored to gain insight for possible integration into a soft robot application.

### 2.4.2 Directional Control Valve

Conventional pneumatic oscillator valves switch a single input pressure between two outputs, a common application is the double-acting cylinder. The switching is done by opening or closing internal channels to direct airflow. The internal workings of pneumatic oscillators are close to, if not precisely, like that of a directional control valve.

A directional control valve directs flow internally through channels that are located on a sliding shuttle, with the direction of the flow being dependant on the position of the shuttle. The position of the shuttle is usually controlled by electromagnets that attract the shuttle to either side. If the shuttle slides back and forth to change the direction of the input pressure between two or more outputs, an oscillating output is achieved. Being able to customise the geometry of the shuttle gives flexibility in the number of outputs and inputs that can be used.

An example of a directional control valve is shown in Figure 2.4.1. In Figure 2.4.1 the spool directs flow between a supply pressure and one of two outputs whilst connecting the other output to a venting channel. The shaded spool indicates the other possible position of the spool which directs the supply pressure to the previously venting output and connects the previously pressurised output to the venting channel.

Directional control valves are almost exclusively used in high-pressure applications and are therefore very large and expensive pieces of equipment especially in the context of soft robotics where smaller and less expensive silicone

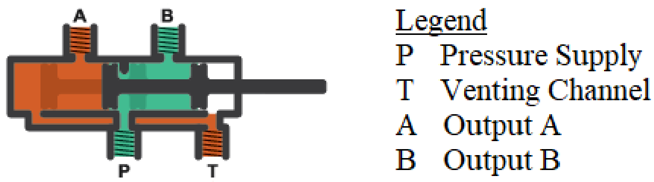


**Figure 2.4.1:** Directional Control Valve Diagram: The dark spool indicates a state wherein B is pressurised and A is vented, while the shaded spool position indicates a state wherein A is pressurised and B is vented

parts are used. The functioning of directional control valves is very simple, therefore it will be possible to be replicate a directional control valve with parts that are 3D printed. This method of manufacturing will reduce cost, and provide flexibility in design. Incorporating permanent magnets for latching and soft membranes for switching will allow the design of a semi-soft oscillator. Therefore, using an adapted directional control valve with soft elements will suffice for this study.

### 2.4.3 Microfluidic Membrane Valve

The field of microfluidics is responsible for the design of small pneumatic circuits that function similarly to digital circuits by developing pneumatic components that are analogous to electronic components. There is an abundance of ways electronic components and circuits can produce oscillating outputs, but there are not many such circuits or components available in the microfluidic world. Therefore a microfluidic analogue of the transistor was designed, with a transistor being an electrical component used for oscillation. Transistors are often used as switches in electronic circuits. The switching operation can be used to form an oscillating circuit by cyclically switching the direction of the input between two outputs. The microfluidic transistor is referred to as a membrane valve. An exploded and assembled view of this mechanism is shown in Figure 2.4.2 which is adapted from [40].

Membrane valves function by blocking the flow of the working fluid through a channel by using an inflating elastomeric membrane controlled by an external control signal. The membrane is squeezed between the top and bottom wafers in which a displacement chamber and a valve seat are etched. When the membrane is not inflated, the flow of the working fluid is allowed to flow from input to output via the valve seat, with the membrane not providing any resistance. When the membrane is inflated by the control signal, it occupies the valve seats and blocks the flow of the working fluid.

[41] has used the membrane valve to produce an oscillating output by using

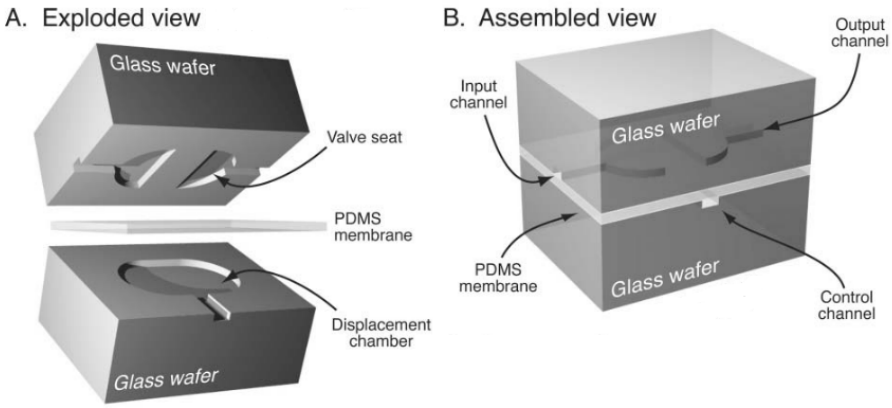


**Figure 2.4.2:** Microfluidic Transistor [40]

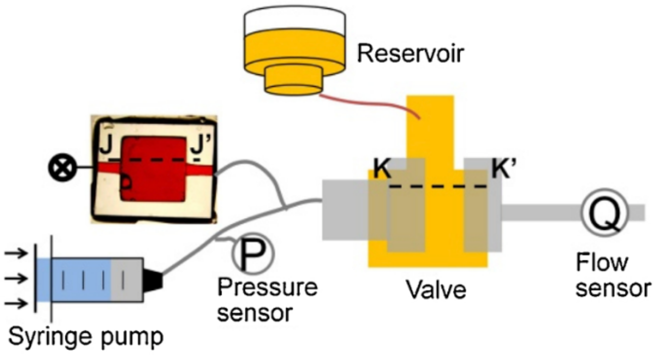


**Figure 2.4.3:** Membrane Valve Oscillating Circuit [41]

a constant input flow rate. A diagram of the circuit is shown in Figure 2.4.3. The circuit consists of a mechanical membrane acting as a fluidic capacitor, which is highlighted in red in Figure 2.4.3, and a membrane valve to which a reservoir is connected to the displacement chamber.

The fluidic capacitor provides a reservoir of working fluid that sustains flow through the valve once the critical pressure of the valve has been reached. The critical pressure is dependant on the counteracting pressure on the membrane that the reservoir provides, which is controlled by varying the level of fluid in the reservoir.

This circuit produces by an oscillating output by using a constant flow rate input that builds up pressure in the capacitor, until a critical pressure is reached at the input of the normally closed membrane valve which then forces the valve open and allows the capacitor to drain until the input pressure reduces to below the critical pressure. This cycle is repeated as long as the constant flow input is supplied.

The frequency of the oscillation is controllable by changing the pressure or the reservoir, with an increase in pressure causing a decrease in frequency and vice-versa. This application is hydraulic, but one will be able to adapt it to work with a pneumatic source.

A problem identified for implementing microfluidics in this project is the scale of the components and their operating conditions. The pressure and flow rate requirements of a microfluidic system is different to that of the soft technology chosen for this project, with the soft oscillator in [42] requiring 34 kPa for a flow rate of 24.5 $\text{pm}^3/\text{s}$, and the latching valve of [40] requiring a vacuum of 85 kPa and positive pressure of 40 kPa for control of a fluid with a maximum pressure of 4 kPa. Such a small flow rate for the working fluid will be an inconvenience if a microfluidic controller is implemented for an EIA based soft robot that is not of the same scale as the controller.

### 2.4.4 Soft Valve

[43] developed a soft valve that has a variety of applications. In [43], the soft valve is used as an oscillator that used in an inching soft robot worm, and as a soft pneumatic switch. The soft valve makes use of buckling elastomer tubes and a bistable membrane. The tubes allow airflow when straightened, and block airflow when buckled. The bistable nature of the membrane allows it to be used as the latching switch that either buckles or straightens the tubes. Figure 2.4.4 shows the soft valve in its two states. The setup in Figure 2.4.4 requires a working fluid input for the top and bottom tubing as well as control inputs for the top and bottom chambers.

In the oscillator setup, the valve requires only one input, where the working fluid is also used as the control fluid. This setup is shown in Figure 2.4.5 were the working fluid pressurises the opposite chamber that, in turn, blocks the working fluid by actuating the membrane and buckling the tube. This setup requires the depressurising of the bottom chamber to stop the valve from latching closed. This is accomplished by having the bottom tubes vent to the atmosphere when straightened. This setup does not strictly have a bistable membrane, seeing as the membrane snaps back into the original state without chamber pressurisation. The output is also a singular positive oscillating pressure, which will not allow one of these oscillators to control either two actuators or a single double-acting one.

The soft valve designed by [43] has been implemented by [44] to create a ring oscillator. The ring oscillator application shows that this design is able to be connected in series to produce lagging oscillating outputs. The lagging peaks of the output pressures of the three soft valves are shown in Figure 2.4.6. An application like this can produce the travelling wave undulations found in the salamander.

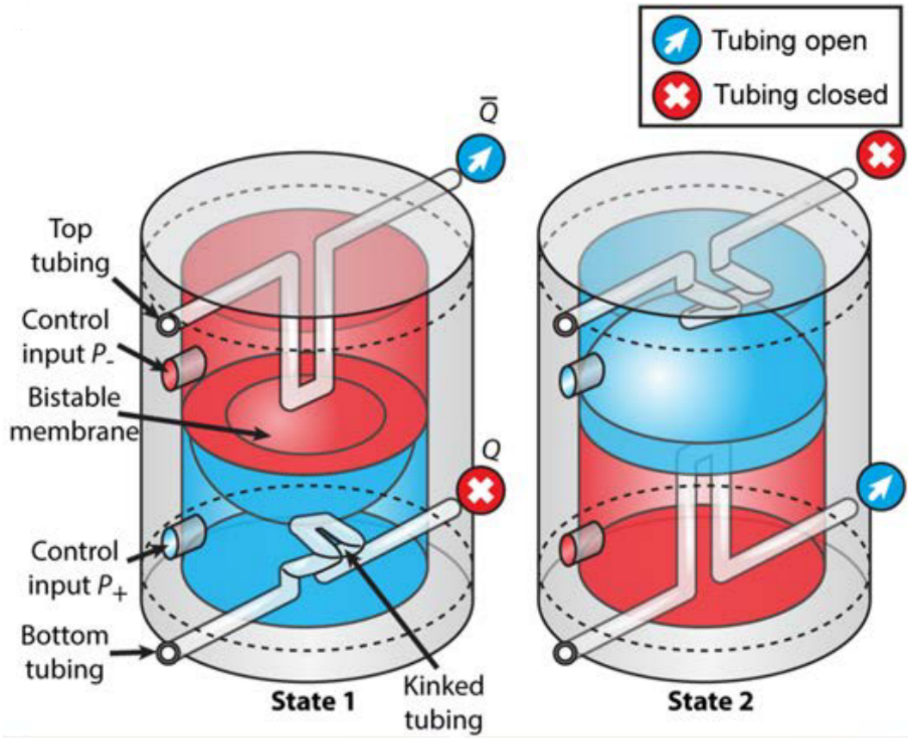


**Figure 2.4.4:** Soft Valve Diagram [43]: State 1 allows flow through the top tubing until Control input $P_+$ is applied at which time snap through of the membrane occurs and the valve transitions to State 2. The top tube is then buckled which causes flow to stop and the bottom tube is relieved which allows flow.

### 2.4.5 Evaluation and Discussion

Of the three oscillator technologies looked at, only the directional control valve and the soft valve are suitable for this project. Doubts with regard to the flow rate achievable using a microfluidic solution does not warrant any further exploration of this technology.

In the preliminary design section the ability of the directional control valve and soft valve to perform the actions of a controller is evaluated and the most promising technology is refined further. The design methodology used to develop and test these technologies must be identified.

## 2.5 Design Methodology

Researching the field of soft robotics it is noted that two design methodologies are commonly followed, namely simulation based design and experiment based design.

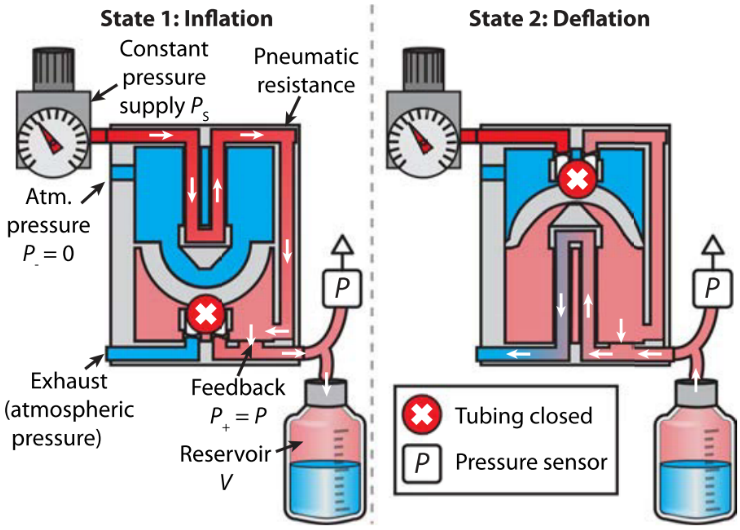


**Figure 2.4.5:** Soft Valve Oscillator Diagram [43]: In State 1 the flow through the top tube increases the pressure of the bottom chamber and the reservoir until critical pressure is reached and snap-through occurs and the valve transitions to State 2. In State 2 the pressure from the chamber and reservoir vents through the bottom tube until a critical pressure differential is reached at which time the membrane snaps back into the initial position.

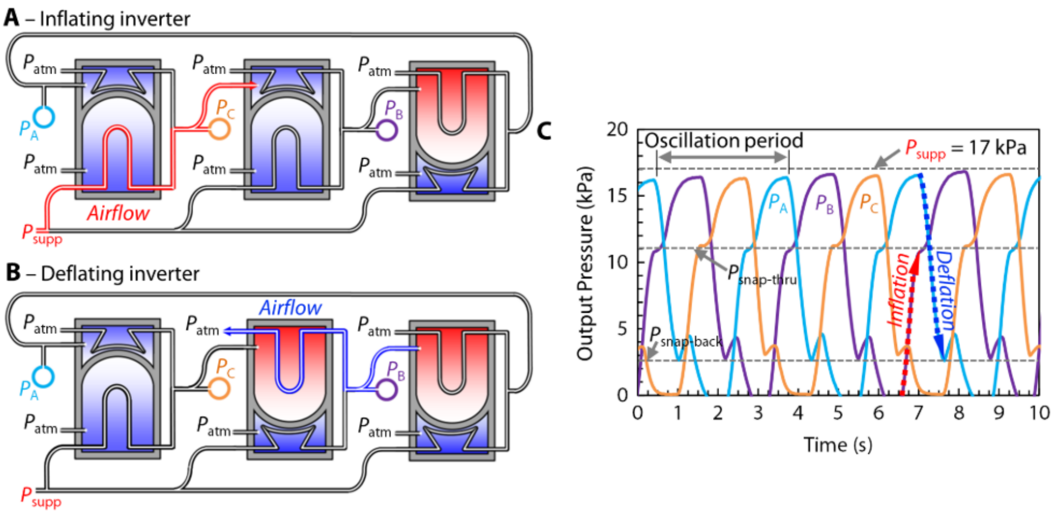


**Figure 2.4.6:** Soft Valve Ring Oscillator Output [44]

### 2.5.1 Simulation Based Design

Simulation based design follows the approach of developing a mathematical or computer based model of a system which is then verified through experiments. This approach is commonly followed in conventional robotic design where the behaviour of the used materials and components are predictable and the physical system is not expected to differ greatly from the simulation. In the soft robotic field simulation based design uses experimental data to verify the accuracy of the material model used in the simulation. This is due to difficulty in developing a material model that can accurately capture the non-linear behaviour of silicone rubbers.

This is shown in [45] where a bending soft actuator for use in hand rehabilitation is modelled using the finite element method (FEM) and compared to experimental data gathered from a manufactured actuator, in order to verify whether the FEM model can be used to accurately predict the bending characteristics of the physical actuator. [17] uses a similar designing method where an SMP is used as a contracting actuator. The contraction rate is defined in a mathematical model and verified with experimental data. [46] and [47] also use experimental data to verify the accuracy of a FEM modelled soft fibre reinforced bending actuator and SMP gripper respectively. [46] also compares the results from an analytical model to the FEM and experimental results.

### 2.5.2 Experiment Based Design

The other common design method is that of experiment based design. This method is used to apply a novel mechanic or material to a use-case and evaluate the functionality of the resulting system. [48] makes use of such a design method to develop artificial muscles driven by the contraction of folded paper in a vacuumed enclosure, as seen in Figure 2.5.1. [48] applies this novel method of contraction to the construction of an artificial muscle and verifies functionality through experimentation. Although values such as the pulling force of the actuator is noted, the aim of the project was to determine feasibility of the novel mechanic.

[27] follows a similar design method to develop a multigait soft robot. A novel design of a five sectioned quadrupedal soft robot was manufactured and tested. The tests were performed to verify whether the arrangement of sections were successful in producing a multigait soft robot.

[43] used a experimental based design approach to develop the soft valve. Alterations to different parameters of the valve were made in order to study the effect of the changes on the functioning of the device.

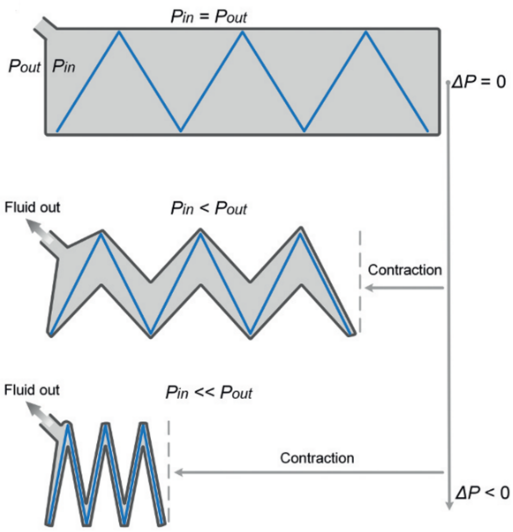


**Figure 2.5.1:** Paper-Based Contracting Actuator: Actuator is seen to be contracting from top to bottom. The difference in air pressure between the external fluid and internal fluid causes contraction [48]

### 2.5.3 Evaluation and Discussion

Simulation based design is a methodology followed when the characterising of a material model is important or when the functionality of the physical system is known to be accurately modelled by either a mathematical or computer model. In the design of a soft controller that makes use of materials with non-linear behaviour where the focused is not placed on the accuracy of the produced system but rather on the functionality of a novel mechanic, it is more applicable to follow a experiment based design. This removes the need to develop an accurate material model and system model, and places emphasis on the functionality of the device. This combines with the rapid prototyping method followed in the project, where prototypes are tested and altered as required until a functional solution is acquired.

## 2.6 Discussion of Literature Review

The literature review provided the identification of the controller type and the soft robotic technology to which it is applied. Along with identifying an oscillator as the type of controller and EIAs as the applicable technology, the identification of the specifications of the operational conditions are defined. The problem is therefore defined as in the conceptual design section of the systems engineering approach, meaning that the literature review is seen as the conceptual design section of this project.

In relation to operating pressures that the oscillator technology will be able to produce, the soft robots of [27], [43], and [44] required pressure inputs ranging from 11 kPa to 130 kPa, while [7] speculated that EIAs are functional for pressure inputs ranging from 20 kPa to 55 kPa, and the pneu-nets of [29] function with pressures from 2 kPa to 60 kPa dependant on material and reinforcements. Therefore, any oscillator that can produce a pressure of above about 5 kPa will be acceptable since EIAs can be designed for a wide range of operating pressures.

From the functioning of CPGs and the type of double actuation required to reproduce the body undulations of a salamander during terrestrial locomotion, the specifications of the output of the oscillator are also defined. The oscillator must produce two positive pressure oscillating outputs from a single, constant positive pressure input. The output pressures must satisfy the operational pressures defined in the previous paragraph.

The frequency of the outputs does not have a defined value, but rather the phase between the two oscillations and the relationship between the frequency and input pressure magnitude is specified. The oscillations must be asynchronous, meaning a phase difference of 180° is required. The output frequency must be linked to the magnitude of the supply pressure in such a way that an increase in supply pressure causes an increase in the output frequency without impacting the phase between the oscillations.

The project is also to follow an experimental design methodology wherein technologies are iterated upon as according to experimental results until functional designs are produced or a design is deemed not appropriate for the application.

# Chapter 3

# Preliminary Design

## 3.1 Introduction

This chapter evaluated the two chosen oscillator technologies identified in the literature review and conceptual design. The technologies were evaluated in regards to their applicability to the chosen soft actuator technology, their suitability to rapid prototyping, and their suitability to being implemented in soft robotics.

With regards to rapid prototyping, the preliminary designs were manufactured using 3D printing technologies. The functionality of the designs using this manufacturing method were evaluated; the manufacturing process must have acceptable tolerances to produce functional oscillators.

The three functional mechanisms that are required to produce a pneumatic oscillator capable of producing two asynchronous outputs for a single constant pressure source are switching, latching, and flow control mechanisms. These functions are critical in terms of functionality. The oscillators are therefore were also evaluated with regards to how well the technologies enabled these mechanisms.

## 3.2 Directional Control Valve

Directional control valves are a widely used pneumatic or hydraulic flow controller that is able to switch a single input pressure between two outputs, this is the type of functionality this project aimed to achieve. A robust solution to the problem addressed in this study was explored through the design of a scaled-down version of a directional control valve that incorporated soft mechanisms and was manufactured using Stereo-lithography Apparatus (SLA) 3D printing. Directional control valves that can deliver functionality that this project aims for, but these solutions do not provide a robust and soft robot focused solution. Therefore, the application of SLA 3D printing to provide a robust and soft robot focused directional control valve solution is explored in this project. SLA 3D printing was selected since it is a technology that is available and delivers printed parts that are more accurate and of higher surface finish quality than conventional fused deposition modelling methods.

The functionality of the scaled-down directional control manufactured with SLA 3D printed parts and the effect of scaling the design down on the required operating pressure was not initially known. The concept was evaluated through testing, to ensure functional switching, latching, flow control at the operational pressures of the scaled-down and 3D printed directional control valve.

In order to design such a scaled-down directional control valve, the components of the valve was split into three segments: the slider and casing, a latching mechanism, and a switching mechanism. These segments are made modular in order to adapt segments without total redesigns.

### 3.2.1 Latching Mechanism

Conventional directional control valves use electromagnets or a system of springs and mechanical or magnetic latches to latch the slider into the correct position, but this requires an input control signal. The design followed in this case makes use of a permanent magnet carefully positioned to create an attractive force to latch a slider into position. Two magnets are used to latch into two different stable positions. The attractive force is matched to the switching force of the switching mechanism.

The magnets used are ring magnets, with inner and outer diameters that integrate with the slider mechanism, which is described in a following section. The ring magnets used are N38 grade, nickel, 11 mm outer diameter, 6 mm inner diameter, and 3 mm thickness neodymium magnets. A graph of the pull away force is shown in Figure 3.2.1, using data from an existing database.

Figure 3.2.1 is used as a reference for the design of the switching and slider modules. The magnet is located on the slider itself, and the steel plate is located in the switching mechanism. The steel plate is located on a screw, to adjust the distance between the plate and the magnet to allow for adjustment in latching force. The latching mechanism is tested along with the switching mechanism in a later section.

### 3.2.2 Switching Mechanism

The switching mechanism is responsible for switching the position of the slider when the controlled actuator has reached the desired pressure. This was done by having a bladder, located between the latching magnet and steel plate, that inflates and pushes the magnetic slider away from the plate to which it is currently latched and towards the steel plate that latches the slider to the other side. The bladder insures that cavity responsible for switching is sealed, reducing the need for the 3D printed parts to be precisely manufactured. The

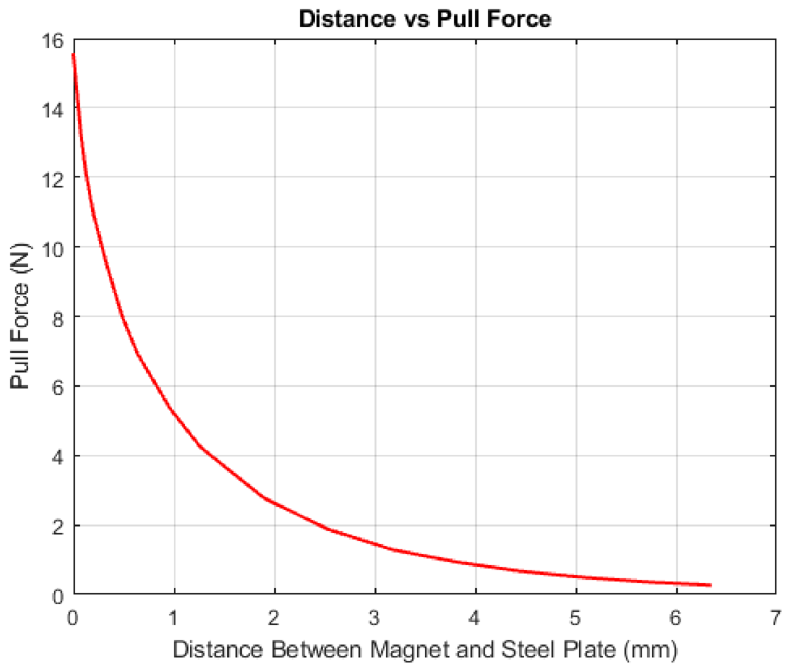


**Figure 3.2.1:** Magnetic Pull Force at Separation Distance

pressurising chamber of the switching mechanism is closed on the side of the steel plate whilst the other face is attached to the slider.

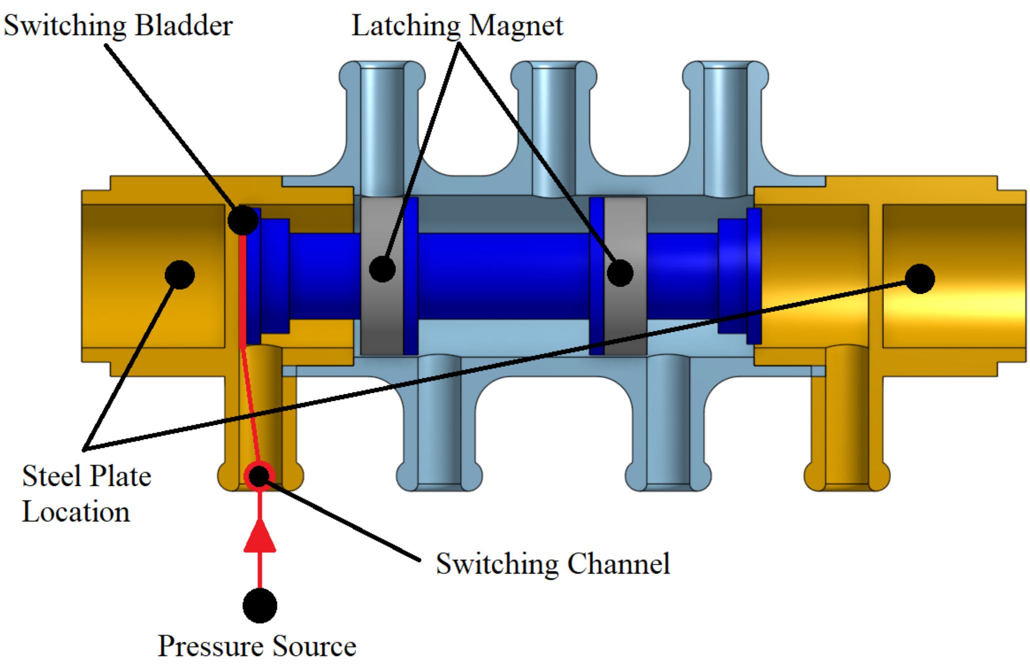


**Figure 3.2.2:** Latching and Switching Mechanisms Test Diagram

### 3.2.3 Slider and Directional Control

The slider along with the directional control module is responsible for directing the flow of the working fluid, locating the latching magnets, and locating one half of the switching module. The directional control module provides channels for input pressure, output pressure, switching pressure, and venting. Figure 3.2.3 shows the directional control valve in one of its operating positions. In the case of Figure 3.2.3, Actuator A is being actuated and on the verge of switching while Actuator B is not connected to the input pressure but is allowed to vent to atmosphere. When the switching module is correctly pressurised, the latching magnet will unlatch and the slider will latch to the opposite side. Then Actuator A will be allowed to vent, and Actuator B will be connected to the input pressure and actuated.

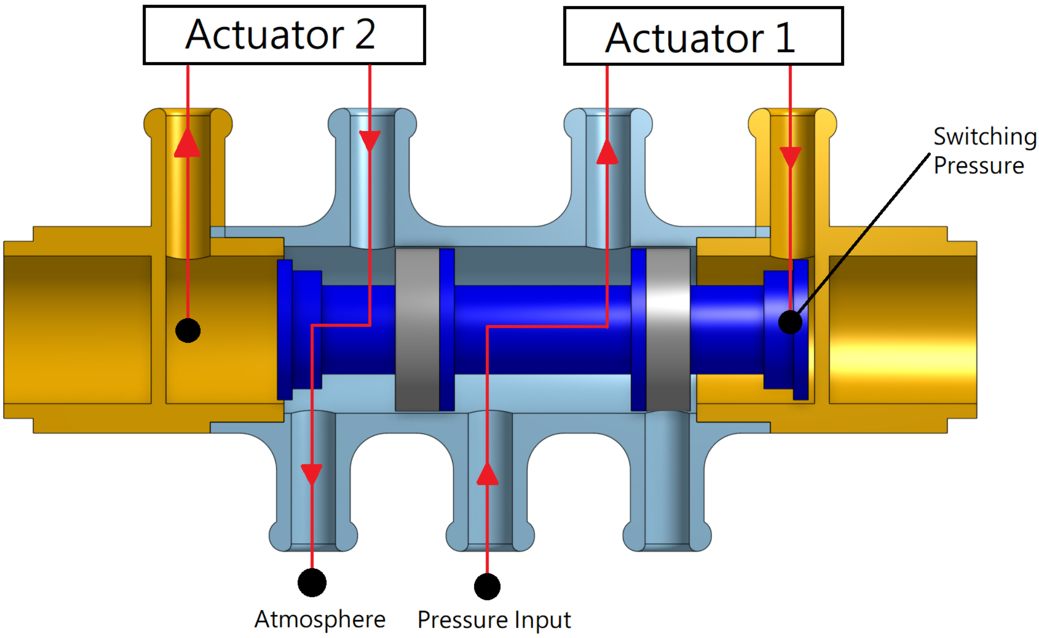


**Figure 3.2.3:** Directional Control Valve in Use

### 3.2.4 Evaluation and Discussion

The valve was manufactured using SLA 3D printing, and balloons were used for the bladder of the switching modules, which provided a cost-effective design that was able to be rapidly iterated on. The minimum distance between the latching plate and magnet could be varied from 3 mm to 15 mm by adjusting the screw and the slider and switching module. This allows for a theoretical latching value of 1.5 N with the currently chosen magnet. Theoretically, the latching value can be increased by using larger magnets and scaling the diameter of the modules up to the accommodate the larger magnet. Two tests were performed to determine the functionality of the switching, latching, and flow control mechanisms.

### Latching and Switching Mechanism Testing

The switching plate is 10 mm in diameter, $D$, and it is assumed that the inflating bladder exerts a force on the complete face of the plate. With the nearest distance the magnet and steel plate are permitted to be from each other being 3 mm, the maximum required switching force is present in this situation. Using equation (3.2.1) and a known pressure, $P$, a theoretical switching force can be determined. For a theoretical relationship between pressure, area and a resulting in a force equation (3.2.1) can be used. Using the situation where the maximum switching force is required, a operational pressure can be determined using equation (3.2.1).

$$F = P \times \pi \times \left(\frac{D}{2}\right)^2 \tag{3.2.1}$$

Using Figure 3.2.1 to determine a maximum switching force of 1.5 N and equation (3.2.1), a theoretical minimum switching pressure at the point of highest required switching force can be determined. A theoretical minimum switching pressure of 19.1 kPa is calculated, which is well within the specified pressure range for EIA applications. The tests are therefore conducted with supply pressures exceeding this value to ensure switching.

The testing setup diagram can be seen in Figure 3.2.2. A pressure source of 20 kPa is connected to the switching channel in order to inflate the switching bladder. The steel plate and magnet are located 4 mm from one another for testing, requiring a minimum theoretical switching pressure of 12.7 kPa.

The test was partially successful. Due to low manufacturing tolerances, the spool is not straight enough to allow smooth translation inside the casing. This causes to spool to jam in the casing and not switch. Rotating the spool into a position that allows smooth translation, the latching and switching mechanism function correctly. The spool switches and latches in the secondary position. More accurate manufacturing techniques will deliver a more functional spool and casing.

### Flow Direction Mechanism Testing

Making use of the directional control setup shown in Figure 3.2.3, the flow control of the directional control valve was tested. This test determines if the design is able to direct flow to inflate a EIA and allow the EIA to deflate when the spool directs the inflated actuator to the venting channel.

Using an input pressure of 20 kPa, the directional control valve initially inflates Actuator 1 and, since the switching mechanism is not being tested, the spool is then manually located to the second position once the actuator is inflated. After the spool is in the second position, it was observed that Actuator 1 started to deflate and Actuator 2 started inflating. When the spool is again returned to the first position, Actuator 2 deflates and Actuator 1 inflates.

During the tests it was noticed that the spool does not translate freely, as expected from the latching and switching mechanism testing. Leaking air was also noted during the initial inflation of Actuator 1, again indicating that the manufacturing accuracy is insufficient for this design due to resulting leakages between the spool and the casing.

#### Discussion

Although functional, the mechanisms are not consistent. The tolerance of the printed parts did not allow for smooth operation, with leakages between the spool and the casing and jamming preventing smooth switching and latching. This design requires another manufacturing technique for further refinement. Therefore the application of SLA printing in producing a variation of directional control valve technology does not produce functional results.

If prefabricated rods and tubes, for the spool and casing respectively, were used during the development of the directional control, the functionality would be increased. The removal of the reliance on the accuracy of the fabrication method is a design choice that will greatly influence the viability of this design. The casing and spool are the components most affected by the tolerance of the fabrication method; the other components that are manufactured by the SLA printer are able to be integrated to system wherein the spool and casing are prefabricated. This option served as a possible solution to the problem of this project if the soft valve technology failed to meet the requirements of the project.

## 3.3 Soft Valve

### 3.3.1 Introduction

The soft valve concept described by [43] is considered for the design of a soft oscillator. In order to use the soft valve as an oscillator, the design must consist of three mechanisms, namely, latching, switching, and flow control mechanisms. The flow control mechanisms are the elastomer tubes that buckle to block the flow, the switching mechanism is the membrane that snaps to either side dependant on the side of the membrane that is pressurised and the latching mechanism is the bistability of the membrane. The membrane was thus designed with both bistability and snap-through behaviour in mind.

### 3.3.2 Flow Control Mechanism

The elastomer tubes used to evaluate the soft valve are Smooth-Sil 950 silicone tubes with an inner diameter of 2 mm and an outer diameter of 5 mm. For initial testing of this concept the tubes are cut to a length of 30 mm to accommodate the full stroke of the membrane described later.

### 3.3.3 Bistable Membrane

The elastomer membrane in [43] is dome-shaped to allow for a snap-through instability, with the snap-through occurring at the switching pressure. The switching pressure for either side of the membrane is not the same. When the membrane is snapped-through from the state it was cast in, there are internal and surface stresses along the membrane that want to return the membrane to its original state. These stresses cause a difference in the pressure required to snap-through the membrane from its original position, and the pressure needed to snap it back to its original position. The position the membrane is cast in is seen as the initial position. This position is more stable than the opposite, or deformed, position. In Figure 3.3.1 the bias towards the initial membrane position can be seen at point A where the switching pressure is reached to snap from the initial position to the opposite side. The pressure at point A is greater than the pressure at point B where the membrane snaps back to the initial position.

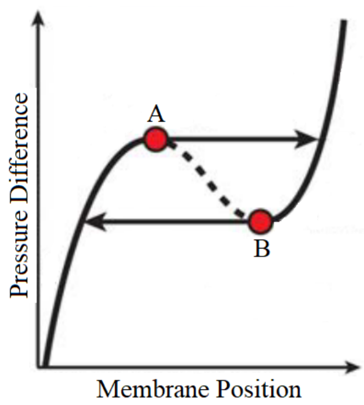


**Figure 3.3.1:** Membrane Stability Diagram

The dome shape of [43] was altered for this initial evaluation to a cone-shaped membrane. The shape change is believed to provide a smaller difference in the two snap-through pressures, making the deformed position more stable. An illustration of the two shapes is shown in Figure 3.3.2, with the dome on the right and the cone on the left. The thin hinges are chosen to reduce stresses where large strains occur, and increase stability. For the preliminary testing, the angle of the cone is initially chosen as 45°, with a thickness of 2 mm, and an outer diameter of 40 mm. According to [49] changing the scale of the soft valve, in a reasonable way, does not influence the functioning, therefore the increase from 20 mm to 40 mm is done to ease manufacturing.

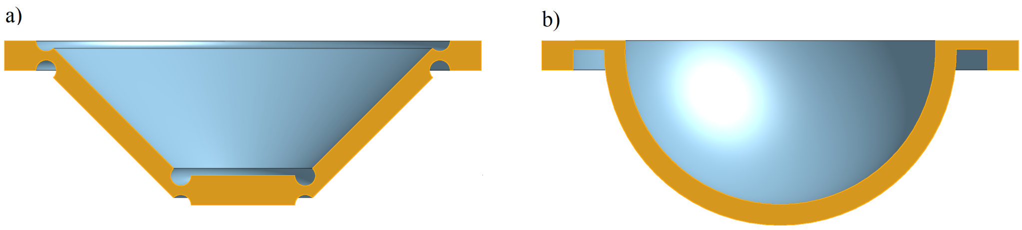


**Figure 3.3.2:** Membrane Shape Comparison

The last component of the soft valve is the wall of the valve. The wall creates the chambers that are pressurised for snap-through and also reinforces the membrane. The thickness of the walls increases the snap-through pressure by increasing the amount of material the membrane must displace to snap-through. A 3 mm wall thickness is used for this concept evaluation, as this is comparable to the valve of [43]. The dimensions of the soft valve used for concept evaluation are given in Table 3.3.1.

**Table 3.3.1:** Dimensions for Soft Valve Used for Concept Evaluation

| **Dimension** | **Value** |
|---|---|
| Wall Thickness | 3 mm |
| Membrane Diameter | 40 mm |
| Membrane Thickness | 2 mm |
| Membrane Angle | 45° |
| Tube Outer Diameter | 5 mm |
| Tube Inner Diameter | 2 mm |

## 3.3.4 Evaluation and Discussion

### Latching and Switching Mechanism Testing

The latching and switching mechanisms of the soft valve are performed by the membrane of the valve. For the latching mechanism to be functional the membrane of the soft valve must be able to passively maintain position in either of the two states. The switching mechanism is enabled by the ability of the membrane to snap-through to either of its stable states when pressurised. These mechanisms are simultaneously tested.

The test was performed by having one side of the membrane open to the atmosphere while the other is sealed and exposed to a steadily increasing pressure, until the critical pressure at which the membrane snaps from one stable position to the other. The pressure at which snap-through occurs was recorded, and the valve is allowed to depressurise. It is also noted that when the membrane switches sides a popping sound is heard, further confirming the snap-through mechanic of the membrane. After the membrane is depressurised, the state of the membrane was recorded to ensure that no passive snap-back occurs.

The test was repeated three times for both sides of the membrane and average critical pressure values used for the final switching pressure. The snap-through pressures for the membrane are shown in Table 3.3.2. These values show that the conical membrane has two stable states that can be switched between by exposing one of the sides of the membrane to a critical pressure. Therefore, the latching and switching mechanisms are functional.

**Table 3.3.2:** Snap-Through Pressures for Concept Evaluation

| **Action** | **Average Pressure (kPa)** |
|---|---:|
| Snap to Initial Position | 5.13 |
| Snap to Deformed Position | 1.27 |

### Flow Control Mechanism Testing

The tubes were tested to see if buckling the tubes produced a seal that does not leak under pressurised conditions equal to or greater than the highest snap-through pressure of the latching and switching mechanism test.

A pressure of 20 kPa was supplied to one end of the tube and the tube was then buckled to confirm if flow through the tube is blocked by the obstruction caused by buckling. For preliminary testing purposes, Smooth-Sil 950 silicone tube lengths of 40 mm to 25 mm in 5 mm intervals were tested. The tubes were pressurised and buckled. If the flow is blocked the length of the tube at which flow is blocked is measured and is referred to as the critical length.

All lengths of tubes tested were able to block flow once buckled. The results in Figure 3.3.3 show the critical lengths of the different tubes tested.

### Discussion

The tests performed on the membrane and tubes establish that these components deliver functional switching, latching, and flow control mechanisms. These components are manufactured using 3D printed SLA moulds, indicating that this method of manufacturing is viable. The tubes are able to maintain a seal.

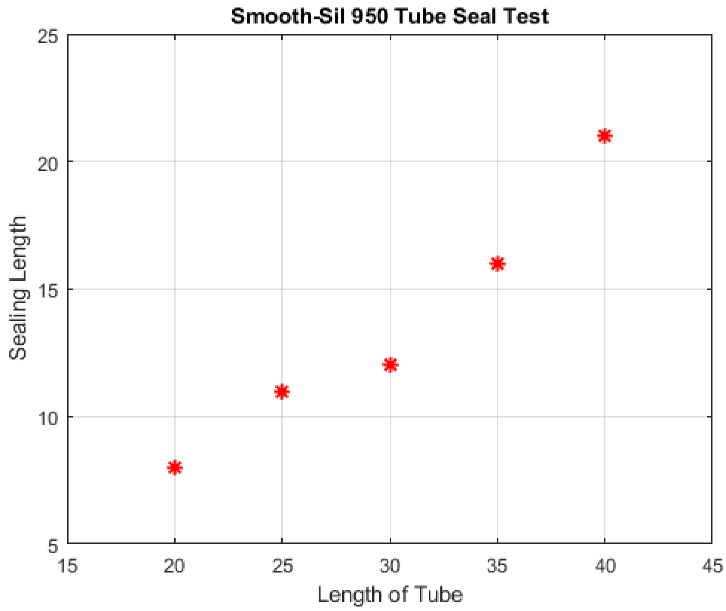


**Figure 3.3.3:** Smooth-Sil 950 Tube Seal Tests

## 3.4 Preliminary Design Discussion

Of the two designs considered, the soft valve is more promising. The switching, latching, and flow control mechanisms of the directional control valve do not function effectively due to the manufacturing technique not producing parts of an acceptable quality. In order to improve the functionality of the design, a different manufacturing process which does not align with the rapid prototyping specification of the project must be used .

The soft valve design is functional with regards to latching, switching, and flow control. The components are functional whilst making use of a manufacturing technique frequently used for rapid prototyping. Along with the functionality of the soft valve mechanisms, the entire silicone composition of the soft valve makes it very favourable in terms of cost and available facilities. The soft valve is chosen for further development for the design of a soft pneumatic oscillator.

# Chapter 4

# Detail Design

## 4.1 Introduction

This section covers the design and manufacturing processes followed to result in a functional soft pneumatic oscillator. The design and manufacturing processes of the tubes and the membrane are followed by the integration of the two parts into a functioning oscillator.

## 4.2 Tube Design, Manufacturing, and Testing

There are many design parameters to consider for the internal tubes of the soft oscillator. The diameter, wall thickness, length, and material are design choices that influence the sealing length, and the quality of seal. These parameters have a drastic effect on the functionality of the soft oscillator. This section explores the methodology followed to select the dimensions and material for the tubes of the oscillator.

The diameter and wall thickness of the tubes and the material of the tubes have a relationship in the the resulting buckling distance and and quality of seal of the tubes. Theoretically a certain diameter and wall thickness of tube has a material that will result in an functional buckling tube. The diameter and wall thickness of the tubes were therefore kept constant for all testing purposes and the material was varied. This also reduces the amount of moulds that were manufactured, adhering to the financial constraints of the project.

### 4.2.1 Tube Material

The material selection for the tubes was determined from the available materials, their effectiveness in sealing when buckled, and the required buckling force. Two different silicone rubbers were considered, namely Smooth-Sil 950 and Mold Star 30, with Shore hardness ratings of 50A and 30A respectively. This provides examples of soft and medium materials as in Figure 4.2.1. More information regarding the silicone is found in Appendix B. The silicone rubbers are evaluated in relation to their buckling force and sealing length.

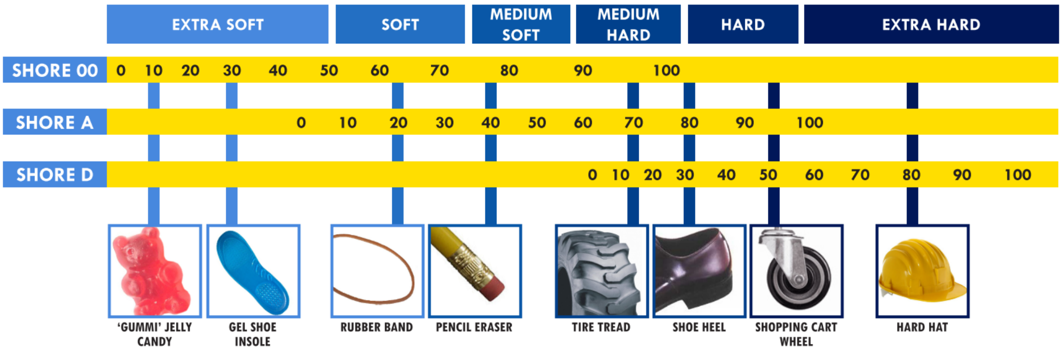


**Figure 4.2.1:** Shore Hardness Scale [50]

### Silicone Preparation Process

All silicone rubbers used are two-part platinum silicone rubbers that cure at room temperature, therefore the preparation process includes measuring, mixing, and vacuum degassing. The measuring process differs for each silicone since the ratios of the two parts required for each silicone differs, therefore the prescribed ratios are measured in to deliver the desired final volume of silicone. After measuring the correct ratios of the two parts, they are thoroughly mixed together. After mixing, the silicone are degassed at a vacuum close to negative one atmosphere until no more bubbles are visible on the surface of the silicone, thereafter the silicone is ready for pouring. After pouring the silicone is left to cure for the prescribed curing time.

## 4.2.2 Tube Diameter and Wall Thickness

The manufacturing process of the tubes need to be considered when designing the tubes to reduce the needs for specialised parts. The wall thickness needs to be thin enough to reduce the buckling force required and thick enough to stay robust and allow buckling. Wall thickness between one and two millimetres was considered.

The outer diameter of the tubes was determined by considering the available pneumatic equipment. In order to simplify later testing an outer diameter of five millimetres was selected as this allows for easy connection to existing equipment and is sufficiently small to stay robust.

The chosen outer diameter required an inner diameter between one and three millimetres. This was achieved by using 12 gauge wiring as a core, with a diameter of 2.06 mm. This provided a wall thickness of 1.47 mm. The chosen dimensions are shown in Table 4.2.1.

**Table 4.2.1:** Tube Dimensions

| Dimension | Value (mm) |
|---|---:|
| Outer Diameter | 5 |
| Inner Diameter | 2.06 |
| Wall Thickness | 1.47 |

### 4.2.3 Tube Manufacturing

The tubes are manufactured using a stereolithography (SLA) printed split mould. More information regarding the printer and resin used is found in Appendix A. This printing technology was chosen due to both the availability of the technology and the precision in comparison to fused deposition modelling (FDM) printing. The two side moulds are responsible for the outer diameter and the inner diameter is created by the 12 gauge wiring that is located by a cap. An illustration of the mould assembly along with the labelling of the parts is shown in Figure 4.2.2, with the wires in various states of insertion and one of the sides removed. The mould produces eight 50 mm in length tubes at a time. Computer aided design (CAD) drawings of the spilt moulds and the cap used to manufacture the tubes are found in Appendix H.

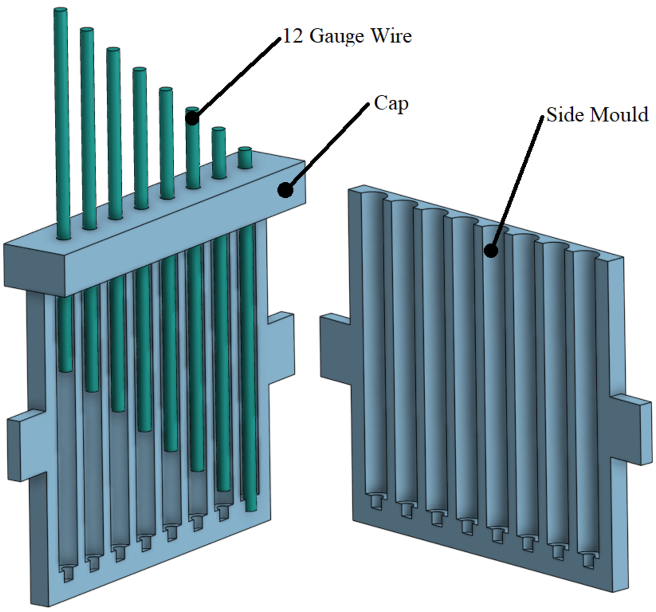


**Figure 4.2.2:** Tube Mould Assembly

### Manufacturing Process

After the silicone was prepared, the two side moulds were fixed together with insulation tape and aligned using the protrusions on each side. The silicone was then injected into the holes using a syringe filled with the chosen silicone, the holes were filled three-quarters of the way. After filling, the cap was placed and each wire was inserted one at a time. This allowed overflow if the mould is overfilled. The process is illustrated in Figure 4.2.3. The mould was kept upright while curing. After curing, the wires were removed first, followed by the cap and then the tape. The two side moulds are separated, and the tubes are extracted. Any cured overflow silicone was removed and the inner diameter was checked for concentricity.

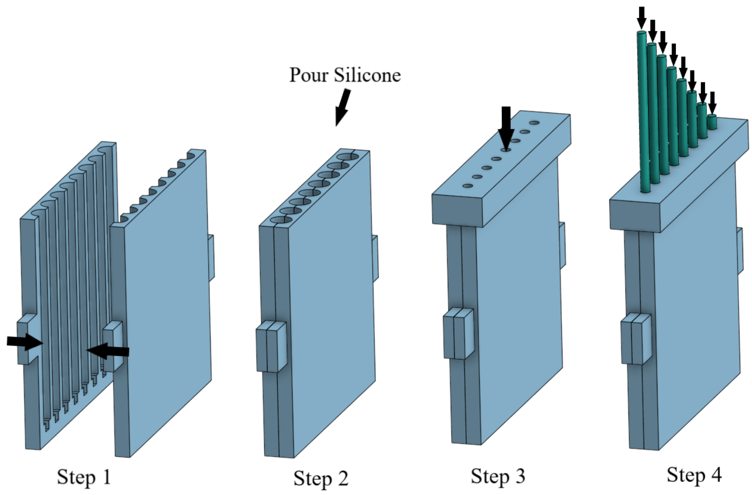


**Figure 4.2.3:** Tube Manufacturing Process: Step 1: Align and tightly secure the split moulds, Step 2: Pour silicone into the tube cavities, Step 3: Place the cap onto the split mould securely, Step 4: Insert the wires one-by-one allowing excess silicone to spill out of open holes

## 4.3 Tube Length and Critical Length

There were two important lengths to consider during the design of the tubes, namely the overall length and the buckled length at which the tube stops airflow, referred to as the critical length. The length of the tube has an effect on the critical length, the relation to between the two was experimentally determined. Since the required lengths of the tubes were not known, a maximum length that still allowed for buckling and sealing was determined along with the critical lengths.

### Tube Testing Methodology and Results

A decision was made to limit the maximum length of the tubes to 40 mm and the minimum to 20 mm, as these are the boundaries at which the tubes consistently sealed when buckled. The experiment for determining the critical length was performed by connecting one end of a tube to a pressure source, fully constraining one end and allowing the other end to translate along the tube axis, and bringing them closer together until the airflow stopped. A diagram showing the setup and measuring positions, with the initial position in a and the critical length in b, is shown in Figure 4.3.1. The length of the tube at which airflow stops was recorded and referred to as the critical length. Tests were done for tube lengths 40 mm to 20 mm in 5 mm intervals. The critical length for a given tube length is shown in Figure 4.3.2. This data did provide a set tube length but will help identify an acceptable length when the parameters of the membrane is known.

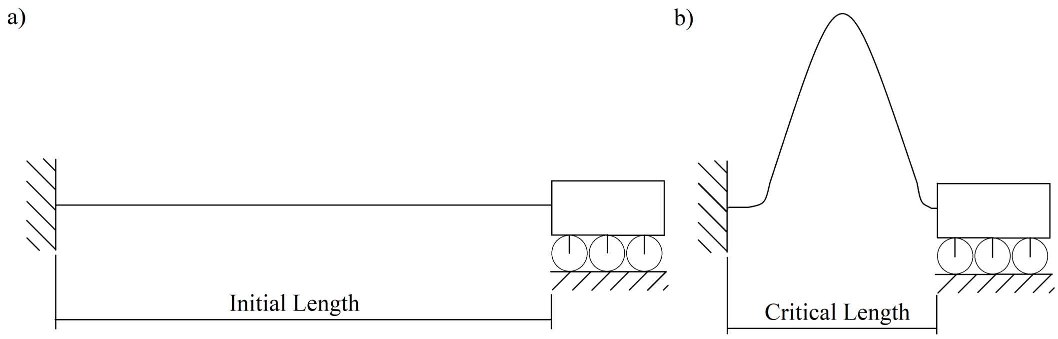


**Figure 4.3.1:** Critical Length Test Setup

The dimensions of the tubes are determined as shown in Table 4.2.1, and a reference for choosing a functional tube length is given in Figure 4.3.2. This information was invaluable in integrating the tubes into the rest of the soft oscillator, as the parameters and their effects are known. The choice between a harder or softer tube was made when their interaction with the membrane was defined.

## 4.4 Membrane Design, Manufacturing, and Testing

The design of the membrane is crucial because this mechanism is responsible for both switching and latching. The manufacturing technique was also important, as simplifying this allowed for a more efficient iterative design process. The design choices, manufacturing processes, and their evaluations are covered in this section.

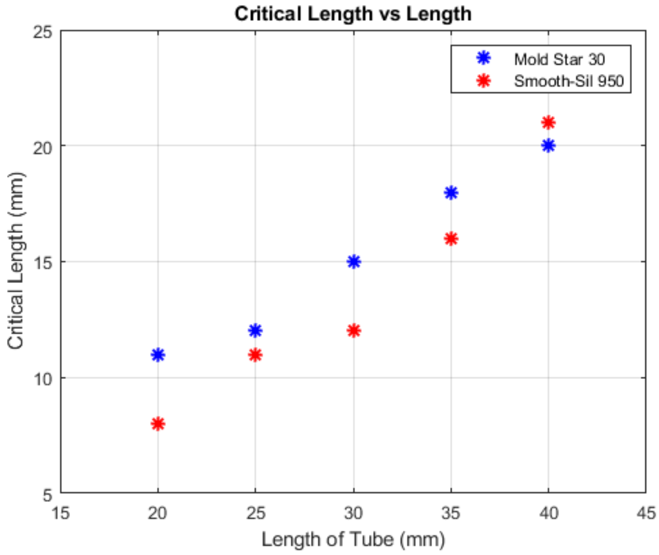


**Figure 4.3.2:** Critical Length Versus Length

## 4.4.1 Membrane Design

The parameters that need to be considered for the design of the membrane are the diameter, thickness, material, hinge, geometry, and slope of the membrane. These parameters all have an effect on the bistability, the snap-through behaviour of the membrane, and the tube length selection.

### Membrane Diameter, Slope, and Wall Length

The membrane slope and diameter determine the actuation distance of the membrane and therefore are also responsible for determining the length of the tube required. A larger diameter with a given slope increases the length of the tube needed.

The slope of the membrane is also a contributing factor to the bistability of the membrane, with a steeper slope requiring more compression of the membrane to snap-through. The increased stability caused by a greater slope also increases the pressure at which the membrane switches. The two pressures at which the snap-through and snap-back motions of the membrane occurs are referred to as the critical pressures. The slope of the membrane is defined as the angle between the slanted wall of the membrane and the horizontal plane. The measurement of the slope dimension is illustrated in a sectioned view of the membrane in Figure 4.4.1.

For testing, a baseline slope was chosen as 45°and the influence of a smaller slope, chosen as 30°, was analysed by comparing the critical pressures of a Mold Star 30 and Smooth-Sil 950 membrane with each of the two slopes. A three-run average value for the critical pressures is shown in Table 4.4.1. Critical pressure 1 refers to the critical pressure required to switch the membrane from its original shape to the deformed state, and critical pressure 2 is the pressure required to switch back. For these tests, a membrane diameter of 40 mm is used, and a membrane thickness of 2 mm is used.

The results of Table 4.4.1 show that a smaller slope decreases the critical pressure. The lowered critical pressures for the 30° cases are neither an advantage or disadvantage in the general sense, but may be important for the operating pressure of a given EIA. For this project it is advantageous for the two critical pressures to be near equal, as the bending actuators will have operating pressures nearer one another. As critical pressures 1 and 2 will be the two operating pressures for the connected two EIAs, more equal pressures will produce a more symmetric actuator output.

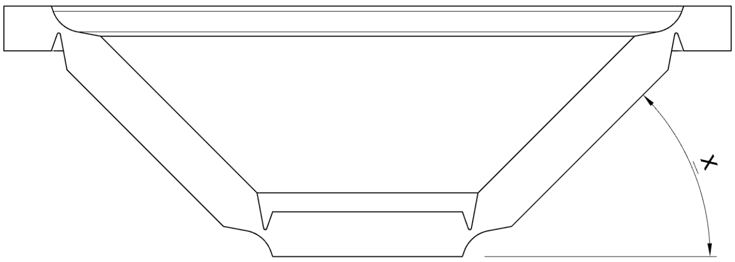


**Figure 4.4.1:** Membrane Slope Diagram

**Table 4.4.1:** Slope and Critical Pressure Relationship

| Membrane Designation | Critical Pressure 1 | Critical Pressure 2 |
|---|---:|---:|
| 30° Smooth-Sil 950 | 4,51 kPa | 1.66 kPa |
| 45° Smooth-Sil 950 | 5.81 kPa | 3.92 kPa |
| 30° Mold Star 30 | 2.08 kPa | 0.64 kPa |
| 45° Mold Star 30 | 5.13 kPa | 1.27 kPa |

Another influence of the membrane slope, is the stroke, $S$, of the switching membrane. The stroke of the membrane is the distance either side of the membrane's horizontal tips travels when the membrane switches sides. The stroke of the membrane influences the chosen length of the buckling tubes used. Figure 4.4.2 shows a sectioned view of a soft valve with an arbitrary slope and wall length. From Figure 4.4.2 it is seen that for a given wall length, the stroke influences the elongated and buckled length of the tubes.

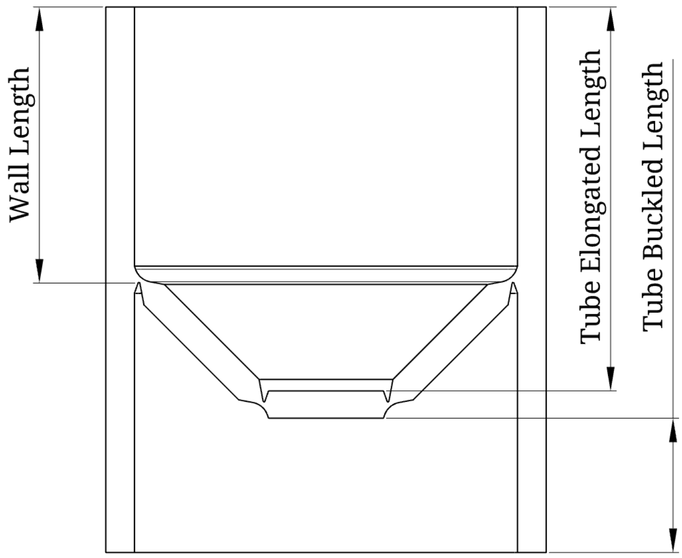


**Figure 4.4.2:** Wall Length and Stroke Illustration

$$\begin{aligned} &L_{\text{wall}} < L_{\text{critical}} < L_{\text{elongated}} \\ &L_{\text{elongated}} \leq L_{\text{tube}} \\ &L_{\text{wall}} \geq \frac{S}{2} + 5\ mm \end{aligned} \tag{4.4.1}$$

Equation (4.4.1) gives the criteria for the selection of tube and wall lengths, $L_{\text{tube}}$ and $L_{\text{wall}}$ respectively, based around the tube critical length, $L_{\text{critical}}$. The criteria ensure that a tube's length and critical length only allows flow when the membrane has snapped through. This prevents the inflating side of the membrane to start venting before the membrane has snapped through.

From Figure 4.4.2 and equation (4.4.1) it is seen that the stroke of the membrane influences the length window for the tube critical length, with a smaller stroke decreasing the window size and a larger stroke increasing the window size. The window of allowable critical length lies between the wall length and the elongated length of the tube, $L_{\text{elongated}}$. The length of the tube must then be greater or equal to the elongated length of the tube, where the elongated length may not always be the maximum length of the tube but rather any length greater than the critical length which allows flow through the tube.

The criteria for the wall length allows for a distance wherein the buckled tube can lie without pressing against the membrane, which may cause the membrane to be slightly switched. This safety length has been chosen as 5 mm. The wall length is adjusted to make a certain length of tube viable.

The critical length of a given tube can be moved into the acceptable length window by changing the length of the wall.

### Membrane and Hinge Geometry

The chosen membrane for this project is cone-shaped since this shape provides a bistable design. Along with bistability, the membrane provides a flat surface for the tubes to be fixed to. A notable difference between the design of this oscillator and the soft valve of [43], is that the tubes do not form a u-shaped bend but are rather two separate tubes that are fastened to the membrane. The flat surface for fastening provided by the cone shaped membrane is more applicable. The diameter of the flats will be large enough to accommodate the two tubes fastened to it.

Another important geometry consideration is the shape of the hinges of the membrane, with the hinge areas highlighted in Figure 4.4.3. The hinges are assumed to be the material between the wall and the membrane and the flat and the membrane. The hinges undergo a great amount of strain when the membrane switches from the initial stable state to the second stable state, therefore the material above and below the neutral axis experience compressive and tensile stresses. These compressive and tensile stresses reduce the stability of the second state, where a large magnitude of stress will cause the second state to be unstable. Therefore, the design is only bistable if the geometry of the hinges produce stresses that allow the membrane to exist in two stable states.

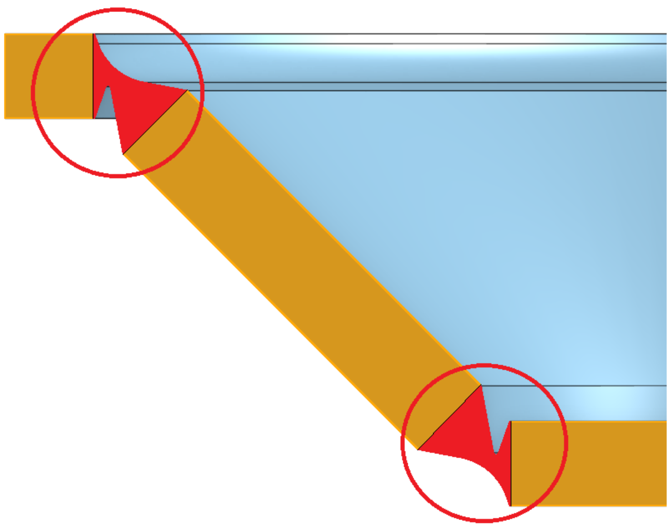

**Figure 4.4.3:** Membrane Hinge Illustration

In order to study the effects of bending on the hinges undergone by switching initial and second positions, the hinge is modelled as a cantilever beam experiencing a moment load shown in Figure 4.4.4. The fixed end of the model represents the horizontal, vertical, and rotational constraints the wall of the soft valve places on the hinge. The free end of the beam represents the attachment to the membrane where the rotation of membrane from the initial state to the second state causes a moment load. The hinge that connects the membrane to the flat undergoes the same amount of bending as the other hinge, therefore the conclusions drawn also apply although the edge supports may differ if modelled.

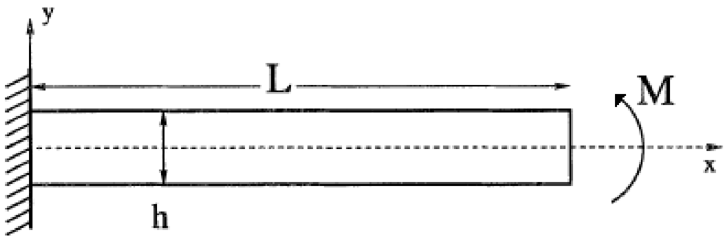


**Figure 4.4.4:** Cantilever Beam Model of Hinge

The beam used to model the hinge is assumed to have a constant thickness, $h$, equal to that of the thinnest part of the hinge with the centroid and normal axis along the centre of the thickness of the beam. As seen in Figure 4.4.5, a beam of original length, $L$ shown equation (4.4.2), subjected to a moment load, $M$, causes bending which in turn causes an elongation of the bottom of the beam and compression of the top of the beam. The changed length of the beam, $L(y)$ at a position $y$ is found using equation (4.4.3), where $r$ represents the radius of curvature and $\theta$ the angle of the arc. With strain being defined as the fractional change of length, the strain along the beam's length, $\varepsilon$, at a position $y$ is determined using equation (4.4.4).

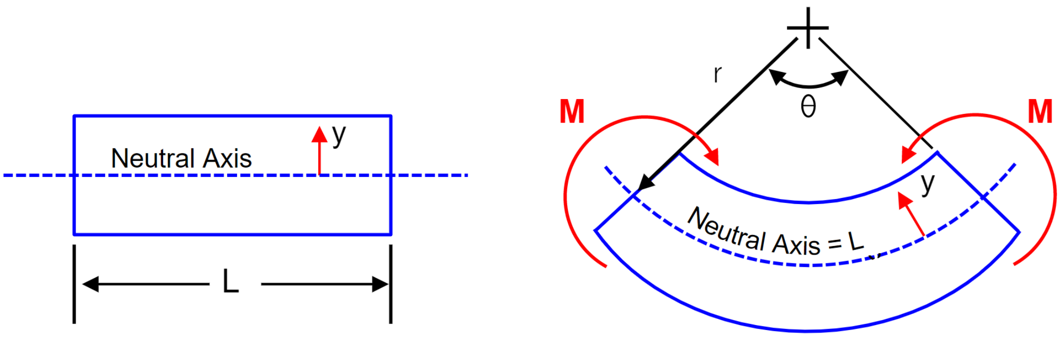


**Figure 4.4.5:** Beam Bending Resulting Strain

$$L = r\theta \tag{4.4.2}$$

$$L(y) = (r - y)\theta \tag{4.4.3}$$

$$\varepsilon = \frac{L(y) - L}{L} = \frac{(r - y)\theta - r\theta}{r\theta} = -\frac{y}{r} \tag{4.4.4}$$

Assuming the hinge undergoes only elastic deformation, the stress in the beam is determined by applying Hooke's Law, shown in equation (4.4.5) with $E$ referring to the Young's modulus of the material, to equation (4.4.4). The stress along the length of the beam, $\sigma$, is calculated using equation (4.4.6).

$$\sigma = E\varepsilon \tag{4.4.5}$$

$$\sigma = -\frac{Ey}{r} \tag{4.4.6}$$

Equation (4.4.6) is used to conclude that for a given material and deformation, the stress in the hinge is reduced by decreasing the thickness of the hinge or by an increase in radius of curvature. Since the radius of curvature is determined by the slope of the membrane, it is considered as a fixed value for hinge thickness determination. The maximum strain, and therefore stress, is experienced on the outer surfaces of the hinge where $y$ is equal to half the thickness of the hinge. The maximum strain and stress are given in equation (4.4.7) and equation (4.4.8) respectively. From these equations it is seen that any fraction reduction in the thickness of the hinge will reduce the strain and the stress by that same fraction.

$$\varepsilon_{\text{max}} = -\frac{h}{2r} \tag{4.4.7}$$

$$\sigma_{\text{max}} = -\frac{Eh}{2r} \tag{4.4.8}$$

The thickness of the hinge is therefore limited by the ability to remain functional during exposure to the the operating pressure of the membrane. At the operation pressure, the hinge must be able to withstand the vertical en horizontal forces caused by the membrane. There is accordingly a range of functional hinge thickness values. The upper bound is a hinge thickness resulting in stresses that are too large to allow bistability and the lower bound is a hinge unable to withstand the forces exerted by the pressurised membrane.

If the hinge fails to vertically locate the membrane under operational conditions, it is assumed to fail due to shear stress caused by the vertical component of the force caused by the pressure experienced by the membrane. The horizontal component of the resulting force is supported by both the wall and the membrane whilst the hinge is the only component that resists the vertical force, therefore the vertical shear stress experienced by the hinge is assumed to be dominant.

The hinge is modelled as a three-dimensional rectangular cantilever beam subject to a vertical shear force. The width, $b$, of the beam is equal to the outer circumference of the hinge and the thickness, $h$, equal to that of the thinnest section of the hinge. The resulting vertical reaction force due to operation pressure is given as $V$. The shear stress, $\tau$, as a result of a shear force in a beam is given in equation equation (4.4.9), where $Q$ is the maximum first moment of area, $V$ is the shear force, and $I$ is the moment of inertia of the cross section.

$$\tau = \frac{VQ}{Ib} \tag{4.4.9}$$

The maximum first moment of area and the moment of inertia of a rectangular beam is shown in equation (4.4.10) and equation (4.4.11) respectively.

$$Q = \frac{bh^2}{8} \tag{4.4.10}$$

$$I = \frac{bh^3}{12} \tag{4.4.11}$$

Substituting equation (4.4.10) and equation (4.4.11) into equation (4.4.9), gives the maximum shear stress experienced by the beam, $\tau_{\max}$, which is shown in equation (4.4.12).

$$\tau_{\max} = \frac{V\frac{bh^2}{8}}{\frac{bh^3}{12}b} = \frac{3V}{2bh} \tag{4.4.12}$$

From equation (4.4.12) it can be concluded that the only dimension that can influence the ability of the hinge to withstand the operational pressure is the thickness of the hinge, since the operational pressure, membrane geometry and slope, and wall diameter are fixed values during the design of the hinge. Therefore, when failure of the hinge to vertically locate the membrane occurs during testing, the thickness of the hinge must be increased.

In conjunction with having thin hinges, the material around the hinges must be designed so that there is no interference when the membrane snaps between positions. There must be clearance between the material making up the slope of the membrane and the material that joins with the wall. The hinge design used to provide both clearance for bending and for the use of thin hinges is shown in Figure 4.4.3, highlighted in red. A CAD drawing with the dimensions of the membrane hinges is found in Appendix H.

The improved membrane hinge geometry was tested for the new critical pressures, which are given in Table 4.4.2. The increase in critical pressure values shows an increase in bistability.

**Table 4.4.2:** Slope and Critical Pressure Relationship For Improved Hinge Design

| **Membrane Designation** | **Critical Pressure 1** | **Critical Pressure 2** |
|---|---:|---:|
| 45° Smooth-Sil 950 | 15.72 kPa | 7.17 kPa |
| 45° Mold Star 30 | 5.12 kPa | 2.29 kPa |

### Membrane Thickness and Material

The membrane thickness and material both have an effect on the bistability, snap-through, and switching pressure. The membrane undergoes deformation from the initial state to the second state. This causes tension and compression stresses either side of the neutral axis of the membrane. Since the membrane thickness and material is chosen before the hinge is designed, the thickness and material can be altered. Therefore it is important to know the relationship between the two attributes.

Hooke's law states the relationship between stress and strain, assuming no plastic deformation takes place. Therefore equation (4.4.5) can be used as guidance for membrane thickness and material choice. A thicker membrane will lead to more strain which results in a higher stress. This leads to a reduction in stability in the second state. However, the stress can be reduced for a certain thickness by making use of a material with a smaller Young's Modulus, as seen in the relationship given by equation (4.4.5). Therefore, a functional combination of the membrane thickness and material exists.

The upper functional bound of the relationship constitutes a combination where the material and thickness result in stress to high to allow for a second stable state, due to either a material with too large a Young's modulus or too high a strain as a result of too thick a membrane.

The lower functional bound of the constitutes a combination where the material and thickness result in a membrane that does not allow for the existence of a second stable state or a membrane that does not exhibit snap-through.

### Membrane Specification

The chosen membrane specifications are given in Table 4.4.3 with the corresponding dimension locations shown in Figure 4.4.6. These specifications provide a bistable membrane, with flexible hinges. The thickness has been chosen as it provides both bistability, a snap-through mechanism, and a desirable operating pressure. The wall length is chosen to allow for the selected tube length of 40 mm. A Mold Star 30 tube of this length has a critical length of 20 mm, which allows compliance to Equation 4.4.1 with a critical length between wall length and elongated length of the tube.

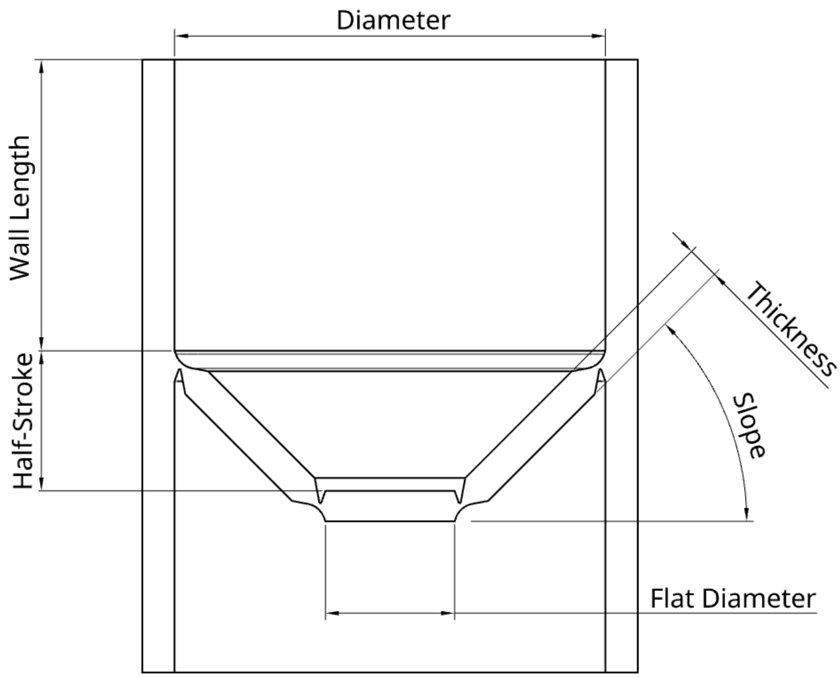


**Figure 4.4.6:** Membrane Dimension Illustration

## 4.4.2 Wall Thickness

The wall thickness is another parameter that influences the critical pressure of the membrane by altering the amount of material the membrane must displace during switching, as seen in [49]. The influence of this parameter is noted, but due to many available parameters that also influence the critical pressure, the

**Table 4.4.3:** Membrane Specifications

| **Parameter** | **Value** |
|---|---:|
| Thickness | 3 mm |
| Slope | 45° |
| Diameter | 40 mm |
| Flat Diameter | 12 mm |
| Material | Smooth-Sil 950 |
| Wall Length | 18 mm |
| Half-Stroke | 13 mm |

wall thickness is chosen as 3 mm to reduce the number of variables that require altering to tune the critical pressure. Adjustment in the wall thickness would also require the printing of new moulds, which needlessly increases costs.

### 4.4.3 Membrane Manufacturing

The membrane and the walls are manufactured as one piece, making use of 3D printed moulds. The moulds are a four-part mould, where two parts make up the cylindrical shape of the walls and the other two are top and bottom inserts that form the cavities of the valve and the shape of the membrane. The design allows for the use of the two wall forming moulds with any inserts that make adaptations on the membrane shape, allowing for a reduction in printing resin use and for faster prototyping.

One half of the mould that forms the outer diameter of the wall is shown in Figure 4.4.7. Two of these moulds are used to form a hollow cylindrical mould in which the inserts that shape the cavities and membrane are inserted. The slit in the top overhang visible in Figure 4.4.7 c) provides a channel for excess silicone to pour out in the manufacturing procedure.

The bottom and top inserts responsible for the creation of the cavities and the shape of the membrane are shown in Figures 4.4.8 and 4.4.9 respectively. These parts are the negative of the membrane design shown in Figure 4.4.6. The slit in the top overhang of the top insert of Figure 4.4.9 lines up with the slit of the outer diameter mould for excess silicone draining. Considering the use of an SLA 3D printer, the parts were designed to have walls that are as thin as possible, the inserts were therefore hollowed out, as seen in the sectioned view of both inserts of Figure 4.4.10. This approach reduced the printing time and costs, therefore also easing the iterative design process. CAD drawings of the outer diameter mould and the bottom and top inserts are found in Appendix H.

The manufacturing process starts by preparing the moulds. The mould preparation process starts by securing the two outer diameter moulds to each other along with the bottom insert with a temporary adhesive that doubles as a seal. The top insert is also placed in position but is not adhered since

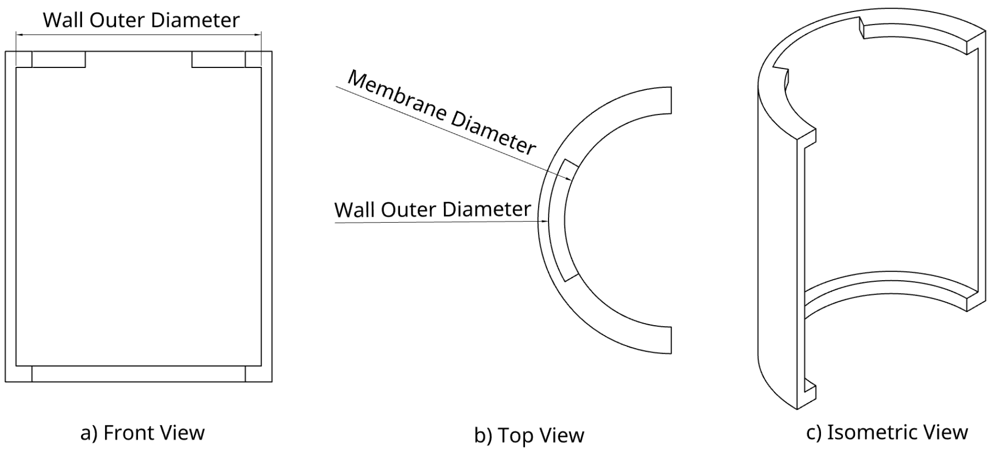


**Figure 4.4.7:** Wall Outer Diameter Mould Illustration

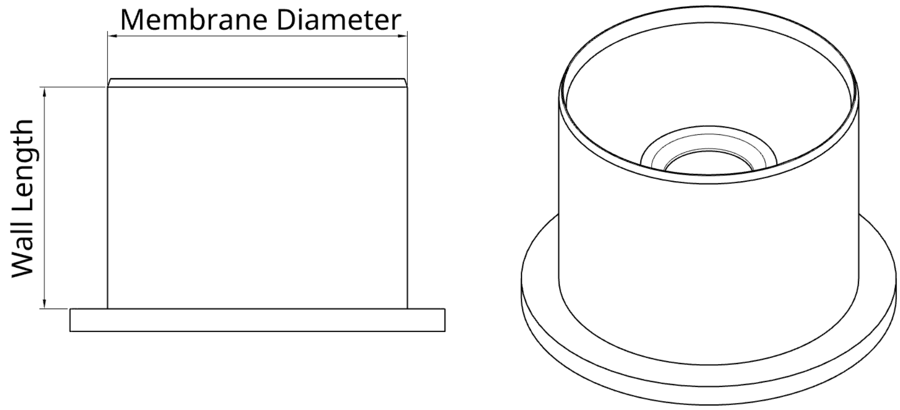


**Figure 4.4.8:** Bottom Mould Insert

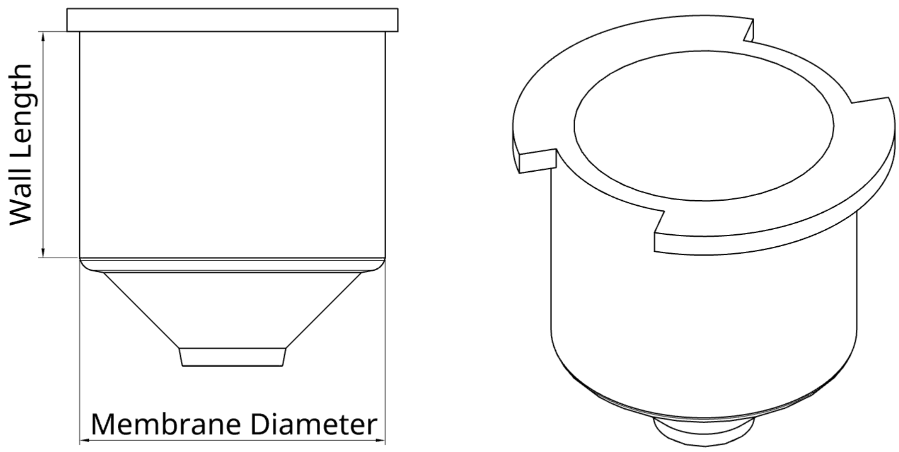


**Figure 4.4.9:** Top Mould Insert

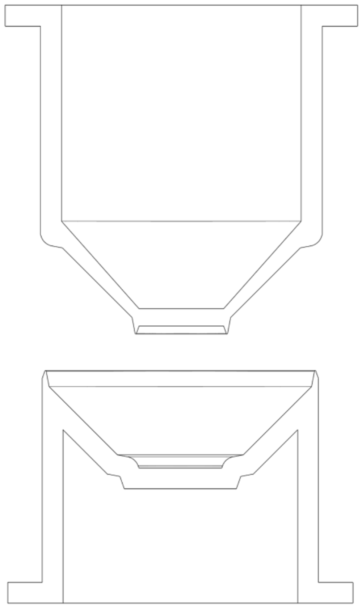

**Figure 4.4.10:** Insert Sectioned View

it must be removed to pour the silicone. After the outer diameter mould and the bottom insert have been fastened and sealed, the top insert is removed. The silicone is then prepared in the same manner as for tube manufacturing as described in Section 4.2.1, and is then poured slowly into the mould until three-quarters full which allows the silicone to seep into the wall cavities. To prevent air bubbles being caught in the outline of the tip of the cone in the top insert, the tip of top insert is coated in the uncured silicone before being inserted into the mould. While the top insert is being inserted, the excess silicone pours from the overflow slits until the insert is in position. Once in position, the top insert is weighed down to prevent movement during curing. After the curing time has elapsed the temporary adhesive is removed, followed by the outer diameter moulds, and finally the inserts are removed. An illustration of the casting process is shown in Figure 4.4.11. The casting vents cause the formation of protrusions, which are cut off to flatten the top of the wall.

## 4.5 End Cap Design and Manufacturing

The final component needed to manufacture the complete oscillator is the end cap that allows the internals of the oscillator to attach to an actuator, a supply pressure, and to vent. The end cap must, therefore, have at least three connection points. A simple design with four connection points with ample room for fastening is required. The diameter of these connection points is the same as the diameter of the buckling tubes. The end cap must have a flat surface for the walls to attach to, and the protrusion of the connection

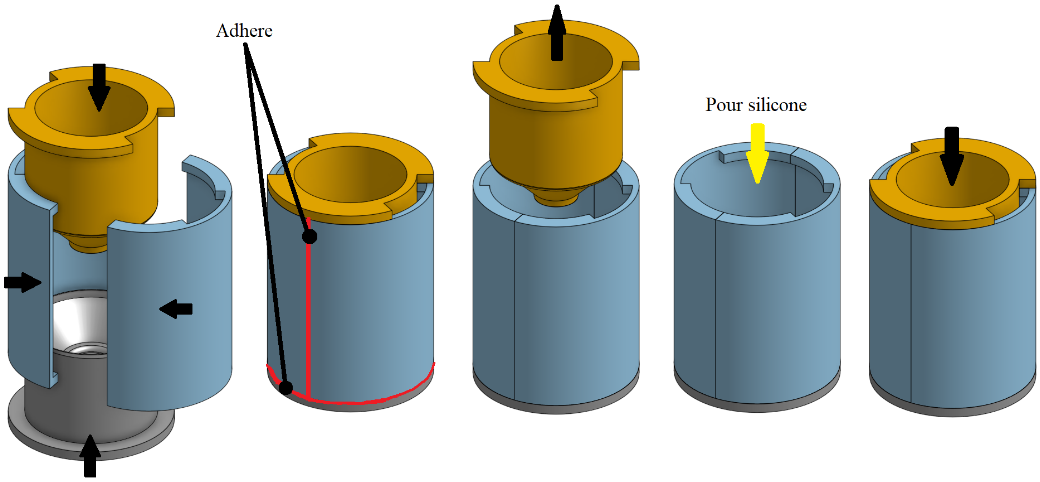


**Figure 4.4.11:** Membrane Mould Casting Process: Step 1: Align the outer diameter moulds and the top and bottom inserts, Step 2: Secure and seal the components with temporary adhesives with the exception of the top insert, Step 3: Remove the top insert, Step 4: Pour silicone into the mould until three-quarters full, Step 5: Coat the the tip of the top insert in silicone and insert into the mould

points provides an area for extra fastening. The end cap design is shown in Figure 4.5.1 and the mould in Figure 4.5.2. The end cap is manufactured by pouring silicone, prepared according to the steps in Section 4.2.1, into the mould and removing once cured. CAD drawings of the the end cap and end cap mould are found in Appendix H.

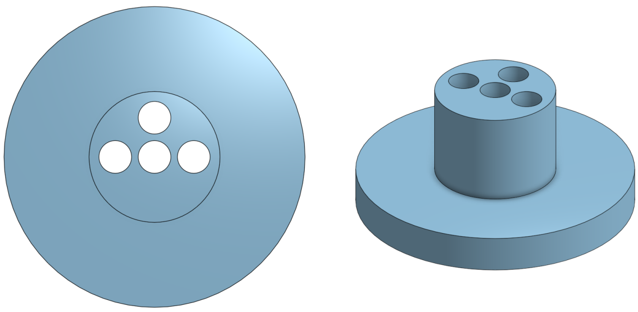

**Figure 4.5.1:** End Cap

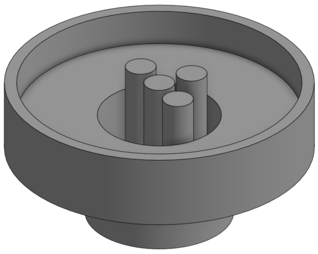

**Figure 4.5.2:** End Cap Mould

## 4.6 Oscillator Design and Manufacturing

### 4.6.1 Introduction

The penultimate step of the design process is integrating the different components into a functional oscillator. To do this, a breakdown of the different functions the oscillator must be able to perform to reach the objectives must be identified. The three functions identified for acceptable functionality are being able to produce two oscillating outputs, each output must be able to inflate and deflate the a connected actuator, and the outputs must oscillate asynchronously. The components enabling these functions must be integrated into a single design and manufactured.

### 4.6.2 Oscillator Functional Analysis

In the diagram Figure 4.6.1 the three functions, the component states, and the output for the given component states are shown, where a value of one equates to a tube allowing flow and zero equates to a blocked tube. Figure 4.6.2 provides a naming guide for the component names in Figure 4.6.1, as well as an illustration of the blocked and flow allowing states of the tubes. The top and bottom cavities of the oscillator are designated as A and B respectively, where an input tube is designated with a suffix one and venting tube is designated with a suffix two; the input tube of Cavity A and venting tube of Cavity B would then be referred to as A1 and B2 respectively. A venting tube is a tube that connects its cavity and connected actuator to the atmosphere to allow for depressurisation, and an input tube is a tube connecting the pressure source to the opposite cavity and its connected actuator. Actuator 1 is the actuator dependant on Cavity A and Actuator 2 is dependant on Cavity B.

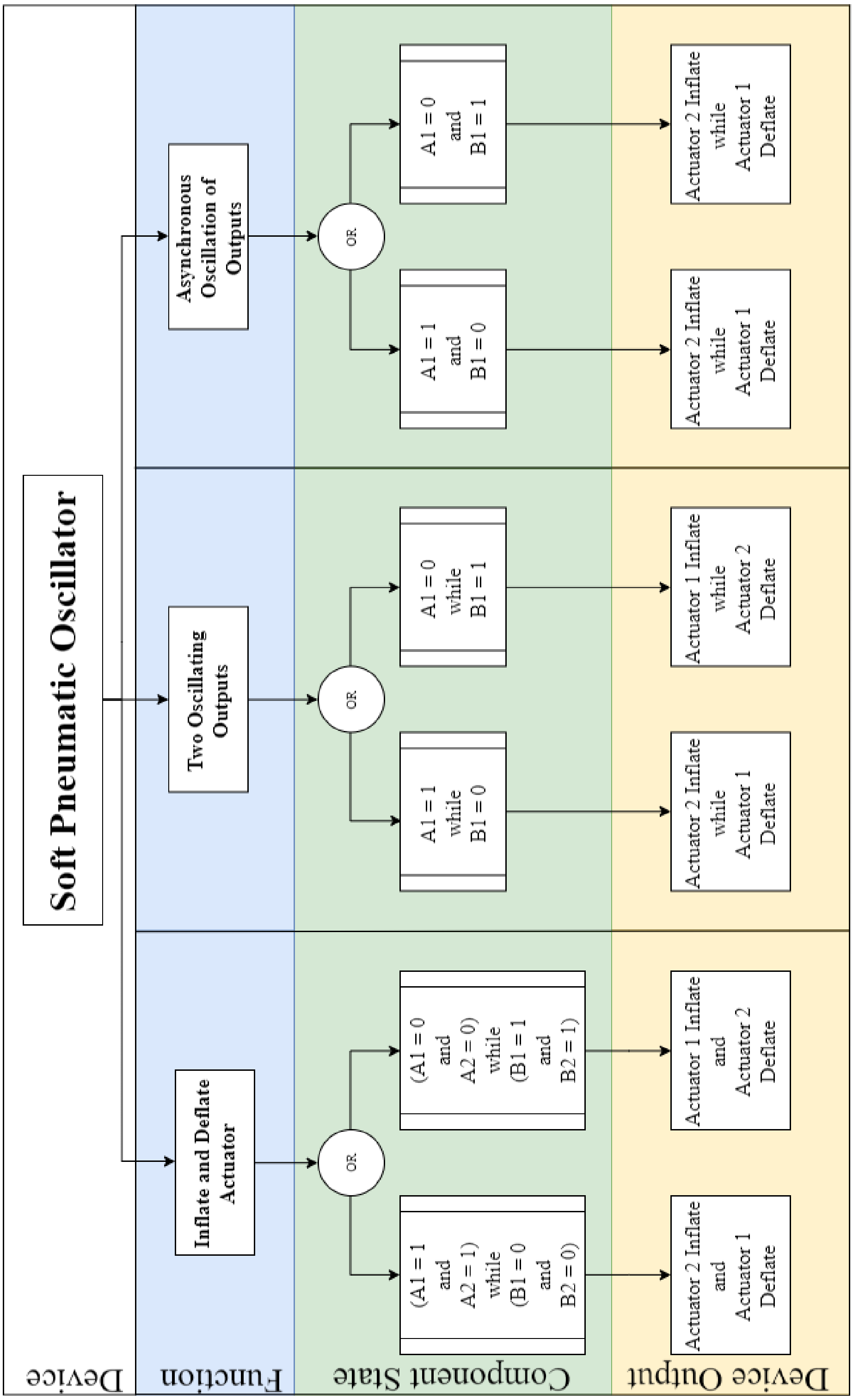


**Figure 4.6.1:** Soft Pneumatic Oscillator Functional Diagram

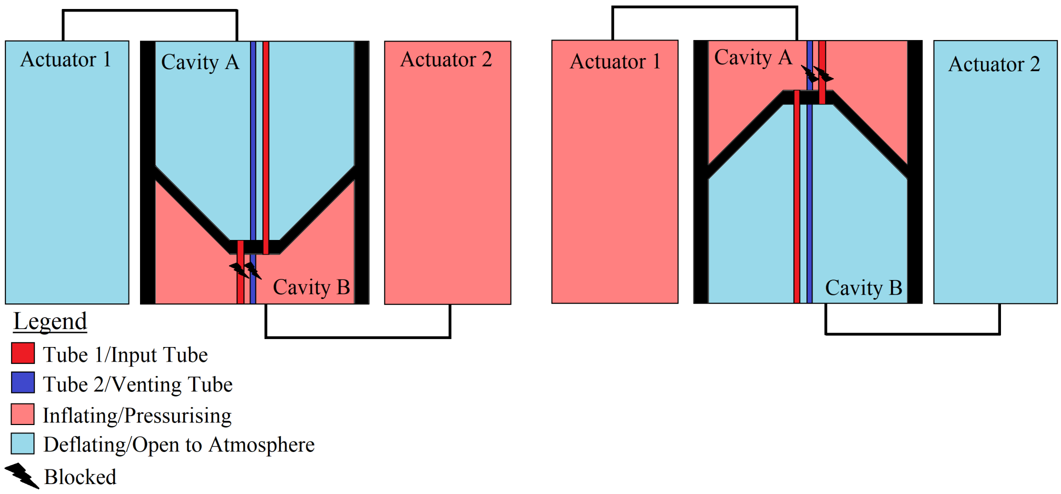


**Figure 4.6.2:** Soft Pneumatic Oscillator Naming Guide and Functioning Illustration

Figure 4.6.2 also shows the two states of the oscillator. In one state Cavity B and Actuator 2 are pressurised by tube A1 and Cavity A and Actuator 1 are exposed to atmosphere by tube A2. In the other state Cavity A and Actuator 1 are pressurised by tube B1 and Cavity B and Actuator 2 are exposed to atmosphere by tube B2.

From Figures 4.6.1 and 4.6.2 it is seen that if the tubes of either of the cavities are buckled, the tubes of other cavity will always allow flow. Therefore, tubes A1 and A2 will always equate to one if tubes B1 and B2 are zero, and A1 and A2, and B1 and B2 will always have the same state as each other. These conditions satisfy all the component states in Figure 4.6.1, and therefore produce the required device outputs.

### 4.6.3 Oscillator Manufacturing

Integrating the tubes, membrane, and end caps into a functioning oscillator requires gluing the parts together and correct spacing and orientation of the tubes.

#### Tube Spacing, Orientation, and Preparation

In order to have the venting and input tubes of the two cavities not hinder each other, their placement on the flat surface of the membrane must be chosen correctly. Figure 4.6.3 shows the layout of the tubes on either side of the membrane. The important consideration for this design is the positioning of the two input tubes, to not interfere with the flow of the working fluid. In the layout of Figure 4.6.3 the inner diameter of the two input tubes are unrestricted.

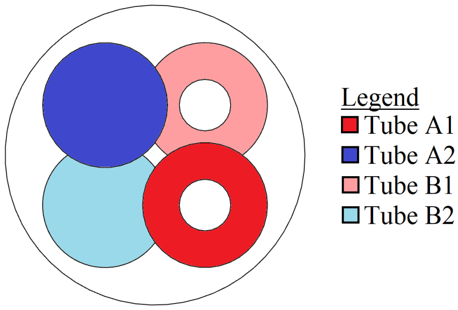


**Figure 4.6.3:** Tube Layout Diagram

Before the venting tubes are installed, the channel that allows the tube to expose the cavity to the atmosphere must be cut into the tube. A 12 gauge needle was used to cut a hole near one of the ends of a tube, this process designates the tube as a venting tube. This hole is the channel that allows air to escape the pressurised cavity. The venting tube must be orientated so that the end with the venting channel is located nearest the membrane, so that the tube may be buckled to stop the flow to atmosphere. The orientation of the tubes with the venting end nearest the membrane in shown in Figure 4.6.4 with the vent on the venting tube highlighted.

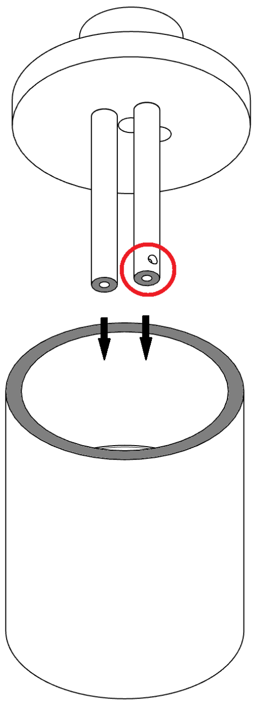

**Figure 4.6.4:** Tube Orientation

The location of the tubes in the end cap is shown in Figure 4.6.5. This positioning allows the input and venting tubes to align with the positioning of the tube on the membrane flats shown in Figure 4.6.3, and indicates the two output connections.

The tubes are cast to an over-specified length to allow for variations in tube lengths, therefore must be cut to the selected length. The length of the tube eventually used for the oscillator must also be over-length by about five millimetres to allow for a surface to glue to the end cap.

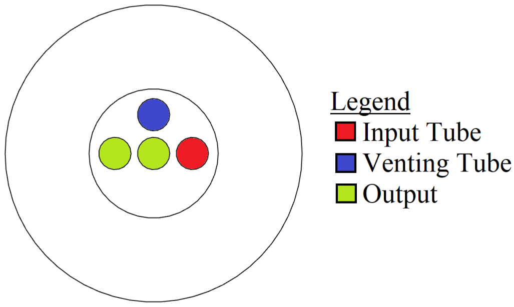


**Figure 4.6.5:** Tube Layout in End Cap Illustration

### Membrane Preparation

The membrane is manufactured with longer than required walls to allow for a variety of tube lengths, therefore the walls must be shortened to the correct length. Using Figure 4.4.6 as an indication for measuring the wall length, the wall is cut to the correct specification for the chosen tube length.

Along with the wall length, the channel between the two cavities must be created. This channel allows the flow through the input tube to bridge between the two cavities. The holes are cut into the flat of the membrane on the locations illustrated in Figure 4.6.3 using a 12 gauge needle.

### Component Integration

After the different components have been manufactured and prepared, they must be glued and combined to form the oscillator. Sil-poxy Silicone Glue from Smooth-On is used to glue the components together, more information regarding the silicone glue is found in Appendix B. The two steps needed to manufacture one side of the oscillator are shown in Figure 4.6.6, these steps are repeated for the other side to manufacture the complete oscillator. The first step is gluing the tubes to the end cap in the positions shown in Figure 4.6.5 and the second step is the gluing of the tubes to the membrane flats in the layout shown in Figure 4.6.3. The tubes used are designed to be compressed slightly while in the elongated position, which allows the end cap to protrude from the wall. This allows a space between the wall and the end cap to allow for the applying of glue in Step 2 of Figure 4.6.6. The silicone glue is applied to the shaded areas of the tubes and wall in Figure 4.6.6, and fixed into position while the glue dries.

After gluing the tubes in Step 1 of Figure 4.6.6, the length of tube protruding from the end cap must be measured to ensure that the tube is not inserted into the end cap beyond the length provided for gluing. This is important for ensuring that the length of tube is present in the cavity.

For manufacturing of the second side of the oscillator, the process is eased by snapping the membrane to the other side. Inserting lengths of 12 gauge wiring in the tubes during manufacturing also eased the process by increasing rigidity the of the tubes and prevents the glue from clogging the tubes and channels.

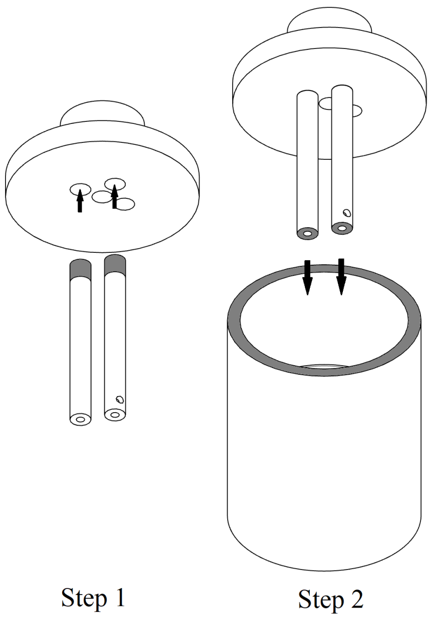


**Figure 4.6.6:** Oscillator Manufacturing Illustration

## 4.6.4 Evaluation and Discussion

Following the design and manufacturing steps of this section, a soft pneumatic oscillator can be manufactured. The needed functionality is achieved by correctly combining the components to control flow based on membrane position. The specifications given in Table 4.4.3 are used for the evaluation of this design, but the specifications are adaptable while Equation 4.4.1 and the snap-through and bistability conditions of the membrane are met.

# Chapter 5

# Soft Pneumatic Oscillator Evaluation

## 5.1 Introduction

The soft pneumatic oscillator is evaluated to ensure the objectives of the project are reached, therefore a test was designed to verify functionality of the oscillator for each of the objectives. The tests are used to confirm that the oscillator delivers in regards to both functionality and application in EIA control, meaning that the oscillator is tested to determine that the output frequency is linked to the supply pressure, as the output of a CPG is linked to input magnitude, and that the oscillator produces two asynchronous outputs capable of deflating and inflating an attached EIA.

## 5.2 Soft Pneumatic Oscillator Testing Methodology

To ensure the satisfaction of the objectives, the oscillator is tested for the three output functionalities identified in Figure 4.6.1. Therefore, two outputs of the oscillator will be tested for asynchronous oscillation of two inflating and deflating EIAs. EIAs must be identified for the test setup of the oscillator, and since this project does not cover the design of a soft robot a placeholder EIAs must be used. The placeholder EIA is theoretically capable of modelling the spinal undulation of a salamander and function similar to an EIA in regards to operation.

### 5.2.1 Placeholder Elastic Inflatable Actuator

The placeholder EIA used for testing must comply with the pressure range as laid out in the conceptual design, namely, the operating pressure must lie within the range of about 5 kPa to 130 kPa. Initially, this is achievable due to the critical pressures for a 45° Smooth-Sil 950 membrane with a diameter of 40 mm falling in the accepted pressure range, as given in Table 4.4.2.

The chosen EIA for the test setup is based on a strain-limited actuator of the rolling soft robot of [44]. The EIA consists of a compliant inflating bladder and deformation constraining component. This allows for actuation until the expansion is restricted and then a pressure build-up that switches the oscillator's membrane.

An EIA of similar function to that of the placeholder EIA can be used to model the spinal bending of the salamander. If a bending actuator is allowed to bend up to a certain point at which the bending is restricted, there is a pressure build-up while no further bending takes place. Assuming the theoretical EIA is designed to function at the operating pressures of the soft oscillator, the placeholder EIA is sufficient for evaluating the performance of the soft oscillator.

The placeholder EIA consists out of an inflatable bladder, a balloon, in this case, encased in a rigid enclosure. The balloon is allowed to inflate until constricted by the enclosure, at which point the pressure increases until the membrane switches. After switching, the inherent elasticity of the balloon will cause it to deflate, testing the venting procedure of the oscillator. Two of the placeholder EIAs are used for testing, each connected to one of the chambers of the oscillator to test asynchronous oscillation of the two actuators.

### 5.2.2 Testing Setup

The important data needed from the evaluation of the oscillator are the input pressure and the pressure inside the two actuators, as these values are used to determine whether the oscillator achieves the functions in Figure 4.6.1. The test setup is illustrated in Figure 5.2.1 where the oscillator is used to actuate two of the placeholder EIAs as described.

Pressure transducers $P_1$ and $P_2$ are connected to Actuator 1 and Actuator 2 respectively as seen in Figure 5.2.1. More information of the differential pressure transducers used are found in Appendix C. The pressure transducers provide the temporal pressure data of the actuators for evaluation the frequency and amplitude of the oscillations. The phase between the two outputs and the frequency of the oscillations is extracted from the measured data. The data is used to conclude whether the oscillations are asynchronous and whether the frequency of the oscillation is linked to the input pressure.

### 5.2.3 Testing Procedure

The data is gathered by supplying the test setup with a supply pressure capable of reaching the higher of the critical pressures of the oscillator. After such pressure is reached, the data from the pressure transducers are logged. For

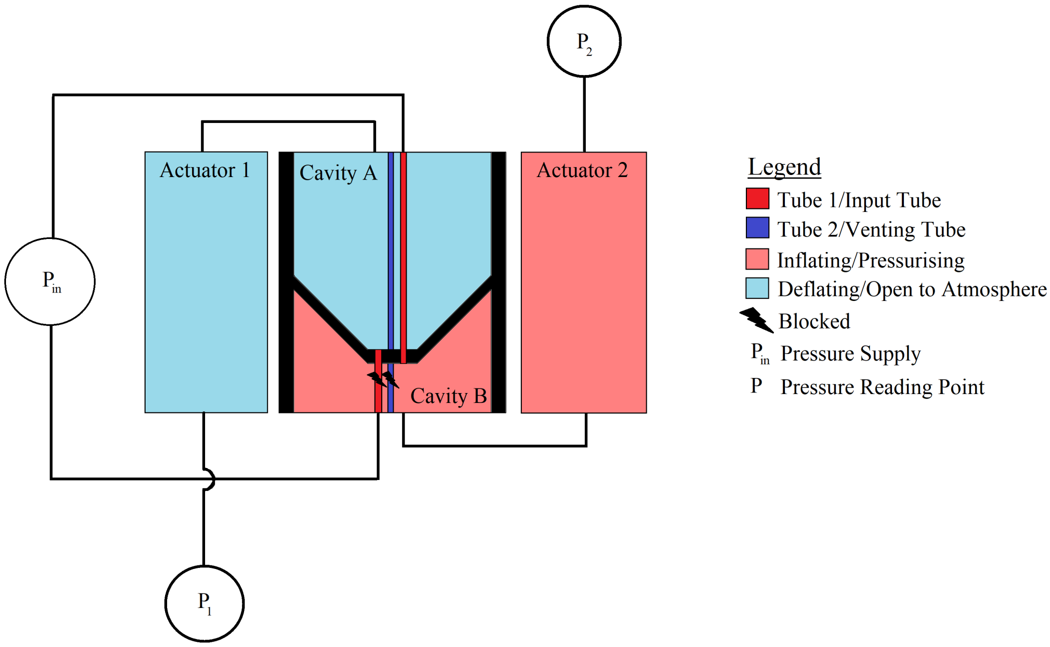


**Figure 5.2.1:** Test Setup Diagram

each test case a sufficient amount of oscillations were recorded for ensuring the procurement of usable data.

A pneumatic system diagram showing the setup and port configuration of the oscillator is shown in Figure 5.2.2. In Figure 5.2.2 the actuators are modelled as reservoirs and the oscillator as a control valve. The outlets are open to atmosphere and the controllers are pressure lines connected to the inflating actuators. The two inlets are connected to a single pressure source.

## 5.3 Results and Discussion

Figure 5.3.1 shows a front, top, and isometric view of a manufactured oscillator. Figure 5.3.2 shows a time-lapse of a single oscillation using the placeholder EIAs. The left actuator is actuated and the right depressurised in the first frame, the rest of the frames depict one cycle. The raw data gathered from the 20 kPa, 24 kPa, and 28 kPa tests are found in Appendices D through F respectively.

### 5.3.1 Inflate and Deflate Functionality

To confirm whether the oscillator is capable of inflating and deflating two connected EIAs, the internal pressures of the actuators are measured. The pressures of the two actuators are expected to increase in pressure during inflation and decrease in pressure during deflation. If these expectations are

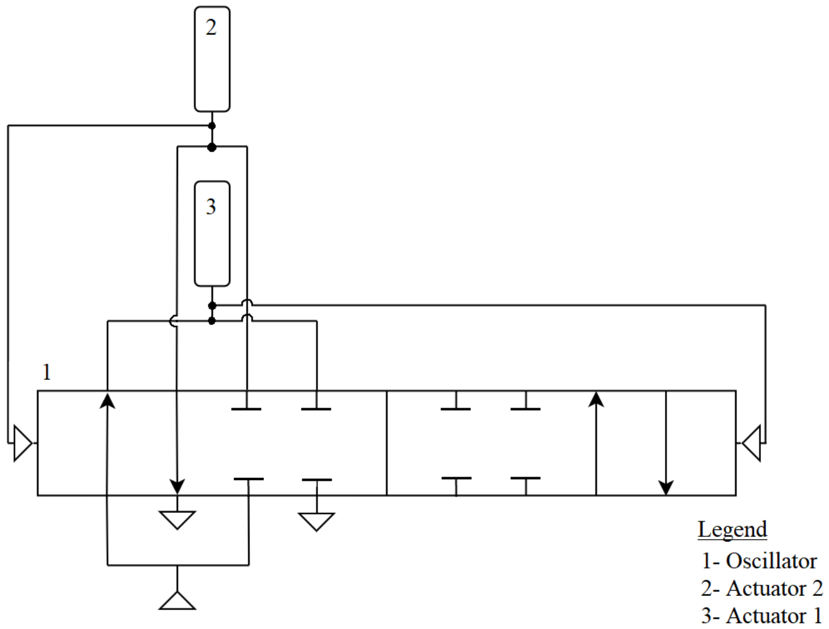


**Figure 5.2.2:** Pneumatic System Diagram of Testing Setup: The initial and secondary states of the oscillator can be seen along with the flow path of the input pressure to the actuators and switches, and the flow path of the output pressure form the actuators to the outlet

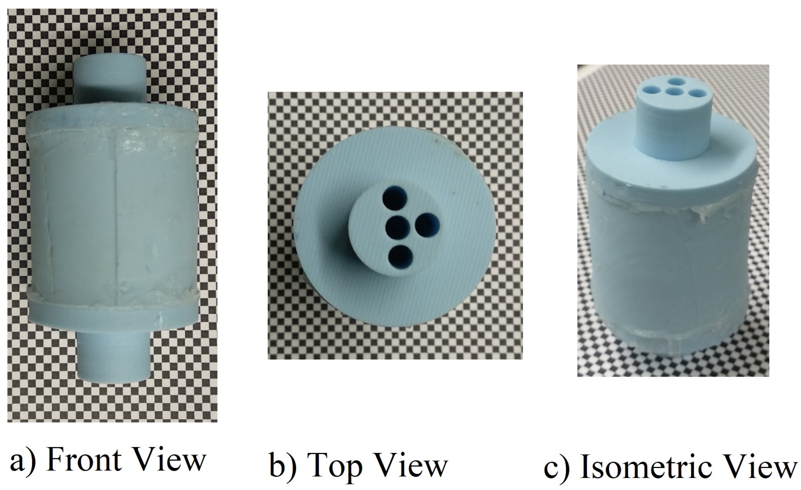


**Figure 5.3.1:** Oscillator: The front (a), top (b), and an isometric (c) view of a fully manufactured soft pneumatic oscillator

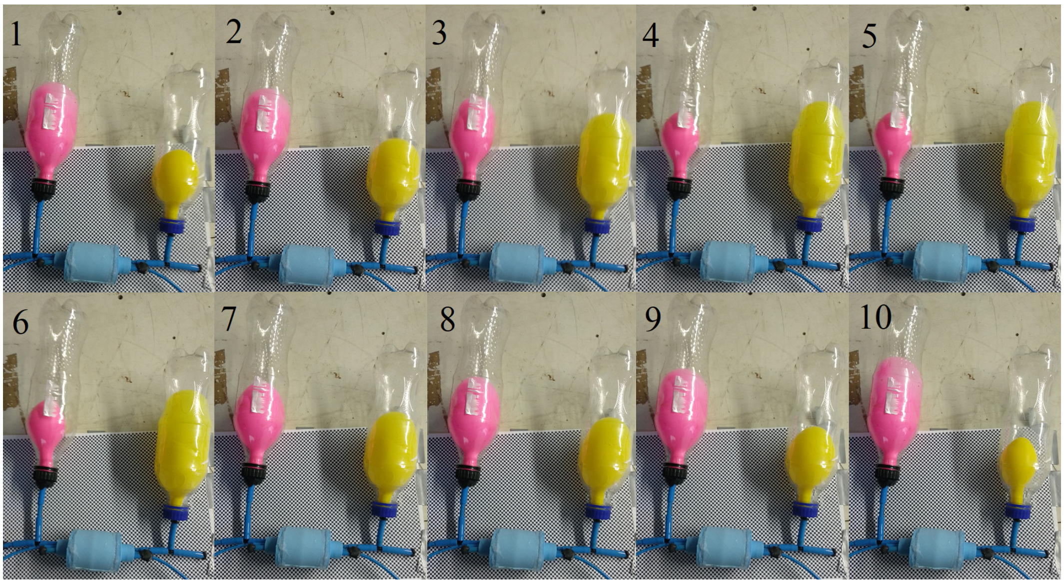


**Figure 5.3.2:** Oscillation Time-Lapse: Frame 1 shows Actuator 1 in a fully inflated state with the membrane just having snapped through allowing Actuator 2 to start inflating. Frames 1 through 5 show the inflation of Actuator 2 and the depressurising of Actuator 1. Between frames 5 and 6 the membrane snaps-through with frame 5 showing the start of the depressurisation of Actuator 2 and the start of inflation of Actuator 1. Frames 6 through 10 Actuator 1 is inflating and Actuator 2 depressurising. Frame 10 shows the start of a new cycle with the Actuators in the same state as Frame 1

met, the oscillator functions correctly.

Inflation and deflation are tested using the test procedure and setup described in this chapter. A supply pressure of 24 kPa is used to test inflation and deflation. The raw test results used are found in Appendix E designated as Test 1.

The results of the test are plotted in Figure 5.3.3. In Figure 5.3.3 it is seen that the pressures inside the actuators increase and decrease, therefore from Figure 5.3.3 it is concluded that the oscillator is functional in regards to enabling the inflation and deflation of two connected EIAs.

### 5.3.2 Two Oscillating Outputs Functionality

To confirm whether the oscillator is capable of producing to oscillating outputs from a single pressure input, the pressure input and two internal pressures of the actuators must be studied. If the oscillator is functional in this regard, a single pressure source connected to the oscillator must produce two outputs that increase and decrease in pressure periodically. If this behaviour is observed, the oscillator functions correctly.

Oscillation is tested by comparing the input pressure to two internal pres-

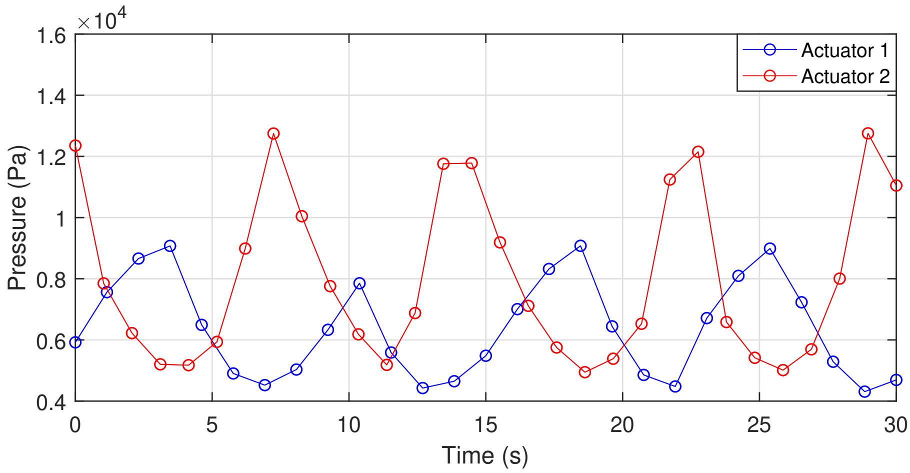


**Figure 5.3.3:** Inflation and Deflation Test Results: Actuator 1 (blue) and Actuator 2 (red) increase and decrease in pressure over time, showing the inflation and deflation functionality of the oscillator

sures of the actuators over a time period. A supply pressure of 24 kPa is used to test for oscillation. The raw test results used are found in Appendix E designated as Test 1.

The results of the test are plotted in Figure 5.3.4. In Figure 5.3.4 it is seen that the pressures inside the actuators increase and decrease periodically whilst the supply pressure remains constant, therefore from Figure 5.3.4 it is concluded that the oscillator is functional in regards to enabling the production of two oscillating pressure outputs from a single constant supply pressure.

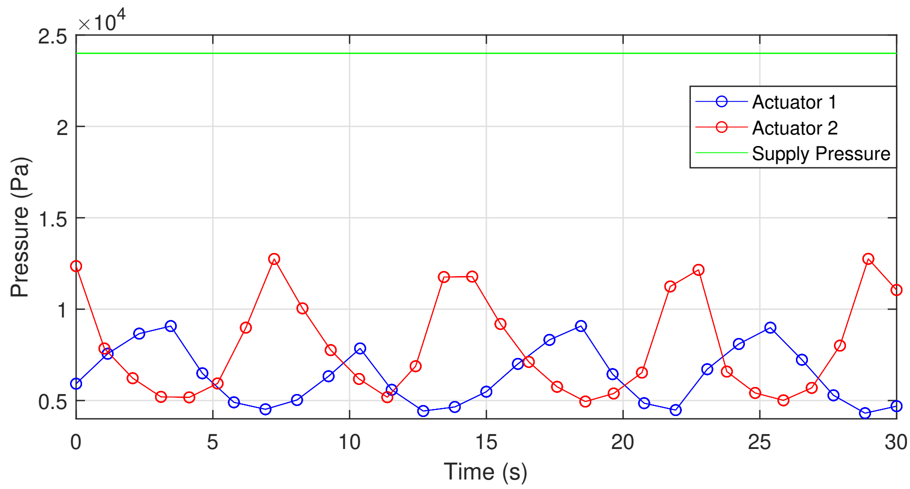


**Figure 5.3.4:** Oscillation Test Results: Actuator 1 (blue) and Actuator 2 (red) increase and decrease in pressure over time while the supply pressure remains constant, showing two oscillating outputs for a single constant output

### 5.3.3 Asynchronously Oscillating Outputs Functionality

To confirm whether the oscillator is capable of producing to asynchronously oscillating outputs, the two internal pressures of the actuators must be studied. If the oscillator is functional in this regard, one actuator must peak in pressure whilst the other experiences its minimum pressure. This behaviour indicates that the oscillations have an 180° phase difference meaning that they are asynchronously oscillating.

To extract the frequency information from the data, the data must be processed into a model from which frequency information can be gathered. The raw data is sufficient for confirming oscillation and inflation-deflation functionality, but is not presented in such a way as to extract the phase difference. The data is therefore fit to a Fourier model. The Fourier model of the data will enable the extraction of the frequency and phase difference of the output pressures.

To gather the data for the Fourier model, three thirty second tests at a supply pressure of 24 kPa are logged. A Fourier fit is done for each set of date and the phase difference between the pressures of Actuator 1 and Actuator 2 for each the three tests is determined. The average phase difference is then determined and used to confirm if the oscillations are asynchronous.

#### Data Trend Checking

Before the data was modelled with a Fourier fit, the data is analysed to determine if there is a trend present in the data. For a Fourier fit to be applied to a data-set, it is required that the data does not have a trend. If a trend is present in the data, the trend is be removed from the data and applied after the fit is applied.

All the data gathered from the three tests at a 24 kPa supply pressure is checked for a trend in the data. The process is explained using the first test as an example. In Figure 5.3.5 the raw data for one of the 24 kPa supply pressure tests is shown along with a scatter plot of values representing the moving mean between the maximum and minimum pressures measured for the test. The moving mean is calculated using a subset of data-points covering the period of a single oscillation.

Figure 5.3.5 also includes the resulting linear fit for the moving mean found using linear regression. The fit to the moving mean is used to determine the trend of the data. This is true for all tests performed at 24 kPa supply pressure. No significant trend is present to influence the Fourier fit, therefore a Fourier fit can be applied to the data.

#### Fourier Fit

A single term Fourier fit is used to maintain a smooth sinusoidal shape whilst still capturing the pressure values with acceptable accuracy. Equation (5.3.1)

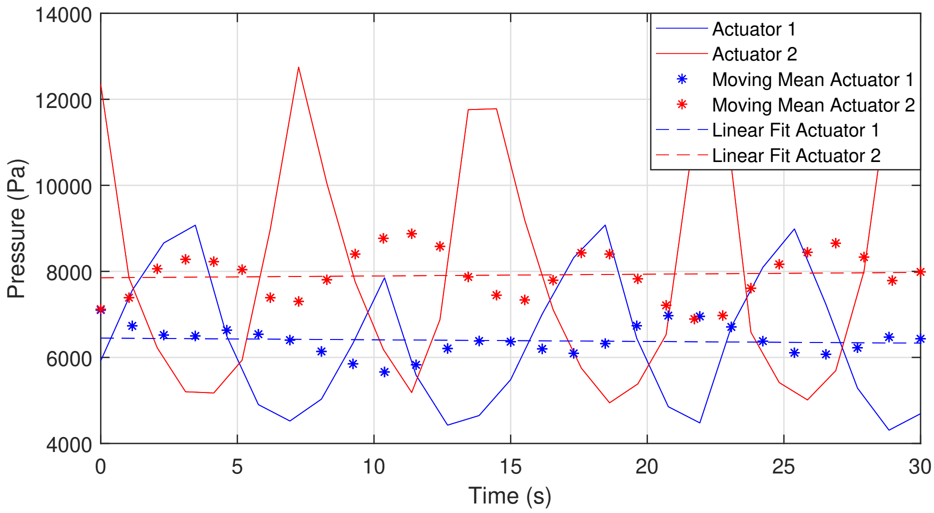


**Figure 5.3.5:** Data Trend Check: A moving mean, with subset of data spanning the time of a single period, is taken of the raw data gathered from a test at 24 kPa supply pressure. A linear fit to the moving mean is done and is used to determine if a trend is present in the data. No significant trend is present.

gives the single term Fourier function used to model the data.

$$f(x) = a_0 + a_1\cos(xw) + b_1\sin(xw) \tag{5.3.1}$$

The important information needed from the Fourier fit is the frequency information, the amplitude information is not necessary for the determination of enabling the functionality of asynchronous oscillations. Due to the nature of the oscillator, the frequency of the pressure oscillations in Actuator 1 and 2 must be the same. Therefore if the Fourier models for the pressure oscillations of Actuator 1 and 2 for each test differ in frequency, the frequency value of the Fourier model is replaced by the mean of the two frequencies. The resulting Fourier fit to the data gathered in the first 24 kPa supply pressure test is shown in Figure 5.3.6.

From Figure 5.3.6 it is concluded that the Fourier fit is successful in capturing the frequency information of the oscillations. The Fourier fit is used to determine the phase difference between the oscillations of the internal pressures of actuator 1 and actuator 2. A phase difference is calculated for each of the three tests, and mean value is determined.The mean value is used to determine of the oscillations are asynchronous.

The phase difference values for each of the three tests can be found in Table 5.3.1. The mean phase difference is then 207.21°. This value is not precisely out phase, but the behaviour is very close to asynchronous behaviour. The behaviour is considered to achieve the asynchronous oscillation functionality.

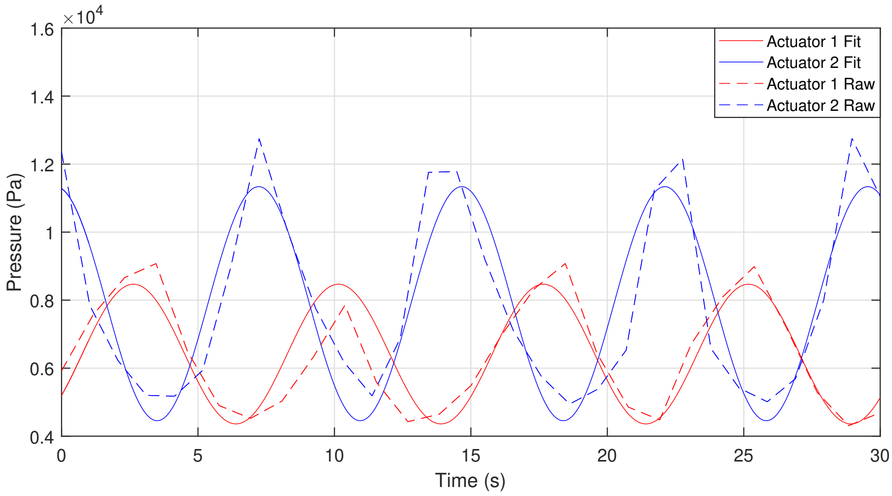


**Figure 5.3.6:** Fourier Fit Results: The Fourier fit for Actuator 1 (blue) and 2 (red).

**Table 5.3.1:** Phase Difference Between Actuator 1 and Actuator 2 Oscillations

| Test | Phase Difference (Degrees) |
|---|---|
| 1 | 208.39 |
| 2 | 207.51 |
| 3 | 205.72 |

### 5.3.4 Oscillation Frequency Dependence on Supply Pressure Magnitude

Along with the three functionalities the oscillator is required to achieve, the oscillator must also mimic the functioning of the CPG with regards to the output frequency being influenced by the magnitude of the input signal. The frequency of the actuators' pressure oscillation must therefore increase along with an increase in supply pressure. Three thirty second test at three supply pressures are performed, and the internal pressures of the actuators are logged. The three supply pressures are 20 kPa, 24 kPa, and 28 kPa. The frequency of the oscillations are expected to increase from the lowest supply pressure to highest supply pressure. If this expectation is met, the oscillator achieves the required behaviour.

The raw data gathered from the test must be processed into a form from which frequency information can be gathered, therefore the data is fit to a Fourier model. The resulting data from each supply pressure test is checked for a lack of trend using the same process followed in the phase difference section. All data was found to be without trend, and therefore fit to a Fourier model.

Each of the three tests for each supply pressure was fit to Fourier model,

**Table 5.3.2:** Mean Oscillation Frequency for Each Test

| Supply Pressure | Frequency (Hz) | | | | |
|---|---|---|---|---|---|
| | Test 1 | Test 2 | Test 3 | Mean | Standard Deviation |
| 20 kPa | 0.104 | 0.096 | 0.095 | 0.0983 | 0.0049 |
| 24 kPa | 0.134 | 0.139 | 0.14 | 0.0983 | 0.0032 |
| 28 kPa | 0.238 | 0.248 | 0.243 | 0.0983 | 0.0072 |

and the frequencies of oscillation were extracted. Due to the nature of the oscillator, the frequency of the pressure oscillations in Actuator 1 and 2 must be the same. Therefore if the Fourier models for the pressure oscillations of Actuator 1 and 2 for each test differs in frequency, the frequency value of the Fourier model is replaced by the mean of the two frequencies. The tests therefore result in three frequency values for each supply pressure. The three frequencies for each supply pressure along with the mean and standard deviation for each supply pressure is shown in Table 5.3.2.

The information in Table 5.3.2 is used in the box plot of Figure 5.3.7 to determine the correlation, if any, between the supply pressure and oscillation frequency.

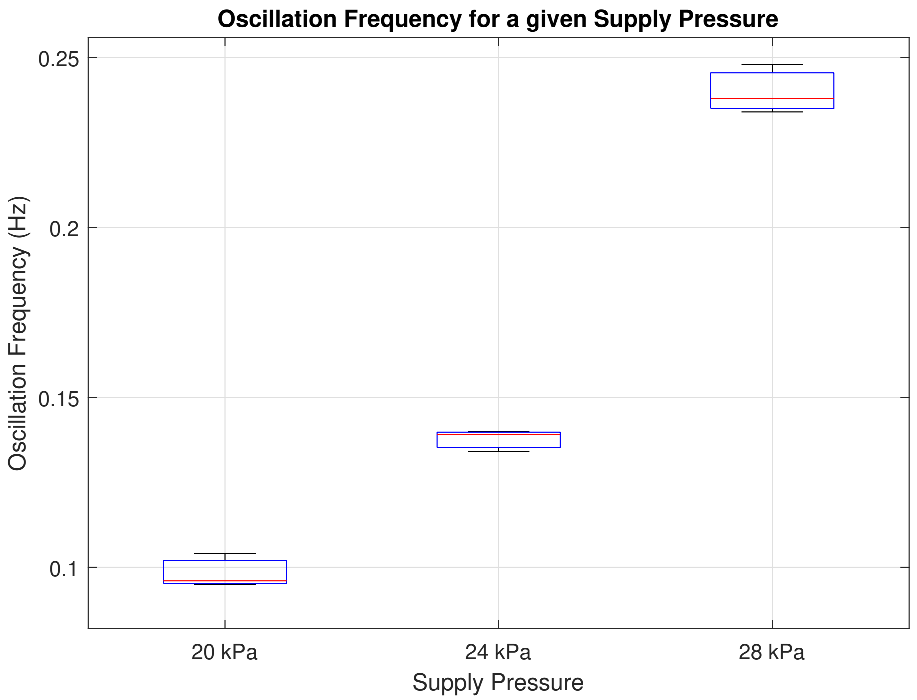


**Figure 5.3.7:** Box Plot of Oscillation Frequency for a given Supply Pressure: An increase in supply pressure is seen to result in an increase in oscillation frequency

### 5.3.5 Oscillation Amplitude and Offset

There are differences in the amplitude and offset of the oscillations for a given actuator at different supply pressures. These differences can be seen in Figure 5.3.8 where the amplitude decreases and the offset increases for each of the actuators along with an increase in supply pressure. The decrease in amplitude can be attributed to the increase in the flow rate of the working fluid. This increase in flow rate decreases the amount of time needed for the internal pressure of the actuators to reach the critical pressure of the oscillator and also decreases the amount of time the actuators have to depressurise.

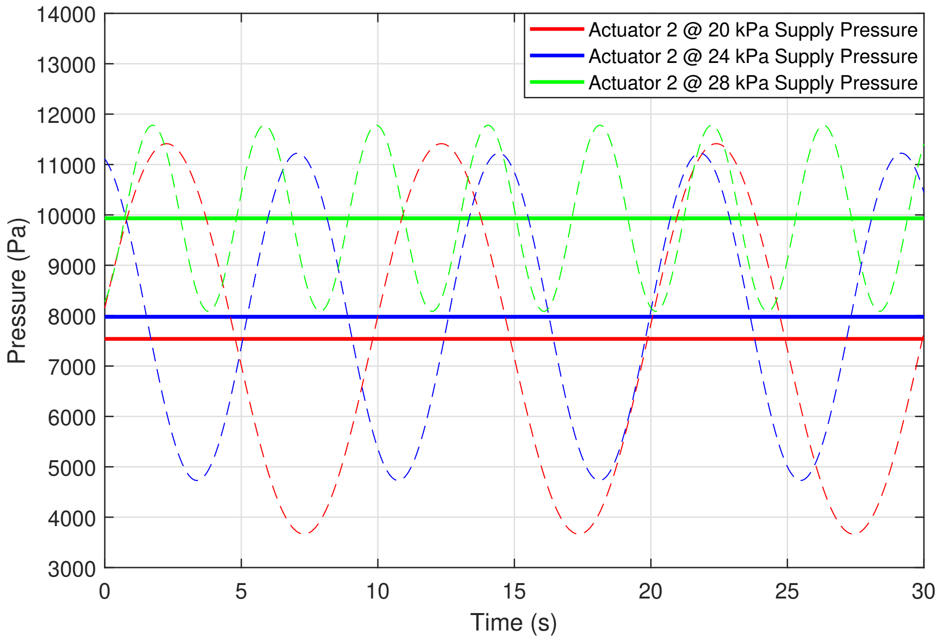


**Figure 5.3.8:** Offset Comparison for Different Supply Pressures: The increase in offset due to a reduction in venting time is seen when the supply pressure is increased from 20 kPa to 28 kPa

### 5.3.6 Oscillator Specifications

The specifications of the oscillator used for testing are given in Table 5.3.3. The physical dimensions such as length and diameter are specific to the chosen membrane diameter and will differ if other values are used. The connector diameters can also be adjusted for a specific case. The oscillator output frequencies will change when the oscillator is used in a system with a different volume, therefore can not be specified. The oscillator is rather specified in regards to switching pressures. The switching pressures for Cavity A and B are extracted from the maximum values of the oscillations gathered during testing. Cavity A and B are designated as in Figure 4.6.2. The pressures of the two cavities are specified for outputs since, as mentioned previously, any connected actuators are seen as an increase in volume of the cavity.

**Table 5.3.3:** Final Oscillator Specifications

| Specification | Value |
|---|---|
| Cavity A Switching Pressure | 14 kPa |
| Cavity B Switching Pressure | 7.5 kPa |
| Port Connection Diameter | 5 mm |
| Oscillator Diameter | 45 mm |
| Oscillator Length | 90 mm |

## 5.4 Discussion

In this chapter, the design process of the soft pneumatic oscillator is laid out. The design choices with regards to dimensions and manufacturing for the tubes, membrane, wall, and end caps were discussed and elaborated on. A testing setup with placeholder EIAs is developed to evaluate the oscillator. The testing setup provides data that is used to conclude the effectiveness of the oscillator in achieving the three required functionalities, namely allow for the inflation and deflation of connected EIAs, oscillation of connected EIAs, and asynchronous actuation of connected EIAs. The test results also indicate that the output frequency of the oscillator is linked to the supply pressure, analogous to the functioning of the CPG.

# Chapter 6

# Conclusion and Future Work

## 6.1 Conclusion

This project followed a systems engineering approach to find a solution to a problem. This process started with a conceptual design process, followed by preliminary and detail design stages. These processes guided the project in regards to identifying a need in the field of soft robotics and then a systematic approach to finding a solution to the defined problem.

This project started with the conceptual design process, in which the problem at hand was conceptualised. This stage started by identifying a need for a soft controller in the field of soft robotics. After an evaluation of the state of soft robotics, it was seen that, of the modern soft robotic technologies, EIAs are in need of a dedicated controller.

EIAs currently make use of conventional pneumatic control systems that are mostly bulky and located off-board of the soft robot. EIA technology was chosen as the technology this project will consider for the design of a soft controller, due to its need for a controller and economic and manufacturing feasibility due to readily available resources. After EIAs were chosen as the technology for this project, research was done on existing EIA based soft robots in order to identify the type of control necessary.

The common use of dual-acting actuators was noticed, where two inputs are required to deliver a single motion. An oscillator was seen as a solution that will decrease the required inputs and deliver the same result as the conventional controllers. Once the type of controller needed was identified, a look was taken at the biological world for inspiration in the design of the controller.

The CPG was seen as a biological controller that is used to simplify control systems. The use of CPGs in the control of salamander locomotion was identified as the case study for this project due to its elegance in simplicity and the readiness for the spinal undulation of the salamander to be modelled by EIAs.

The final stage of the conceptual design stage covered the investigation into existing technologies that can produce an oscillating mechanism. Three technologies- namely the microfluidic membrane valve, directional control valve, and the soft valve- were identified. After a look at the feasibility of the technologies, the directional control valve and the soft valve were chosen as potential candidates and were further explored in the preliminary design process.

The conceptual design process provided the objectives for the project, namely the need for a soft robot focused pneumatic oscillator that can, from a single constant supply pressure, produce two oscillating outputs that should be able to produce two asynchronous outputs that can be used to actuate EIAs. The oscillator must also mimic the functioning of the CPG by having the output frequency be dependant on the supply pressure.

The next stage of the project was the preliminary design stage. This stage identified three functions necessary to produce two oscillating outputs from a single supply pressure, namely latching, switching, and flow control. In this stage, the directional control valve and soft valve are investigated to judge their ability to produce the oscillator needed for this project. The directional control valve was explored first.

A reduced scale directional control valve was designed and manufactured to test the viability of SLA 3D printing in producing a variation of the conventional directional control valve. The spool was responsible for flow control, an inflating bladder was responsible for switching, and a magnet and latching plate was responsible for latching. The design, and therefore the chosen manufacturing method, was not functional due to the manufacturing method not producing components with a sufficiently low tolerance.

A soft valve with a conical membrane was manufactured and tested. The soft valve used a bistable membrane for switching and latching and tubes for flow control. The soft valve was seen as functional and a favourable option due to its ease of manufacturing and soft structure. The soft valve was then chosen as the technology from which the oscillator would be designed in the detail design process.

In the detail design stage of the project, the design, manufacturing, and testing processes of the components of and eventually the complete oscillator. A criterion for buckling tubes based on critical length was developed as well as a manufacturing procedure for the tubes. A membrane that is bistable with a prominent snap-through mechanism was designed, and its manufacturing and testing discussed. After the different components are determined to be functional, they are integrated to form the oscillator.

The manufacturing process of the oscillator is discussed and a testing methodology for the oscillator is developed. The testing requires a placeholder EIA. A placeholder EIA is developed for testing, the placeholder mimics the functioning of an EIA that makes use of fibre reinforcement to limit actuation. The test produces data that validates the functionality of the oscillator in regards to the required functions identified in the detail design section. The tests were done at three supply pressures to compare the oscillation frequencies for different supply pressures.

The results of the tests indicate that the oscillator meets the objectives of the project. The oscillator produces two asynchronous oscillating outputs capable of actuating two EIAs from a single constant supply pressure, with the oscillating frequency being dependant on the supply pressure.

## 6.2 Future Work

### 6.2.1 Manufacturing Technique

In order to increase repeatability and tighten tolerances, higher quality moulds can be used. Moulds that are machined to tolerances higher than that of 3D printed parts should produce oscillators that function at closer operating conditions to one another and also increase the confidence in the consistency of the design parameters of the oscillator.

### 6.2.2 Parametric Study

Performing a parametric study on parameters such as wall-thickness and tube-thickness would produce a clearer idea of their impact on the functioning of the oscillator. The amount of parameters that have to be considered during the design of the oscillator makes identifying the impact of each parameter in detail a timely task.

The parametric study could produce a design guide that can enable one to produce an oscillator for a specific operating pressure. A quantitative link between wall thickness, membrane thickness and material, and membrane slope could be found.

Testing a greater range of tube thickness and diameter values could also increase the flow rate allowed by the tubes. This could possibly lower the offsets seen in Figure 5.3.8. The minimum pressure values of the two outputs of the oscillator could also be decreased to a pressure value closer to atmosphere by allowing the inflated volumes to vent more rapidly.

# Appendix A

# Stereolithographic Apparatus Information

## A.1

**Table A.1.1:** Stereolithographic Apparatus Information

| Component | Product ID | Serial Number | Firmware Version |
|---|---|---|---|
| 3D Printer | Formlabs Form 2 | B0768JSZ8J | 1.19.12 |
| Resin | Clear Resin Cartridge for Form 2 | RS-F2-GPCL-04 | N/A |
| Printer Software | Preform | N/A | 3.2.0 |

# Appendix B

# Silicone Information

## B.1

**Table B.1.1:** Silicone Technical Specifications

| **Silicone** | **Specific Gravity (g/cc)** | **Pot Time** | **Cure Time** | **Shore A Hardness** | **Tensile Strength (psi)** | **Elongation at Break (%)** |
|---|---|---|---|---|---|---|
| Sil-Poxy | 1.12 | 5 min | 12 min | 40 | 750 | 750 |
| Mold Star 30 | 1.12 | 45 min | 6 hrs | 30 | 420 | 339 |
| Smooth-Sil 950 | 1.24 | 45 min | 18 hrs | 50 | 725 | 320 |

# Appendix C

# Differential Pressure Transducers Specifications

## C.1

**Table C.1.1:** Differential Pressure Transducers Parameters

| **Designation** | **Model** | **Serial Number** | **Operating Pressure** | **Operating Temperature** |
|---|---|---|---|---|
| $P_1$ | PMD75 | AB08EC0109D | -10...10 kPa | -40 to +85° C |
| $P_2$ | PMD55 | KC00A221121 | -50...500 mbar | -40 to +85° C |

# Appendix D

# Test Data for 20 kPa Supply Pressure

## D.1

**Table D.1.1:** Raw Test Data from 20 kPa Tests

| **Time (s)** | **Test 1** | | **Test 2** | | **Test 3** | |
|---|---|---|---|---|---|---|
| | $P_1$ **(Pa)** | $P_2$ **(Pa)** | $P_1$ **(Pa)** | $P_2$ **(Pa)** | $P_1$ **(Pa)** | $P_2$ **(Pa)** |
| 0 | 6917 | 3681 | 4419 | 6667 | 4193 | 7041 |
| 1.0345 | 5252 | 4482 | 4028 | 11065 | 3724 | 11547 |
| 2.0690 | 4415 | 5449 | 2805 | 13926 | 3100 | 13782 |
| 3.1034 | 4011 | 8732 | 3989 | 11288 | 4438 | 10916 |
| 4.1379 | 2847 | 13363 | 5141 | 8606 | 4946 | 8331 |
| 5.1724 | 4062 | 12769 | 5689 | 6731 | 5199 | 6507 |
| 6.2069 | 4857 | 9786 | 6632 | 5484 | 5788 | 5292 |
| 7.2414 | 5503 | 5416 | 7317 | 3347 | 6784 | 4562 |
| 8.2759 | 6363 | 3679 | 5814 | 4093 | 6784 | 3703 |
| 9.3103 | 7228 | 4578 | 4687 | 4894 | 5353 | 3748 |
| 10.3448 | 4789 | 5713 | 4158 | 6726 | 4467 | 7380 |
| 11.3793 | 4123 | 9201 | 3612 | 11145 | 4061 | 11950 |
| 12.4138 | 3452 | 13849 | 3246 | 13885 | 3046 | 13584 |
| 13.4483 | 3541 | 11860 | 4535 | 11206 | 3674 | 10641 |
| 14.4828 | 4672 | 8989 | 4967 | 8543 | 4723 | 8088 |
| 15.5172 | 5002 | 5135 | 4967 | 6688 | 5010 | 6314 |
| 16.5517 | 5309 | 4440 | 6226 | 5431 | 5337 | 5208 |
| 17.5862 | 5833 | 3474 | 7154 | 4661 | 6088 | 4499 |
| 18.6207 | 5833 | 3996 | 6652 | 4123 | 7020 | 3603 |
| 19.6552 | 5878 | 4787 | 5141 | 4918 | 6858 | 3806 |
| 20.6897 | 4755 | 6294 | 4378 | 6815 | 6858 | 4608 |
| 21.7241 | 4198 | 10511 | 4007 | 11258 | 4324 | 12111 |
| 22.7586 | 3703 | 14025 | 2775 | 13876 | 3907 | 13433 |
| 23.7931 | 3702 | 11468 | 4109 | 10963 | 2821 | 10452 |
| 24.8276 | 4694 | 8692 | 4870 | 8317 | 4210 | 7952 |
| 25.8621 | 5007 | 6757 | 5119 | 6499 | 4883 | 6223 |
| 26.8966 | 5325 | 4347 | 5608 | 5308 | 5131 | 5129 |
| 27.9310 | 6072 | 3359 | 7352 | 4590 | 5646 | 4433 |
| 28.9655 | 6824 | 4080 | 5854 | 3752 | 6596 | 3495 |
| 30.0000 | 5250 | 4882 | 4769 | 4974 | 7312 | 3892 |

# Appendix E

# Test Data for 24 kPa Supply Pressure

## E.1

**Table E.1.1:** Raw Test Data from 24 kPa Tests

| Time (s) | Test 1 | | Test 2 | | Test 3 | |
|---|---|---|---|---|---|---|
| | $P_1$ (Pa) | $P_2$ (Pa) | $P_1$ (Pa) | $P_2$ (Pa) | $P_1$ (Pa) | $P_2$ (Pa) |
| 0 | 4836 | 12354 | 8446 | 8554 | 5765 | 5402 |
| 1.0345 | 5921 | 7848 | 8818 | 6710 | 7316 | 5078 |
| 2.0690 | 7561 | 6222 | 4530 | 5511 | 8461 | 5759 |
| 3.1034 | 8661 | 5202 | 5256 | 4890 | 5471 | 8542 |
| 4.1379 | 9074 | 5174 | 6690 | 9747 | 4309 | 12864 |
| 5.1724 | 6492 | 5936 | 8116 | 12674 | 5544 | 10802 |
| 6.2069 | 4903 | 8988 | 8991 | 10161 | 7061 | 8313 |
| 7.2414 | 4522 | 12748 | 6931 | 7876 | 8316 | 4986 |
| 8.2759 | 5031 | 10045 | 5098 | 6250 | 8544 | 6913 |
| 9.3103 | 6330 | 7758 | 4341 | 5190 | 6132 | 9765 |
| 10.3448 | 7852 | 6183 | 5826 | 5121 | 4469 | 11858 |
| 11.3793 | 5588 | 5184 | 8737 | 5896 | 5066 | 9257 |
| 12.4138 | 4426 | 6878 | 7681 | 9107 | 8146 | 7195 |
| 13.4483 | 4649 | 11759 | 5556 | 12820 | 8793 | 5797 |
| 14.4828 | 5483 | 11781 | 4398 | 10498 | 6354 | 4917 |
| 15.5172 | 7006 | 9189 | 4582 | 5770 | 4779 | 5439 |
| 16.5517 | 8320 | 7114 | 5398 | 4909 | 4398 | 7058 |
| 17.5862 | 9077 | 5752 | 6877 | 5369 | 4888 | 9321 |
| 18.6207 | 6443 | 4945 | 8249 | 6730 | 6155 | 12485 |
| 19.6552 | 4855 | 5385 | 8957 | 11575 | 7685 | 9939 |
| 20.6897 | 4478 | 6528 | 6488 | 11950 | 8720 | 8289 |
| 21.7241 | 6713 | 11243 | 4870 | 9350 | 7060 | 6234 |
| 22.7586 | 8095 | 12151 | 5060 | 7259 | 5463 | 5225 |
| 23.7931 | 8987 | 6584 | 6406 | 5840 | 4589 | 6168 |
| 24.8276 | 7231 | 5416 | 7814 | 4962 | 5206 | 10105 |
| 25.8621 | 5287 | 5012 | 8778 | 5285 | 5629 | 12582 |
| 26.8966 | 4309 | 5692 | 7165 | 12766 | 7536 | 10073 |
| 27.9310 | 4692 | 8005 | 5256 | 10916 | 8213 | 7778 |
| 28.9655 | 5658 | 12754 | 4328 | 8409 | 8026 | 6182 |
| 30.0000 | 7198 | 11049 | 4705 | 6577 | 7256 | 5749 |

# Appendix F

# Test Data for 24 kPa Supply Pressure

## F.1

**Table F.1.1:** Raw Test Data from 28kPa Tests

| **Time (s)** | **Test 1** | | **Test 2** | | **Test 3** | |
|---|---|---|---|---|---|---|
| | $P_1$ **(Pa)** | $P_2$ **(Pa)** | $P_1$ **(Pa)** | $P_2$ **(Pa)** | $P_1$ **(Pa)** | $P_2$ **(Pa)** |
| 0 | 8504 | 9040 | 5790 | 11854 | 5849 | 11152 |
| 1.0345 | 6112 | 12505 | 7516 | 9194 | 5406 | 12142 |
| 2.0690 | 5328 | 11492 | 7672 | 7650 | 7042 | 9571 |
| 3.1034 | 6798 | 8911 | 5582 | 9774 | 8136 | 7750 |
| 4.1379 | 8530 | 7546 | 5541 | 12657 | 5771 | 9596 |
| 5.1724 | 6282 | 9744 | 7343 | 7698 | 5527 | 12711 |
| 6.2069 | 7098 | 12336 | 5347 | 10864 | 7184 | 10282 |
| 7.2414 | 8271 | 9696 | 6902 | 12218 | 5308 | 7930 |
| 8.2759 | 5865 | 7678 | 8380 | 9601 | 5821 | 8307 |
| 9.3103 | 5414 | 9010 | 5957 | 7675 | 7575 | 9816 |
| 10.3448 | 7049 | 12838 | 5339 | 9173 | 7730 | 7658 |
| 11.3793 | 8247 | 10644 | 6851 | 12793 | 5605 | 8813 |
| 12.4138 | 5887 | 10131 | 5757 | 10455 | 5452 | 12735 |
| 13.4483 | 5403 | 12662 | 5418 | 8069 | 7051 | 10660 |
| 14.4828 | 6972 | 10059 | 6959 | 8246 | 8303 | 8214 |
| 15.5172 | 8454 | 7775 | 8339 | 12581 | 5851 | 7988 |
| 16.5517 | 6041 | 8807 | 5956 | 7666 | 5439 | 12258 |
| 17.5862 | 7346 | 12803 | 5352 | 8561 | 7032 | 11531 |
| 18.6207 | 7875 | 10751 | 6898 | 12743 | 5504 | 8927 |
| 19.6552 | 5634 | 8248 | 8421 | 10886 | 5611 | 7789 |
| 20.6897 | 5576 | 8041 | 6067 | 8395 | 7376 | 10790 |
| 21.7241 | 7202 | 12259 | 5329 | 7799 | 7687 | 8213 |
| 22.7586 | 8004 | 11615 | 6787 | 11708 | 5507 | 8163 |
| 23.7931 | 5692 | 8440 | 5685 | 11828 | 5683 | 12482 |
| 24.8276 | 5512 | 12759 | 5481 | 9147 | 7378 | 11295 |
| 25.8621 | 7125 | 11025 | 7078 | 7660 | 7896 | 8716 |
| 26.8966 | 8141 | 8456 | 8347 | 10040 | 5523 | 7800 |
| 27.9310 | 5789 | 7956 | 5839 | 8660 | 5469 | 11157 |
| 28.9655 | 5465 | 11978 | 5564 | 7760 | 7231 | 11784 |
| 30.0000 | 7223 | 12320 | 7310 | 9565 | 8023 | 8921 |

# Appendix G

# Raw Data and Fourier Curve Fit Data Comparison

## G.1

**Table G.1.1:** Raw Data and Fitted Data Comparison

| **Parameter** | **20 kPa Supply Pressure** | | | | **24 kPa Supply Pressure** | | | | **28 kPa Supply Pressure** | | | |
|---|---|---|---|---|---|---|---|---|---|---|---|---|
| | **Actuator 1** | | **Actuator 2** | | **Actuator 1** | | **Actuator 2** | | **Actuator 1** | | **Actuator 2** | |
| | **Raw** | **Fit** | **Raw** | **Fit** | **Raw** | **Fit** | **Raw** | **Fit** | **Raw** | **Fit** | **Raw** | **Fit** |
| **Maximum Pressure (Pa)** | 7352 | 6443 | 14025 | 11410 | 9077 | 8372 | 12864 | 11220 | 8530 | 7735 | 12838 | 11780 |
| **Minimum Pressure (Pa)** | 2775 | 3520 | 3347 | 3663 | 4309 | 4535 | 4890 | 4729 | 5308 | 5463 | 7546 | 8086 |
| **Amplitude (Pa)** | 2288.5 | 1461 | 5335.5 | 3872 | 2384 | 1942 | 3987 | 3243 | 1611 | 1136 | 2646 | 1847 |
| **Offset (Pa)** | 5063.5 | 4982 | 8694.5 | 7538 | 6693 | 6430 | 8877 | 7977 | 6919 | 6599 | 10192 | 9933 |
| **Frequency (rad/s)** | 0.63 | 0.6116 | 0.63 | 0.6242 | 0.95 | 0.8731 | 0.95 | 0.8524 | 1.43 | 1.514 | 1.43 | 1.534 |

# Appendix H

# Drawings

## H.1 Valve Split Mould

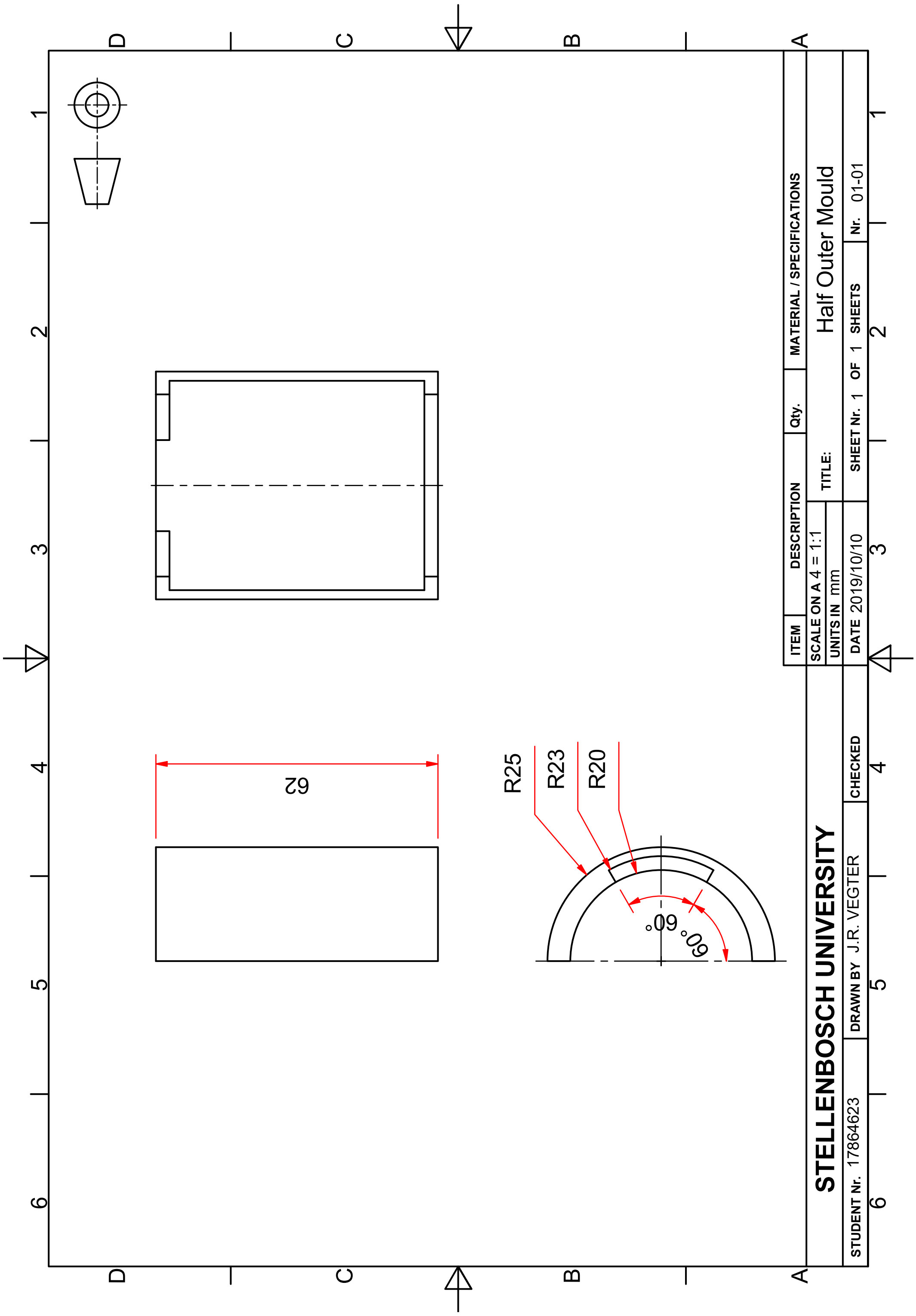
62
R25
R23
R20
60°
60°
ITEM
DESCRIPTION
Qty.
MATERIAL / SPECIFICATIONS
SCALE ON A 4 = 1:1
UNITS IN mm
TITLE:
Half Outer Mould
DATE 2019/10/10
SHEET Nr. 1 OF 1 SHEETS
Nr. 01-01
STELLENBOSCH UNIVERSITY
STUDENT Nr. 17864623
DRAWN BY J.R. VEGTER
CHECKED

## H.2 Top Insert

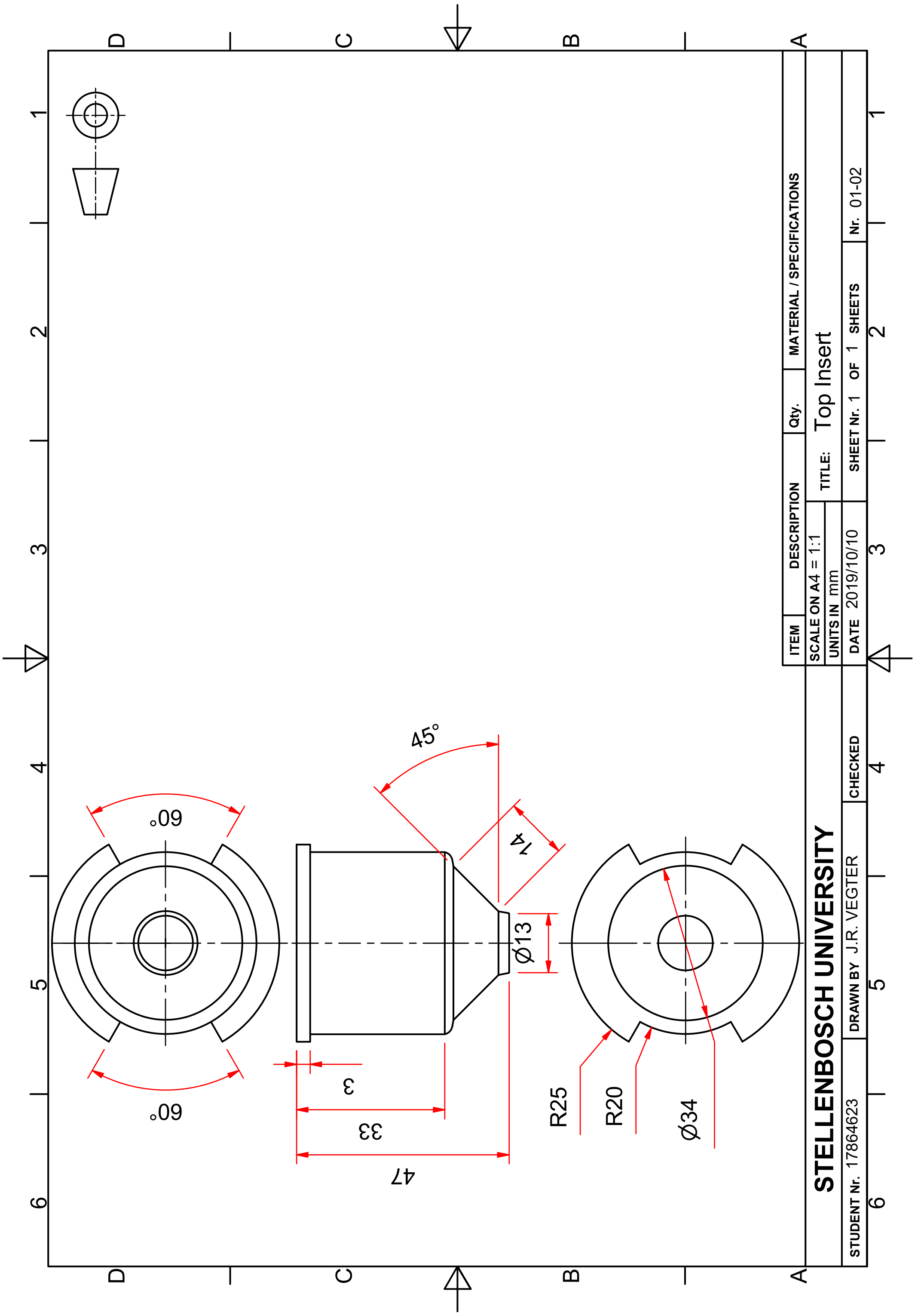
60°
60°
45°
14
Ø13
3
33
47
R25
R20
Ø34
ITEM
DESCRIPTION
Qty.
MATERIAL / SPECIFICATIONS
SCALE ON A4 = 1:1
UNITS IN mm
TITLE: Top Insert
STELLENBOSCH UNIVERSITY
DATE 2019/10/10
SHEET Nr. 1 OF 1 SHEETS
Nr. 01-02
STUDENT Nr. 17864623
DRAWN BY J.R. VEGTER
CHECKED

## H.3 Bottom Insert

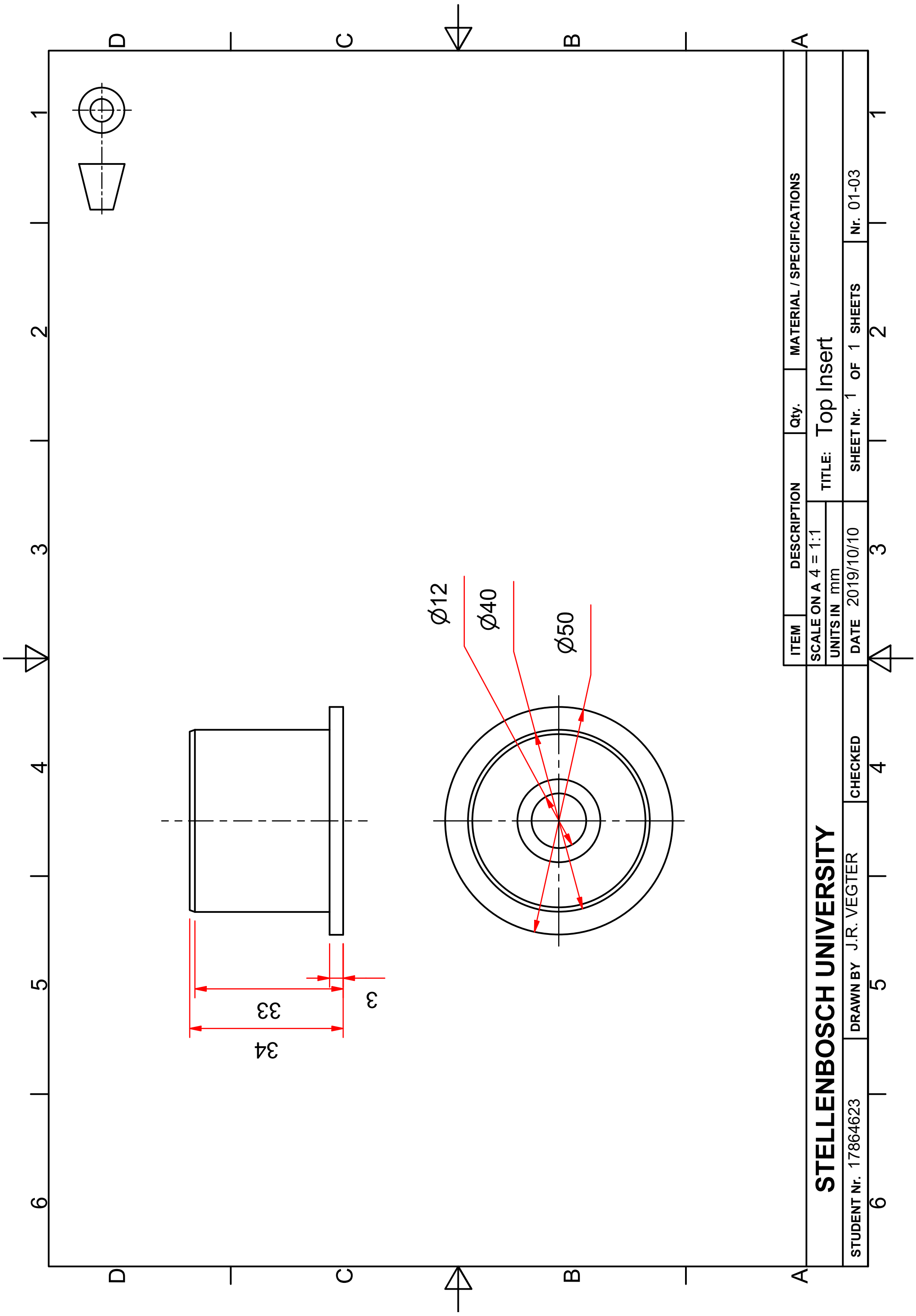

Ø12
Ø40
Ø50
33
34
3
ITEM
DESCRIPTION
Qty.
MATERIAL / SPECIFICATIONS
SCALE ON A 4 = 1:1
UNITS IN mm
TITLE: Top Insert
STELLENBOSCH UNIVERSITY
DATE 2019/10/10
CHECKED
DRAWN BY J.R. VEGTER
STUDENT Nr. 17864623
SHEET Nr. 1 OF 1 SHEETS
Nr. 01-03

## H.4 Membrane Detail Section

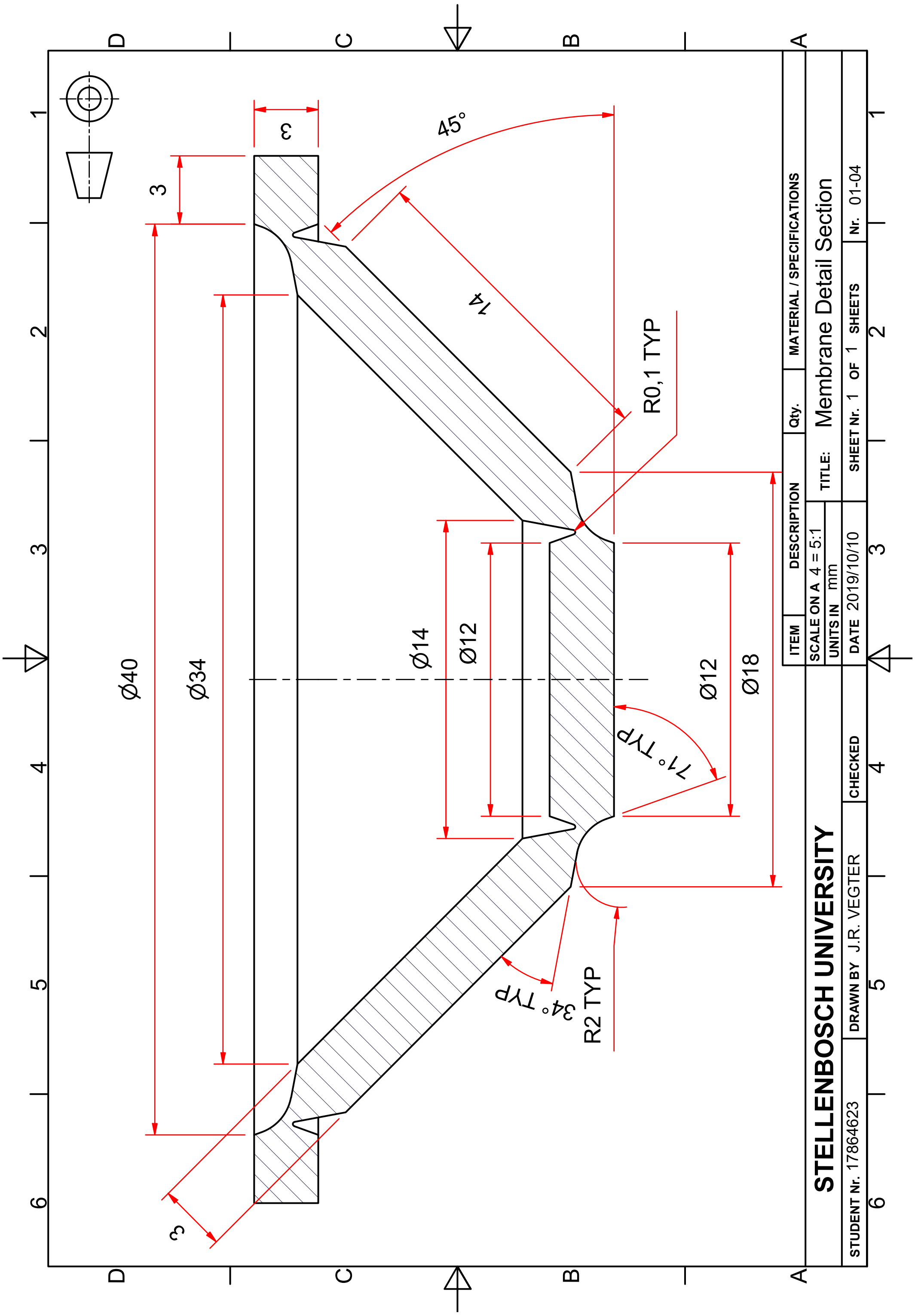

Ø40
Ø34
Ø14
Ø12
Ø12
Ø18
3
3
3
45°
14
R0,1 TYP
R2 TYP
34° TYP
71° TYP
ITEM
DESCRIPTION
Qty.
MATERIAL / SPECIFICATIONS
SCALE ON A 4 = 5:1
UNITS IN mm
TITLE: Membrane Detail Section
STELLENBOSCH UNIVERSITY
DATE 2019/10/10
SHEET Nr. 1 OF 1 SHEETS
Nr. 01-04
CHECKED
DRAWN BY J.R. VEGTER
STUDENT Nr. 17864623

## H.5 Tube Split Mould

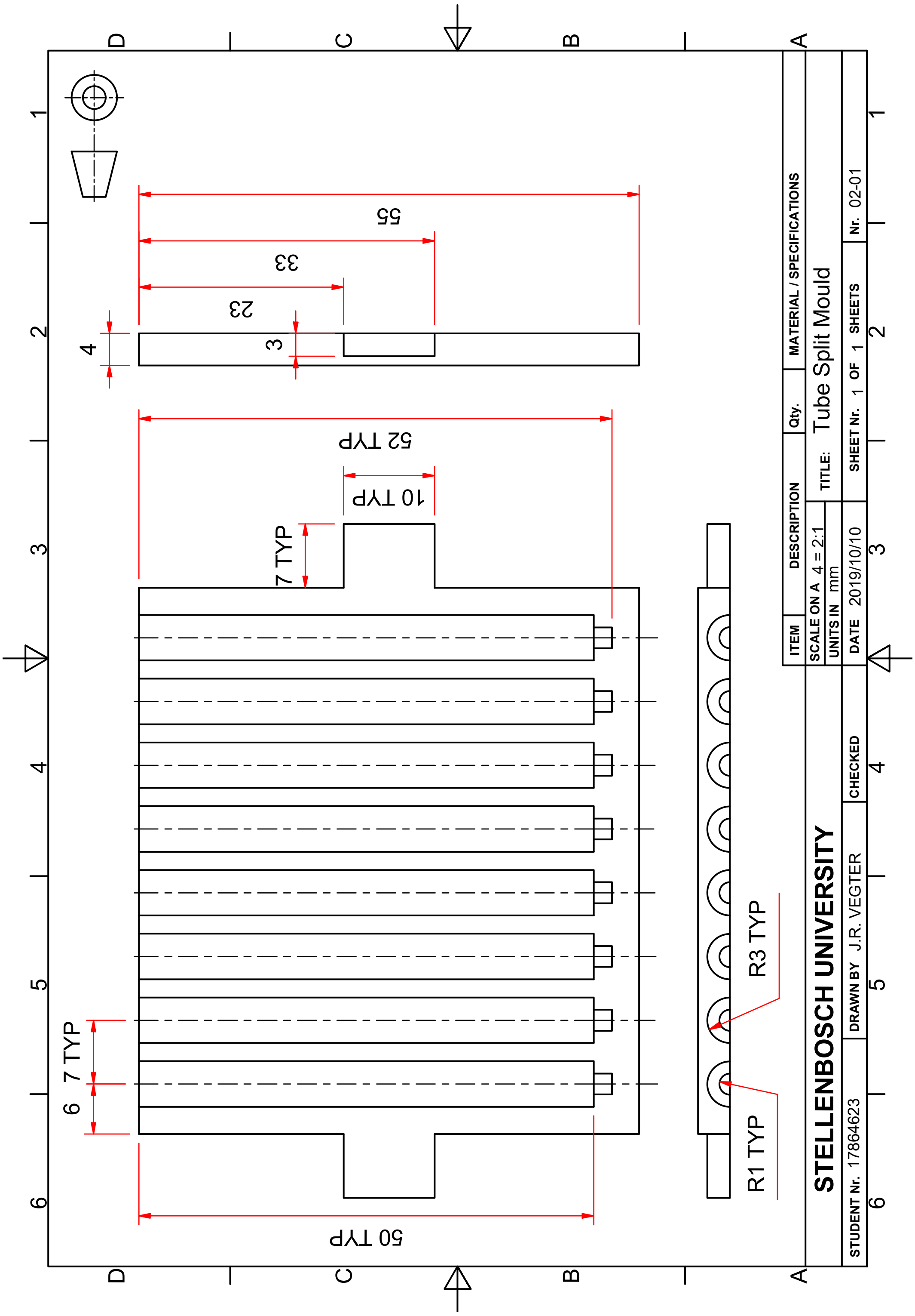
55
33
23
4
3
52 TYP
10 TYP
7 TYP
7 TYP
6
50 TYP
R3 TYP
R1 TYP
ITEM
DESCRIPTION
Qty.
MATERIAL / SPECIFICATIONS
SCALE ON A 4 = 2:1
UNITS IN mm
TITLE: Tube Split Mould
STELLENBOSCH UNIVERSITY
DATE 2019/10/10
SHEET Nr. 1 OF 1 SHEETS
Nr. 02-01
CHECKED
DRAWN BY J.R. VEGTER
STUDENT Nr. 17864623

## H.6 Tube Spilt Mould Cover

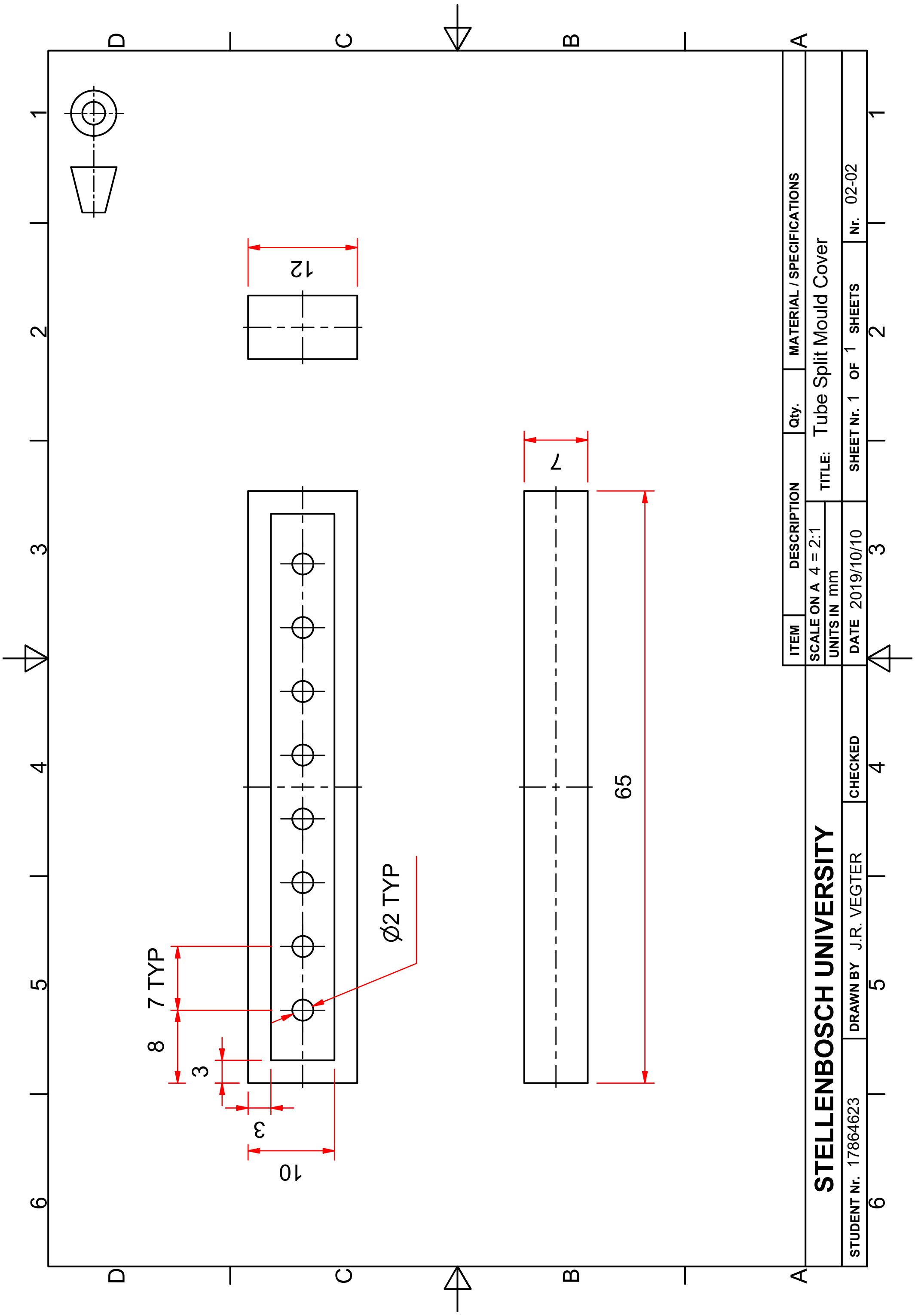
12
7
65
Ø2 TYP
7 TYP
8
3
3
10
ITEM
DESCRIPTION
Qty.
MATERIAL / SPECIFICATIONS
SCALE ON A 4 = 2:1
UNITS IN mm
TITLE: Tube Split Mould Cover
DATE 2019/10/10
SHEET Nr. 1 OF 1 SHEETS
Nr. 02-02
STELLENBOSCH UNIVERSITY
STUDENT Nr. 17864623
DRAWN BY J.R. VEGTER
CHECKED

## H.7 End Cap Mould

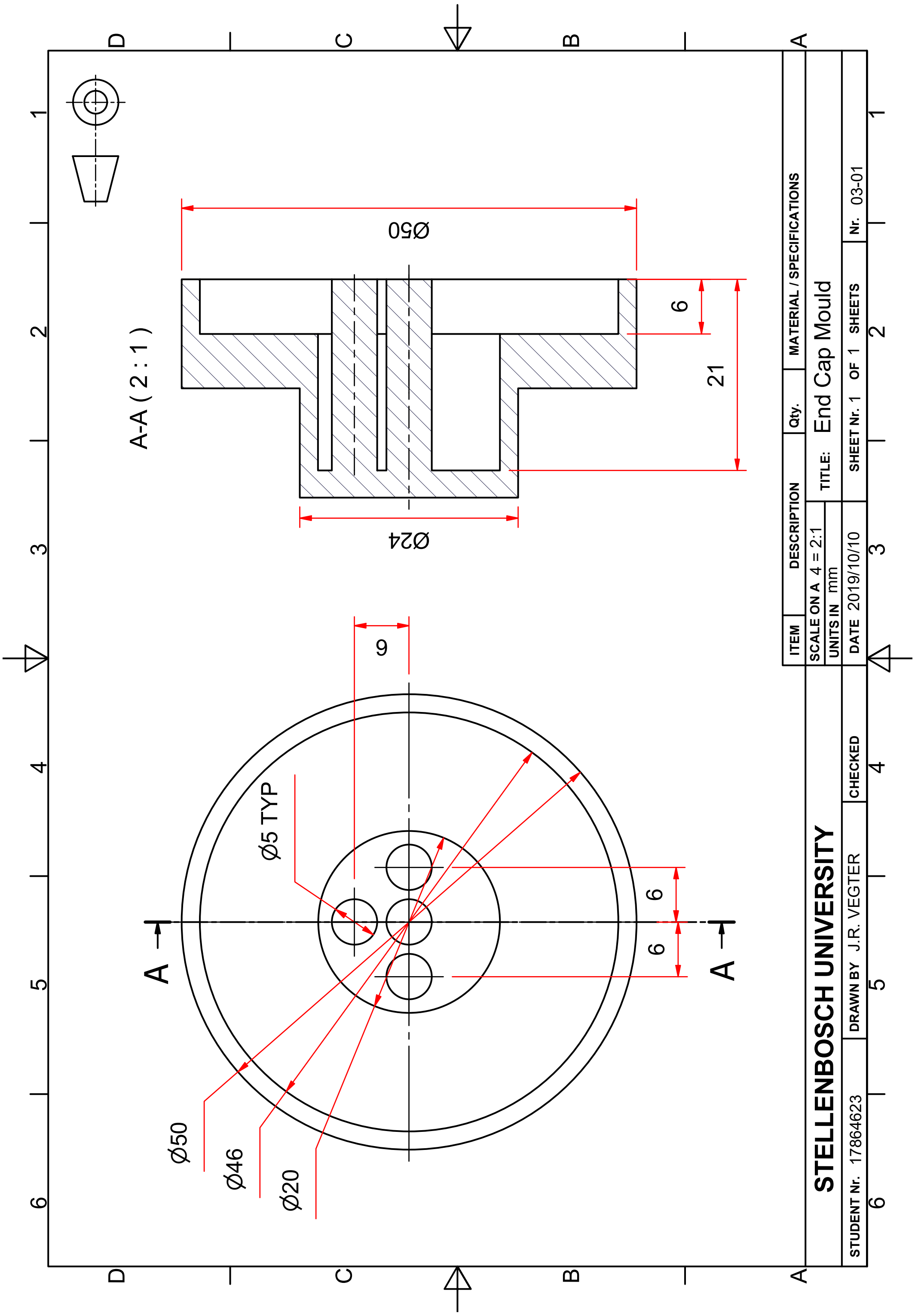
A-A ( 2 : 1 )
Ø50
6
21
Ø24
9
Ø5 TYP
6
6
A
A
Ø50
Ø46
Ø20
ITEM
DESCRIPTION
Qty.
MATERIAL / SPECIFICATIONS
SCALE ON A 4 = 2:1
UNITS IN mm
TITLE: End Cap Mould
DATE 2019/10/10
SHEET Nr. 1 OF 1 SHEETS
Nr. 03-01
STELLENBOSCH UNIVERSITY
STUDENT Nr. 17864623
DRAWN BY J.R. VEGTER
CHECKED

## H.8 End Cap

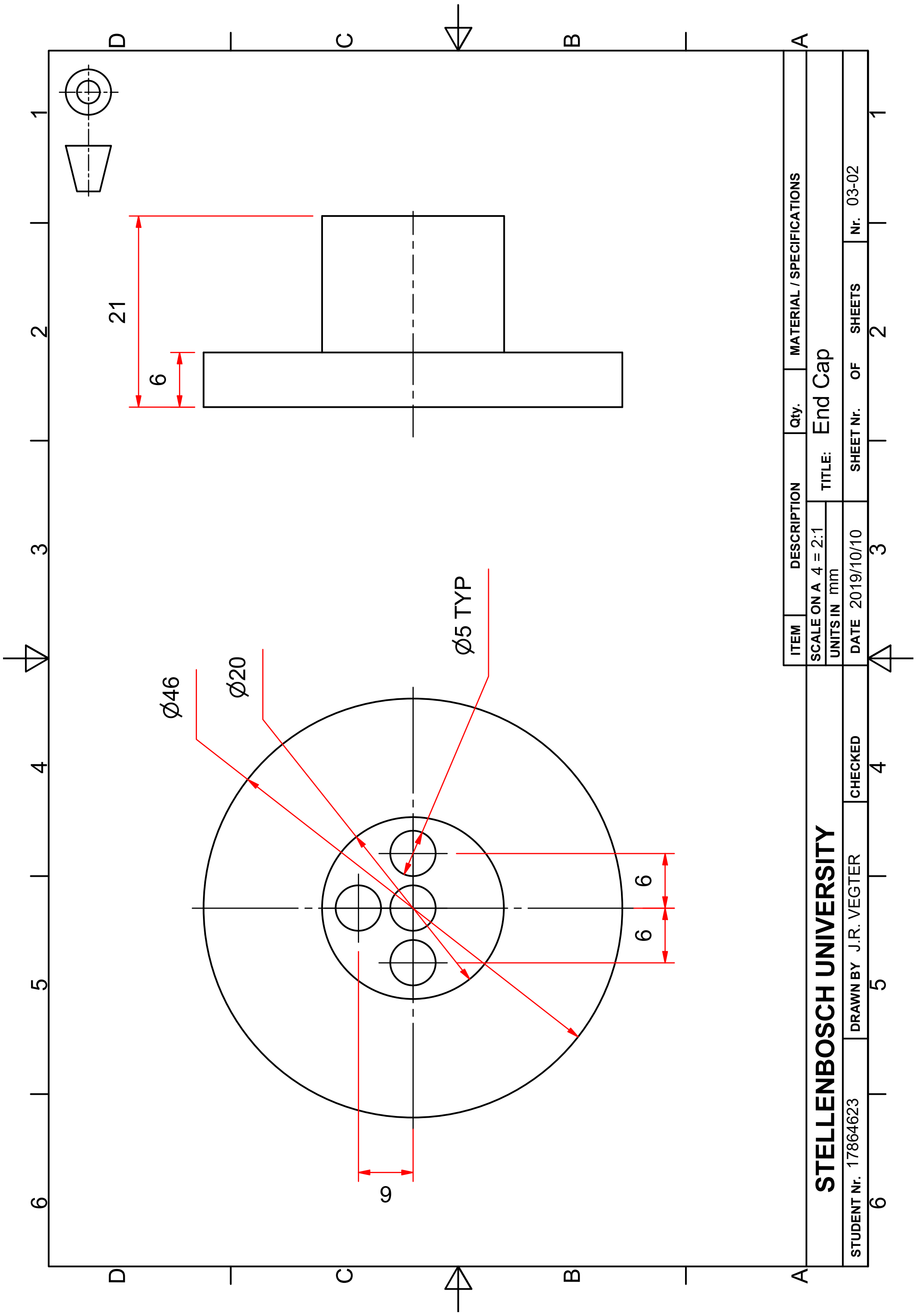
21
6
Ø46
Ø20
Ø5 TYP
6
6
9
ITEM
DESCRIPTION
Qty.
MATERIAL / SPECIFICATIONS
SCALE ON A 4 = 2:1
UNITS IN mm
TITLE: End Cap
DATE 2019/10/10
SHEET Nr.
OF
SHEETS
Nr. 03-02
STELLENBOSCH UNIVERSITY
STUDENT Nr. 17864623
DRAWN BY J.R. VEGTER
CHECKED

# Bibliography

[1] Rus, D. and Tolley, M.: Design, Fabrication and Control of Soft Robots with Fluidic Elastomer Actuators. *Nature*, vol. 521, no. 7443, p. 139 199, 2015.

[2] Majidi, C.: Soft Robotics : A Perspective — Current Trends and Prospects for the Future. , no. July, pp. 4–11, 2018.

[3] Ijspeert, A.J.: Central pattern generators for locomotion control in animals and robots: A review. *Neural Networks*, vol. 21, no. 4, pp. 642–653, 2008. ISSN 08936080. NIHMS150003.

[4] Ijspeert, A.J., Crespi, A., Ryczko, D. and Cabelguen, J.M.: From swimming to walking with a salamander robot driven by a spinal cord model. *Science*, vol. 315, no. 5817, pp. 1416–1420, 2007. ISSN 00368075.

[5] Wang, W., Rodrigue, H., Kim, H.I., Han, M.W. and Ahn, S.H.: Soft composite hinge actuator and application to compliant robotic gripper. *Composites Part B: Engineering*, vol. 98, pp. 397–405, 2016. ISSN 13598368.
Available at: http://dx.doi.org/10.1016/j.compositesb.2016.05.030

[6] Laschi, C. and Cianchetti, M.: Soft Robotics: New Perspectives for Robot Bodyware and Control. *Frontiers in Bioengineering and Biotechnology*, vol. 2, no. January, pp. 1–5, 2014. ISSN 2296-4185.
Available at: https://tinyurl.com/y483kghh

[7] Marchese, A.D., Katzschmann, R.K. and Rus, D.: A Recipe for Soft Fluidic Elastomer Robots. *Soft Robotics*, vol. 2, no. 1, pp. 7–25, 2015. ISSN 2169-5172.
Available at: http://online.liebertpub.com/doi/10.1089/soro.2014.0022

[8] Rodrigue, H., Bhandari, B., Han, M.W. and Ahn, S.H.: A shape memory alloy-based soft morphing actuator capable of pure twisting motion. *Journal of Intelligent Material Systems and Structures*, vol. 26, no. 9, pp. 1071–1078, 2015. ISSN 15308138.

[9] Cianchetti, M., Licofonte, A., Follador, M., Rogai, F. and Laschi, C.: Bioinspired Soft Actuation System Using Shape Memory Alloys. *Actuators*, vol. 3, no. 3, pp. 226–244, 2014. ISSN 2076-0825.
Available at: http://www.mdpi.com/2076-0825/3/3/226/

[10] Trimmer, B.A., Lin, H.-t., Baryshyan, A., Leisk, G.G. and Kaplan, D.L.: Towards a biomorphic soft robot : design constraints and solutions. , no. D, pp. 599–605, 2012.

[11] Lantada, A.D., De Blas Romero, A. and Tanarro, E.C.: Micro-vascular shape-memory polymer actuators with complex geometries obtained by laser stereolithography. *Smart Materials and Structures*, vol. 25, no. 6, 2016. ISSN 1361665X.

[12] Liu, Y., Lv, H., Lan, X., Leng, J. and Du, S.: Review of electro-active shape-memory polymer composite. *Composites Science and Technology*, vol. 69, no. 13, pp. 2064–2068, 2009. ISSN 02663538.
Available at: `http://dx.doi.org/10.1016/j.compscitech.2008.08.016`

[13] Bar-Cohen, Y. and Zhang, Q.: Electroactive Polymer Actuators and Sensors. *Materials Research Society Bulletin*, vol. 33, no. March 2008, pp. 173–181, 2008.

[14] Ilievski, F., Mazzeo, A.D., Shepherd, R.F., Chen, X. and Whitesides, G.M.: Soft robotics for chemists. *Angewandte Chemie - International Edition*, vol. 50, no. 8, pp. 1890–1895, 2011. ISSN 14337851. `79951804311`.

[15] Shintake, J.: Functional Soft Robotic Actuators Based on Dielectric Elastomers. *Thesis*, vol. 6855, p. 149, 2016.

[16] Shahinpoor, M., Bar-Cohen, Y., Xue, T., Harrison, J.S. and Smith, J.: Ionic Polymer-Metal Composites as Biomimetic Sensors and Actuators-Artificial Muscles. pp. 25–50, 1999. ISSN 00976156.
Available at: `http://pubs.acs.org/doi/abs/10.1021/bk-1999-0726.ch003`

[17] Jung, H.S., Yang, S.Y., Cho, K.H., Song, M.G., Nguyen, C.T., Phung, H., Kim, U., Moon, H., Koo, J.C., Nam, J.D. and Choi, H.R.: Design and fabrication of twisted monolithic dielectric elastomer actuator. *International Journal of Control, Automation and Systems*, vol. 15, no. 1, pp. 25–35, 2017. ISSN 20054092.

[18] Tongqing, L., Zhibao, S., Qian, S. and T.J., W.: Bioinspired bicipital muscle with fiber-constrained dielectric elastomer actuator. *Extreme Mechanics Letters*, vol. 6, pp. 75–81, 2016.

[19] Kang, R., Guo, Y., Chen, L., Branson, D.T. and Dai, J.S.: Design of a Pneumatic Muscle Based Continuum Robot with Embedded Tendons. *IEEE/ASME Transactions on Mechatronics*, vol. 22, no. 2, pp. 751–761, 2017. ISSN 10834435.

[20] Giousouf, M. and Kovacs, G.: Dielectric elastomer actuators used for pneumatic valve technology. *Smart Materials and Structures*, vol. 22, no. 10, 2013. ISSN 09641726.

[21] Nguyen, C.T., Phung, H., Nguyen, T.D., Lee, C., Kim, U., Lee, D., Moon, H., Koo, J., Nam, J.D. and Choi, H.R.: A small biomimetic quadruped robot driven by multistacked dielectric elastomer actuators. *Smart Materials and Structures*, vol. 23, no. 6, 2014. ISSN 1361665X.

[22] Carpi, F., Frediani, G., Turco, S. and De, R.D.: Bioinspired tunable lens with muscle-like electroactive elastomers. *Advanced Functional Materials*, vol. 21, no. 21, pp. 4152–4158, 2011. ISSN 1616301X.

[23] Miriyev, A., Stack, K. and Lipson, H.: Soft material for soft actuators. *Nature Communications*, vol. 8, no. 1, pp. 1–8, 2017. ISSN 20411723.
Available at: `http://dx.doi.org/10.1038/s41467-017-00685-3`

[24] Andrikopoulos, G., Nikolakopoulos, G. and Manesis, S.: A survey on applications of pneumatic artificial muscles. pp. 1439–1446, 2011.

[25] Greer, J.D., Morimoto, T.K., Okamura, A.M. and Hawkes, E.W.: Series pneumatic artificial muscles (sPAMs) and application to a soft continuum robot. *Proceedings - IEEE International Conference on Robotics and Automation*, pp. 5503–5510, 2017. ISSN 10504729. `/dx.doi.org/10.1002/adma.201603483`.

[26] Gorissen, B., Reynaerts, D., Konishi, S., Yoshida, K., Kim, J.W. and De Volder, M.: Elastic Inflatable Actuators for Soft Robotic Applications. *Advanced Materials*, vol. 29, no. 43, pp. 1–14, 2017. ISSN 15214095.

[27] Shepherd, R.F., Ilievski, F., Choi, W., Morin, S.A., Stokes, A.A., Mazzeo, A.D., Chen, X., Wang, M. and Whitesides, G.M.: Multigait soft robot. *Proceedings of the National Academy of Sciences*, vol. 108, no. 51, pp. 20400–20403, 2011. ISSN 0027-8424. `84855503964`.
Available at: `http://www.pnas.org/cgi/doi/10.1073/pnas.1116564108`

[28] Onal, C.D. and Rus, D.: Autonomous undulatory serpentine locomotion utilizing body dynamics of a fluidic soft robot. *Bioinspiration and Biomimetics*, vol. 8, no. 2, 2013. ISSN 17483182.

[29] Mosadegh, B., Polygerinos, P., Keplinger, C., Wennstedt, S., Shepherd, R.F., Gupta, U., Shim, J., Bertoldi, K., Walsh, C.J. and Whitesides, G.M.: Pneumatic networks for soft robotics that actuate rapidly. *Advanced Functional Materials*, vol. 24, no. 15, pp. 2163–2170, 2014. ISSN 16163028.

[30] Yang, D., Mosadegh, B., Ainla, A., Lee, B., Khashai, F., Suo, Z., Bertoldi, K. and Whitesides, G.M.: Buckling of Elastomeric Beams Enables Actuation of Soft Machines. *Advanced Materials*, vol. 27, no. 41, pp. 6323–6327, 2015. ISSN 15214095.

[31] Bicanski, A., Ryczko, D., Cabelguen, J.M. and Ijspeert, A.J.: From lamprey to salamander: An exploratory modeling study on the architecture of the spinal locomotor networks in the salamander. *Biological Cybernetics*, vol. 107, no. 5, pp. 565–587, 2013. ISSN 03401200.

[32] Harischandra, N., Cabelguen, J.M. and Ekeberg, r.: A 3D musculo-mechanical model of the salamander for the study of different gaits and modes of locomotion. *Frontiers in Neurorobotics*, vol. 4, no. DEC, pp. 1–10, 2010. ISSN 16625218.

[33] Buchanana, J.T.: The neuronal network for locomotion in the lamprey spinal cord : Evidence for the involvement of commissural interneurons * Fictive swimming Spinal interneurons. *J Physiology*, , no. 89, pp. 221–233, 1995.

[34] Bicanski, A., Ryczko, D., Knuesel, J., Harischandra, N., Charrier, V., Ekeberg, Ö., Cabelguen, J.M. and Ijspeert, A.J.: Decoding the mechanisms of gait generation in salamanders by combining neurobiology, modeling and robotics. *Biological Cybernetics*, vol. 107, no. 5, pp. 545–564, 2013. ISSN 03401200.

[35] Ashley-Ross, M.: Hindlimb Kinematics During Terrestrial Locomotion in a Salamander (Dicamptodon Tenebrosus). *The Journal of experimental biology*, vol. 193, pp. 255–83, 1994. ISSN 1477-9145.
Available at: `http://www.ncbi.nlm.nih.gov/pubmed/23667046`

[36] Karakasiliotis, K., Schilling, N., Cabelguen, J.M. and Ijspeert, A.J.: Where are we in understanding salamander locomotion: Biological and robotic perspectives on kinematics. *Biological Cybernetics*, vol. 107, no. 5, pp. 529–544, 2013. ISSN 03401200.

[37] Frolich, L.M. and Biewener, A.A.: Kinematic and Electromyographic Analysis of the Functional Role of the Body Axis During Terrestrial and Aquatic Locomotion in the Salamander Ambystoma Tigrinum. *Journal of Experimental Biology*, vol. 162, no. 1, pp. 107–130, 1992. ISSN 00220949.

[38] Kyriakatos, A., Mahmood, R., Ausborn, J., Porres, C.P., Buschges, A. and El Manira, A.: Initiation of Locomotion in Adult Zebrafish. *Journal of Neuroscience*, vol. 31, no. 23, pp. 8422–8431, 2011. ISSN 0270-6474.
Available at: `https://tinyurl.com/y5c83eqh`

[39] Ryczko, D., Auclair, F., Cabelguen, J.M. and Dubuc, R.: The mesencephalic locomotor region sends a bilateral glutamatergic drive to hindbrain reticulospinal neurons in a tetrapod. *Journal of Comparative Neurology*, vol. 524, no. 7, pp. 1361–1383, 2016. ISSN 10969861.

[40] Grover, W.H., Ivester, R.H.C., Jensen, E.C. and Mathies, R.A.: Development and multiplexed control of latching pneumatic valves using microfluidic logical structures. *The Royal Society of Chemistry*, pp. 623–631, 2006.

[41] Li, Z., Dey, P. and Kim, S.-j.: Sensors and Actuators B : Chemical Microfluidic single valve oscillator for blood plasma filtration. *Sensors & Actuators: B. Chemical*, vol. 296, no. June, p. 126692, 2019. ISSN 0925-4005.
Available at: `https://doi.org/10.1016/j.snb.2019.126692`

[42] Duncan, P.N., Nguyen, T.V. and Hui, E.E.: Pneumatic oscillator circuits for timing and control of integrated microfluidics. *Proceedings of the National Academy of Sciences*, vol. 110, no. 45, pp. 18104–18109, 2013. ISSN 0027-8424.

[43] Rothemund, P., Ainla, A., Belding, L., Preston, D.J., Kurihara, S., Suo, Z. and Whitesides, G.M.: A soft, bistable valve for autonomous control of soft

actuators. *Science Robotics*, vol. 3, no. 16, p. eaar7986, 2018. ISSN 2470-9476. Available at: `https://tinyurl.com/yynstgnt`

[44] Preston, D.J., Jiang, H.J., Sanchez, V., Rothemund, P., Rawson, J., Nemitz, M.P., Lee, W.-K., Suo, Z., Walsh, C.J. and Whitesides, G.M.: A soft ring oscillator. *Science Robotics*, vol. 4, no. 31, p. eaaw5496, 2019. ISSN 2470-9476. Available at: `https://tinyurl.com/y5cr3pnm`

[45] Polygerinos, P., Lyne, S., Wang, Z., Fernando, L., Mosadegh, B., Whitesides, G.M. and Walsh, C.J.: Towards a Soft Pneumatic Glove for Hand Rehabilitation. pp. 1512–1517, 2013.

[46] Wang, Z., Polygerinos, P., Overvelde, J.T., Galloway, K.C., Bertoldi, K. and Walsh, C.J.: Interaction Forces of Soft Fiber Reinforced Bending Actuators. *IEEE/ASME Transactions on Mechatronics*, vol. 22, no. 2, pp. 717–727, 2017. ISSN 10834435.

[47] Shian, S., Bertoldi, K. and Clarke, D.R.: Dielectric Elastomer Based "grippers" for Soft Robotics. *Advanced Materials*, vol. 27, no. 43, pp. 6814–6819, 2015. ISSN 15214095.

[48] Li, S., Vogt, D.M., Rus, D. and Wood, R.J.: Fluid-driven origami-inspired artificial muscles. *Proceedings of the National Academy of Sciences*, vol. 114, no. 50, pp. 13132–13137, 2017. ISSN 0027-8424.

[49] Rothemund, P., Ainla, A., Belding, L., Preston, D.J., Kurihara, S., Suo, Z. and Whitesides, G.M.: Supplementary Materials for A soft , bistable valve for autonomous control of soft actuators. 2018.

[50] Smooth-On: Shore hardness scales. 2019.
Available at: `https://www.smooth-on.com/assets/pdf/durometer_chart.pdf`